Nigerian Journal of Renewable Energy Research

Volume 1, Number 1, 2023: eISSN 1597-8907: pISSN 1597-8877

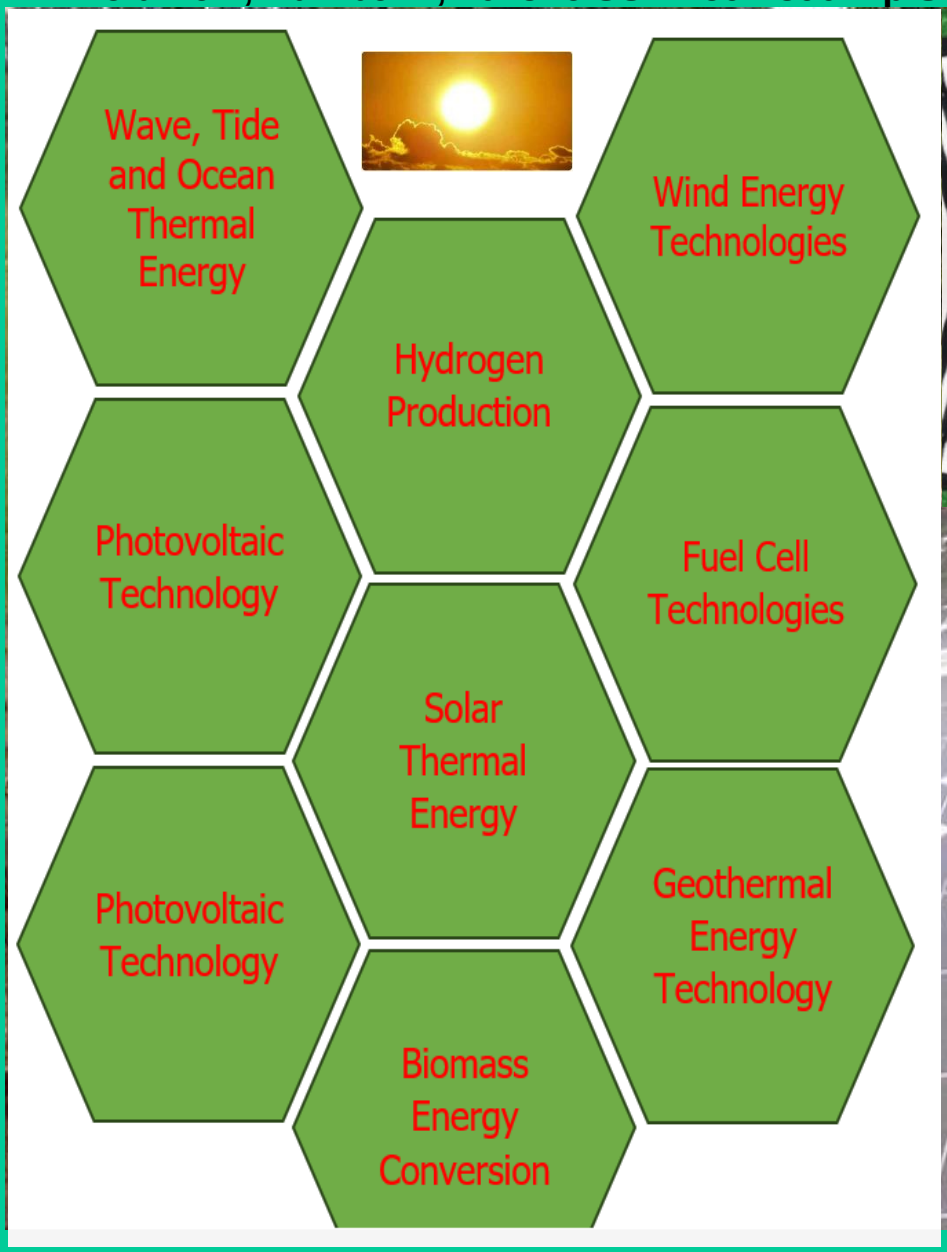

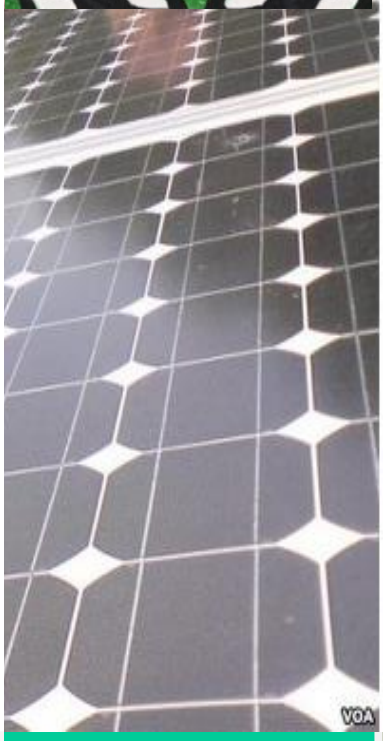

Published by the TETFund Centre of Excellence for Renewable Energy, Kaduna Polytechnic, Kaduna, Nigeria ©2023

This volume was published with funds provided by Tertiary Education Trust Fund.

Acknowledgement

The Centre wishes to acknowledge the funds provided for this Publication by TETFund Centre of Excellence for Renewable Energy, Kaduna Polytechnic, Kaduna, Nigeria. The funds were provided by the Tertiary Education Trust Fund (TETFUND), Nigeria, under the TETFUND Special Intervention for Establishment of Centres of Excellence (TETF/ES/DS&D/KADPOLY/COE /2021/VOL11).

"Technology has given us this wonderful opportunity to have low energy costs. We have to seize that, rather than keep debating and discussing and fighting over it."

Michael Porter

Nigerian Journal of Renewable Energy Research (NJRER)
Volume 1, Number 1, 2023 eISSN 1597-8907: pISSN 1597-8877

About Nigerian Journal of Renewable Energy Research (NJRER)

The *Nigerian Journal of Renewable Energy Research (NJRER)* is a Peer-reviewed, Open Access journal that publishes papers relating to the science and technology of energy generation, distribution, storage, and management. It also publishes studies into the environmental, societal, and economic impacts of renewable energy use and policy.

Amongst others, the journal considers articles relating to Solar energy (thermal and photovoltaic), biofuels and energy from biomass, geothermal energy, hydropower (conventional hydroelectricity, tidal and wave power), Wind power, Wave, Tide and Ocean, Thermal Energy Innovations, Hydro Power, Climatology and Meteorology, Hydrogen Production and Fuel Cell Technologies and Socio-economic Aspects and Policy Discussions on Renewable Energy. NJRER invites submissions that uphold high scientific standards and importance. Once accepted, articles typically appear within half a year. All entries in NJRER undergo a peer review process.

The Nigerian Journal of Renewable Energy Research is published twice a year.

Types of paper

Regular articles: Such pieces should outline fresh and thoroughly validated discoveries. The experimental methods must be detailed enough to allow others to replicate the study. The article's length should be concise, only as long as necessary to clearly convey and explain the research.

Short Communications: A Short Communication is apt for documenting outcomes of minor yet complete studies, or for sharing new concepts, pioneering techniques, or equipment. The structure doesn't have to mirror that of longer articles. These notes span 2 to 4 printed pages, equivalent to roughly 6 to 14 handwritten pages.

Reviews: Contributions offering reviews and insights on contemporary subjects are appreciated and encouraged. Reviews ought to be succinct, spanning between 4-6 printed pages (equivalent to 12 to 18 written pages). Nonetheless, reviews analysing methods and designs might extend to a maximum of 30 printed pages. All review articles undergo a peer review process.

Editorial Policy

Any paper presented to the *Nigerian Journal of Renewable Energy Research* must assert that the research detailed hasn't been previously published (barring its presence as an abstract, a part of a public lecture, academic dissertation, or conference notes). Furthermore, it shouldn't be under review elsewhere. Every author must endorse its publication, and it must also receive either implicit or explicit approval from the pertinent institutions where the research took place. Upon acceptance, the content mustn't be

republished elsewhere, digitally or otherwise, in its current format, whether in English or any other language, without the explicit permission of the rights owner.

Copyright Notice

Authors who publish in this Journal agree to the following legal terms:

1. Authors maintain their copyright but give the Journal the privilege of first-time publication. Concurrently, the work is licensed under a Creative Commons Attribution License. This allows others to distribute the work, provided they credit the original authorship and its first publication in any journal overseen by the Centre for Renewable Energy Research and Development.
2. Authors have the flexibility to engage in separate, supplementary agreements for the non-exclusive dissemination of the version of the work published by the Journal, always acknowledging its first appearance in this Journal.
3. Once their manuscript is accepted, authors are both allowed and advised to upload their work online and supply (in print form) to local libraries. This is to promote fruitful discussion and broader referencing of the published material.

For further information, please contact

The Editor in Chief; Nigerian Journal of Renewable Energy Research
email: help@njrer.org or editor@njrer.org; Phone: +234-8037619719
Website: https://www.njrer.org

NIGERIAN JOURNAL OF RENEWABLE ENERGY RESEARCH
Volume 1, Number 1, 2023 eISSN 1597-8907: pISSN 1597-8877

SCOPE

The **Nigerian Journal of Renewable Energy Research** delivers intricate papers to the research community, aimed at sparking additional studies or advancements. This publication is annual. Within its pages, the Journal presents original articles, detailed reports, and critical reviews. Authors are urged to contribute manuscripts that address essential voids in the field of Renewable Energy research and evolution.

The Nigerian Journal of Renewable Energy Research is dedicated to advancing and sharing knowledge on the diverse topics and technologies related to renewable energy systems and components. Its objective is to assist professionals such as researchers, engineers, economists, manufacturers, NGOs, associations, and societies to stay updated with the latest advancements in their respective areas, ensuring the integration of sustainable energy alternatives into existing practices.

This multi-disciplinary journal focuses on renewable energy science, engineering, technology, and research. It aspires to establish itself as a top-tier, peer-reviewed medium, providing authoritative insights and findings in the renewable energy domain.

The research scope of the Nigerian Journal of Renewable Energy Research includes:

- Photovoltaic Technology Transformation
- Applications of Solar Thermal Energy
- Advancements in Geothermal Technology
- Wave, Tide and Ocean Thermal Energy Innovations
- Advancements in Hydro Power
- Biomass Energy Conversion
- Wind Energy Technologies
- Water Desalination Techniques
- Innovations in Solar and Low-Energy Building Designs
- Studies in Climatology and Meteorology
- Developments in Hydrogen Production and Fuel Cell Technologies
- Socio-economic Aspects and Policy Discussions on Renewable Energy

Additionally, while the Journal is open to topics related to renewable energy, it emphasises the necessity of the papers being focused on power generation via renewable or sustainable means. As an illustration, studies on materials designed for renewable energy systems that don't evaluate the energy they'll produce are not considered relevant.

Original research articles and review papers are accepted by the **Nigerian Journal of Renewable Energy Research**. However, review papers are by the Editor-in-Chief's invitation only. Prospective authors for review papers are advised to submit an outline of

their proposed paper along with a brief CV of the main author/s to the Editor-in-Chief for prior approval.
Contributions aligning with the United Nations' sustainable development goals, especially SDG 7 (Affordable and Clean Energy) and SDG 13 (Climate Action), are particularly welcomed.

NIGERIAN JOURNAL OF RENEWABLE ENERGY RESEARCH
Volume 1, Number 1, 2023 eISSN 1597-8907: pISSN 1597-8877

NIGERIAN JOURNAL OF RENEWABLE ENERGY RESEARCH
Volume 1, Number 1, 2023 eISSN 1597-8907: pISSN 1597-8877

FOREWORD

Renewable energy is derived from sources that naturally replenish within a short span. This includes solar, wind, water, biomass, and geothermal energy. Although 'green energy' aligns closely with renewable energy, it is a specific category that offers maximum environmental advantages. Clean energy sources, which produce minimal carbon emissions, comprise renewable energies as well as nuclear power.

Historically, renewable energy has been employed for heating and power, and in more modern contexts, electricity generation. In Nigeria, like many developing nations, renewable energy hasn't made a significant mark in primary energy utilization. Despite a heavy reliance on fossil fuels for heating, electricity, and transport, events like the 1970s oil crises urged investments in alternative energies. Likewise, the adverse impacts of climate change have amplified the public's call for energy not derived from fossil fuels, with this call being further bolstered by governmental incentives and standards.

The **Nigerian Journal of Renewable Energy Research** is committed to providing essential resources centered on the commerce of renewable energy production and distribution. Augmenting renewable energy's role in sustainable development encompasses:

a. Backing initiatives that address the environmental, economic, health, and social repercussions and advantages of renewable energy, promoting transparency, and ensuring sustainability in energy development through collaborations at various levels.
b. Amplifying stakeholder involvement, including that of local, indigenous communities and women, to actively partake in renewable energy projects, including post-operational mine closures and site rehabilitation.
c. Encouraging sustainable practices in renewable energy utilization by offering financial, technical, and capacity-building support to developing nations, promoting value-added processing, and focusing on site restoration.

Renewable energy is crucial for every nation, especially the developing ones, given its pivotal contributions to the global economy and contemporary societies. To capitalize on this sector, judicious investments are essential. In Nigeria, the sector's potential remains untapped. Effective management of renewable energy can propel comprehensive economic growth, alleviate poverty, and help nations achieve global developmental milestones, such as the Sustainable Development Goals.

For Nigeria to benefit from the renewable energy sector, it must invest rightly, instate robust legal frameworks, ensure economic and social benefits, minimize adverse impacts, uphold biodiversity, and counter illegal financial outflows from mining operations. Despite the significance of the sector, Nigeria has faced hurdles in drawing investments from

domestic and international renewable energy firms. This hesitancy stems from the unpredictability of this sector's investments in the country. To counter this, a cohesive effort involving the national and local governments, industry stakeholders, and the public is needed to ensure a stable investment landscape.

A thriving renewable energy industry is paramount for Nigeria's vision of a well-rounded and robust economy, offering opportunities to all. The nation should consistently bolster the renewable energy sector, focusing on research, clean energy utilization, and environmental safeguards. The right research can spur economic growth by luring investments and initiating auxiliary projects, which, in turn, can provide job and business prospects for its citizens.

This Journal is dedicated to advancing research endeavors in renewable energy. We see this publication as a testament to our commitment to a pivotal economic sector and our allegiance to environmental conservation.

S.N. Mumah, *PhD, FNSChE*
Director, TETFund Centre of Excellence for Renewable Energy,
Kaduna Polytechnic, Kaduna, Nigeria.

NIGERIAN JOURNAL OF RENEWABLE ENERGY RESEARCH
Volume 1, Number 1, 2023 eISSN 1597-8907: pISSN 1597-8877

TABLE OF CONTENTS

Nigerian Journal of Renewable Energy Research
Volume 1, Number 1, pp 1-14, 2023
 eISSN 1597-8907: pISSN 1597-8877

ENERGY SAVING OF NAPHTHA HYDROTREATING (NHU) PLANT USING HEAT INTEGRATION

[1,2,*]Akande H. F., [3]Nwafulugo F.U., [1,2]Mumah S.N., [4]Suleman N., [4]Onifade K. R.
[1]TETFund Centre for Renewable Energy, Kaduna Polytechnic, Kaduna, Nigeria
[2]Department of Chemical Engineering, Kaduna Polytechnic, Kaduna, Nigeria
[3]Department of Chemical Engineering, Federal Polytechnic, Oko, Anambra State, Nigeria
[4]Federal University of Technology, Minna, Niger State, Nigeria

[*] Corresponding author: hassan.akande@kadunapolytechnic.edu.ng
https://doi.org/10.5281/zenodo.11501360
https://www.njrer.org/download/vol_1_No_1_pap_1.pdf

ARTICLE INFORMATION

Article history:
Received 21 May, 2023
Revised 22 Jul, 2023
Accepted 08 Oct, 2023
Available online 30 Dec, 2023

Keywords:
Pinch Analysis
NHU
Energy Target
Aspen Energy Analyzer
Composite Curve

Abstract

Energy is fundamental necessary for any industrial economy, yet it is often overlooked in the drive for profitability. Recent energy market development, including deregulation, increasing oil and gas prices as well as effect of combustion gas on the environment has created a new emphasis on energy management. Pinch technology is a vital tool to achieve this objective. Therefore, energy Integration of Naphtha Hydrotreating Unit (NHU) of Kaduna Refinery and Petrochemicals Company was carried out using Pinch Technology. Optimum minimum approach temperature of 10^{o}C was obtained. The pinch point was found to be 488 K. The utility and capital cost for optimum MTA of 10^{o}C are \$2.80664 x 10^{6} and \$1.2798 x 10^{6} respectively. The cold utility requirements of traditional energy approach and pinch analysis of HDS obtained are 22,492.4 kW and 15,408.4 kW respectively while the hot utility requirements of traditional energy approach and pinch analysis are 24,516.0 kW and 18,246.1 kW respectively resulting in energy saving of 28.5% of total energy. Pinch analysis as an energy integration technique saves more energy and utilities cost than the traditional energy technique.

1. Introduction

Pinch technology is a complete methodology derived from simple scientific principles by which it is possible to design new plants with reduced energy and capital costs as well as where the existing processes require modification to improve performance. An additional major advantage of the Pinch approach is that by simply analyzing the process data using its methodology, energy and other design targets are predicted such that it is possible to assess the consequences of a new design or a potential modification before embarking on actual implementation (Akande, 2007).

Pinch analysis originated in the petrochemical sector and is now being applied to solve a wide range of problems in mainstream chemical engineering. Wherever heating and cooling of process

materials take place, there is a potential opportunity. The technology, when applied with imagination, can affect reactor design, separator design and the overall process optimization in any plant. It has been applied to process problems that go far beyond energy conservation. It has been employed to solve problems as diverse as improving effluent quality, reducing emission, increasing product yield and debottlenecking, increasing throughput and improving the flexibility and safety of the process (Akande, 2007).

Energy saving in the Nigerian industrial sector has several possibilities, due to the fact that, almost all the industrial equipment stock in Nigeria were imported during the era of cheap energy. Consequently, they are inherently energy inefficient. Furthermore, given the fact that energy prices had been kept at a low level up to 1985, energy cost has not been a significant fraction of total production cost even for energy intensive industry like refineries in Nigeria. The improvement of energy efficiency can provide substantial benefit in general to all the sectors of the economy (Dayo, 1994). The Naphtha Hydrotreating Unit is a sweetening process involving removal of impurities, like sulfur, nitrogen, oxygen etc, that constitute catalyst poison in the presence of a catalyst. Therefore, major reactions include; Desulphurization, denitrification and hydrogenation reactions (Joseph, 2010). The Naphtha Hydrotreating Unit, NHU is designed to provide suitable feed, treated heavy Naphtha cut of sulfur content less than 1.00ppm for the Catalytic Reforming Unit (CRU) (Chiyoda, 1980). Catalytic treatment of Whole naphtha for the removal of impurities by reaction with hydrogen Separation of Whole naphtha into its fractions (Chiyoda, 1985)

Process integration using Pinch Technology offers a novel approach to generate targets for minimum energy consumption before heat recovery network design. The Pinch design can reveal opportunities to modify the core process to improve heat integration. Pinch Analysis is used to identify energy cost and heat exchanger network (HEN) capital cost targets for a process and recognizing the pinch point. The procedure first predicts, ahead of design, the minimum requirements of external energy, network area, and the number of units for a given process at the pinch point. Next a heat exchanger network design that satisfies these targets is synthesized. Finally, the network is optimized by comparing energy cost and the capital cost of the network so that the total annual cost is minimized. Thus, the prime objective of energy integration is to achieve financial savings by better process heat integration (maximizing process-to-process heat recovery and reducing the external utility loads) (Akande, 2007).

2. Pinch Technology

Most processes need to consume energy at one temperature level and reject it at another level. This is achieved using utilities. Energy is provided to a process using such utilities as steam, hot water, flue gas etc. it is rejected to cooling water, air, refrigerant or in heat recovery steam rising. Heat recovery is used to reduce the utility cost of a process. Evaluation of heat recovery involves a balancing of utility against the capital cost of the heat recovery system. The utility cost not only depends upon the amount of energy consumed and rejected but on the utility actually used. Cooling water is cheaper than refrigerant, low pressure steam is cheaper than high pressure steam (Adefila, 2002).

2.1 Principle of pinch technology

Pinch analysis is a rigorous, structured approach that can be used on a wide range of process and site utility related problems. Such as lowering operating costs, de-bottlenecking processes, raising efficiency and reducing capital investment (Linhoff and Hindmarch, 1983). Looking at its application in terms of energy improvement, we start by considering the heat and material balance, of the process in question. The majority of processes consist of streams that need to be heated up and streams that need to be cooled down. For each stream that requires heating or cooling, there are two basic choices. The heat can either be exchanged between two process streams or it can be exchanged between the process and the utility system. A fundamental strength of pinch analysis is that it determines the most appropriate set of heat exchange matches. In doing so, it reduces the cost of hot and cold utilities by minimizing the cascade of heat from the expensive, high temperature region down to ambient and also from ambient down to expensive, sub ambient temperatures (Linhoff and Parker, 1984).

The power of pinch technology lies in two factors (Linhoff and Vredeveld, 1984):

1. Its ability to quickly evaluate the economics of heat recovery for a given process.
2. The guidance it provides regarding how a process can be modified in order to reduce associated utility needs and costs.

It is these two factors that attract the use of pinch technology to analyze and design the heat exchanger network of any system. Here, only the source and target temperature, heat capacity and mass flow rates of the process streams are required to carry out the analysis and it works on certain established principles or concepts such as Problem Table Calculation, Composite Curve, Grand Composite Curve, Super Target, Grid representation etc (Linhoff and Vredeveld, 1984).

2.2 Targets

Targets are theoretical values that represent the ideal or perfect situation. They are very important as an analysis tool as it provides a comparison for how close the current design is to the optimal design (Linnhoff and Parker, 1984).

2.3 Energy Targets

Energy targets are the minimum amount of utilities needed to satisfy the process stream requirements (Linnhoff and Parker, 1984). In pinch software, the energy target values are calculated depending on the Utility Load Allocation Method and pinch temperature. The hot and cold utility energy targets are both displayed (Linnhoff and Parker, 1984).

2.4 Pinch Temperature

The pinch temperature is used in designing the optimal HEN by identifying the following (Linnhoff and Parker, 1984):

- Impossible heat transfer between streams when the temperature difference between streams is equal or less than the pinch temperature.
- Unnecessary use of cold utility, when a cold utility is used to cool hot streams in the region above the pinch.
- Unnecessary use of hot utility, when a hot utility is used to heat cold streams in the region below the pinch.

2.5 Plots

Plots provide a visual analysis of key variables and trends for the heat integration in a given stream data. pinch software has a wide variety of plots available.

Composite Curve

A Composite Curve is a graphical combination (or composite) of all hot or cold process streams in a heat exchange network (Linnhoff and Vredeveld, 1984). The Composite Curve plot displays both the hot composite curve and cold composite curve on the same plot. The closest temperature difference between the hot and cold composite curves is known as the minimum approach temperature, ΔT_{min}. The composite curves are moved horizontally such that the minimum approach temperature on the plot equals the minimum approach temperature you specified (Linnhoff and Vredeveld, 1984).

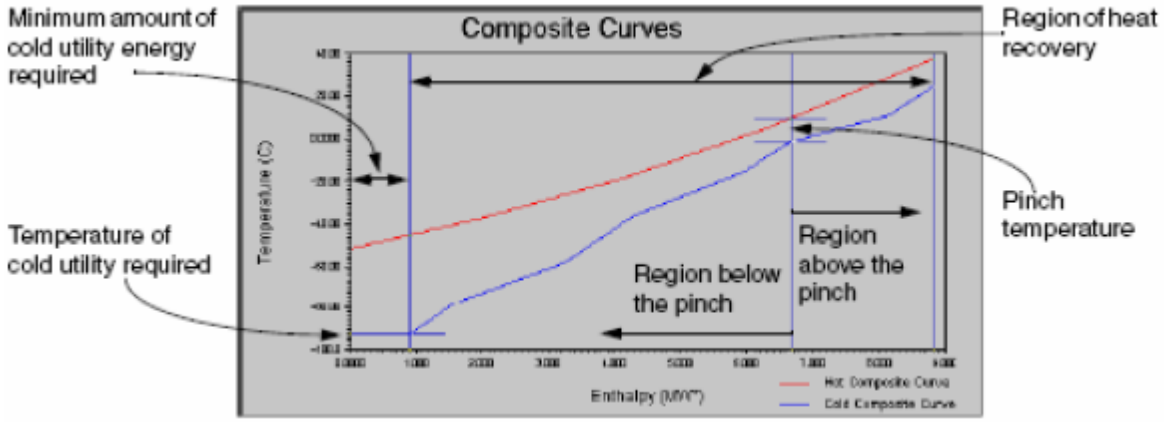

Figure 1. Composite Curve

Shifted Composite Curve

The Shifted Composite Curve is constructed the same way as the Composite Curve (Linnhoff, 1983). However, the Hot Composite Curve (HCC) is shifted down by $\Delta T_{min/2}$ and the Cold Composite Curve (CCC) is shifted up by $\Delta T_{min/2}$. The following equations show how the shifted temperatures are calculated:

$$Shifted\ Hot\ Stream\ Temperature = Unshifted\ Hot\ Stream\ Temperature - \frac{\Delta T_{min}}{2} \quad (1)$$

$$Shifted\ Cold\ Stream\ Temperature = Unshifted\ Cold\ Stream\ Temperature + \frac{\Delta T_{min}}{2} \quad (2)$$

The result is that the hot and cold composite curves meet at the pinch location. The Figure 2 displays the unshifted and shifted composite curves. It can be observed that the two curves are shifted vertically.

Grand Composite Curve

The Grand Composite Curve is a plot of shifted temperatures versus the cascaded heat between each temperature interval (Linnhoff and Hindmarch, 1983). It shows the heat available in various temperature intervals and the net heat flow in the process (which is zero at the pinch). A grand composite curve sample is displayed in the figure below (Linnhoff and Hindmarch, 1983).

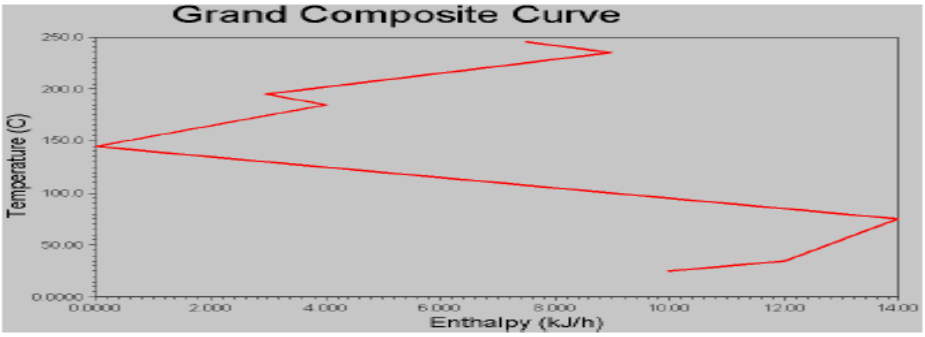

Figure 2. Grand Composite Curve

2.6 Degrees of Freedom

The value of the degrees of freedom indicates whether the HEN design can be controlled or not (Linnhoff and Hindmarch, 1983):

- $N_{DoF} < 0$ indicates that there are not enough manipulated variables in the HEN design and it is not possible to control all target temperatures.
- $N_{DoF} = 0$ indicates that there are enough manipulated variables in the HEN design to control the target streams' temperatures.
- $N_{DoF} > 0$ indicates that there are enough manipulated variables in the HEN design and you can implement more sophisticate control structures. The number of degrees of freedom is calculated using the following equation:

$$N_{DOF} = N_{mv} - N_{ts} \tag{3}$$

2.7 Area Targets

The area targets are the minimum amount of heat transfer area required for the hot and cold streams in a heat exchanger network (HEN) to achieve their specified temperature values. This equation is also known as the Uniform BATH Formula. The basic equation used to calculate the area target is:

$$A = \sum\left(\frac{1}{F_l \times \Delta T_{LM}}\right)_i \sum_j \left[\left(dT_h \times \sum_{jh}\left(\frac{MC_p}{h}\right)_{jh} + (dT_c)_i \sum_{jc}\left(\frac{MC_p}{h}\right)_{jc}\right)\right] \tag{4}$$

2.8 Number of Units Targets

Unit and shell targeting involve the calculation of the minimum number of units and shells in the heat exchanger network. The calculation is based on Euler's Network Theorem (Linnoff, 1983).

$$N_{u,\min} = N_i + N_l - N_i \tag{5}$$

Equation (5) is the minimum number of units in the heat exchanger network, not considering the existence of the pinch. The primary reason for calculating subsets is to simplify networks with a large number of streams. The minimum overall unit target can be expressed as:

$$N_{u,\min} = N_s - 1 \tag{6}$$

Equation (6) is the minimum number of units in the heat exchanger network, not considering the existence of the pinch. In order to consider maximum energy recovery in the calculation of the

minimum number of units in the heat exchanger network, the existence of the pinch must be considered (Linhoff, 1983).

The minimum number of units considering the pinch is calculated as follows in Equation 7:

$$N_{u,\min} = (N_A - 1) + (N_B - 1) \quad (7)$$

2.9 Cost Targets

The total annual cost of a heat exchanger network (HEN) is comprised of two parts: the capital cost and the operating cost.

- The operating cost network is the cost required to operate the process ($/yr).
- The capital cost of the network is a single investment required to build the heat exchanger network ($).

The target capital cost depends largely on how the area targets were calculated and what heat exchanger configurations are used in the HEN design (Linhoff, 1983).

3. Methodology

This chapter presents all the steps involved in the analysis, designing and optimization of Heat Exchangers Network of Naphtha Hydrotreating Unit (NHU) of Kaduna Refining and Petrochemical Company. The procedures involved data extraction, process simulation and pinch analysis which are shown under Figure 3. The procedure involved analyzing of the existing Heat Exchangers Network of the unit in order to extract all the necessary information required for the analysis. As mentioned earlier, the use of pinch technology in the energy conservation area remains the focus of this work.

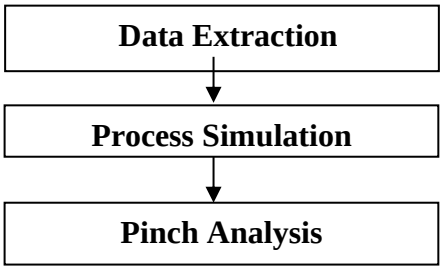

Figure 3. Steps involved in the energy integration of NHU unit of KRPC

3.1 Data Extraction

In the analysis of the existing network, a thorough study of the Process Flow Diagram (PFD) as shown in figure 8, Piping and Instrumentation Diagram (P&ID) and Laboratory analysis of the NHU feed and Products (treated kerosene) of NHU were carried out in order to extract all the necessary and available information require to carry out the process simulation of the NHU plant. The feed and product compositions of the laboratory analysis were used in carrying out the process simulation. The stream temperatures, mass flow rates, pressures were also extracted from PFD and P&ID for carrying out the pinch analysis as shown in Table 1.

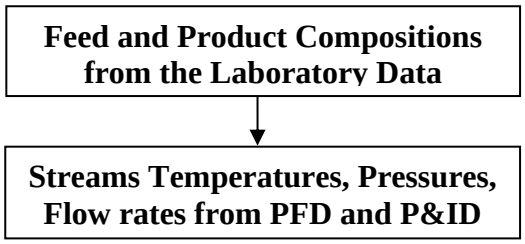

Figure 4. Data Extraction Steps

3.2 Process Simulation Procedure

Hysys Process Simulator was used for the process simulation of the plant streams. The source and target temperatures of all the streams, mass flow rates, feed and product compositions of the feed and product of the plant were used for obtaining the enthalpies of the streams. The stream enthalpies of the process and utility heat exchangers are shown in Table 2.

3.3 Simulation Procedure

Aspen Energy Analyzer procedure for carrying out pinch analysis is shown in Figure 6.

4. Results and Discussion

4.1 Data extraction

Heat loads and temperatures for all the streams in the process are required for the heat integration carried out in this project. The Target and supply temperatures for the streams involved were identified as shown in Table 2. A furnace provides utility heating in the NHU Unit. The furnace design which was represented for fired heaters for the Pinch analysis as a heat sources as a single temperature that is hot enough to satisfy any anticipated heat load in the NHU Unit. The air-cooling and water-cooling likewise can each be represented as heat sinks at a single temperature

4.2 Minimum Temperature Approach

In order to generate targets for minimum energy targets the ΔT_{min} value was set for the problem. ΔT_{min}, or minimum temperature approach, is the smallest temperature difference that was allowed between hot and cold streams in the heat exchanger where counter-current flow was assumed. This parameter reflects the trade-off between capital investment (which increases as the ΔT_{min} value gets smaller) and energy cost (which goes down as the ΔT_{min} value gets smaller). For the purpose of this project, typical ranges of ΔT_{min} values that have been found to represent the trade-off for each class of process have been used. Table 5 shows typical numbers that are appropriate for many refinery units such as NHU Units, cokers, crude units, hydrotreaters and reformers.

In this study a ΔT_{min} value of 10°C was used, which is fairly aggressive for NHUs. This is applied to all process-to-process heat exchanger matches. Rather different trade-offs apply for heat transfer between process streams and utilities, separate ΔT_{min} values for each utility was defined. Table 5 show that a minimum temperature approach (ΔTmin) required for the NHU plant is 20 K. This is the closest approach temperature that is allowable between two streams exchanging heat. Typically, in a petrochemical plant such as NHU plant, a value of 10 to 20 K is reasonable (Linhoff, 1983). However, the optimum value of 20 K of this parameter is significantly affected by the

relative costs of energy and heat exchange area, and this is the primary parameter that was optimized in the *pinch* design program. Table 6 shows the optimum value of 20 K obtained as minimum temperature obtained for the pinch analysis of NHU plant.

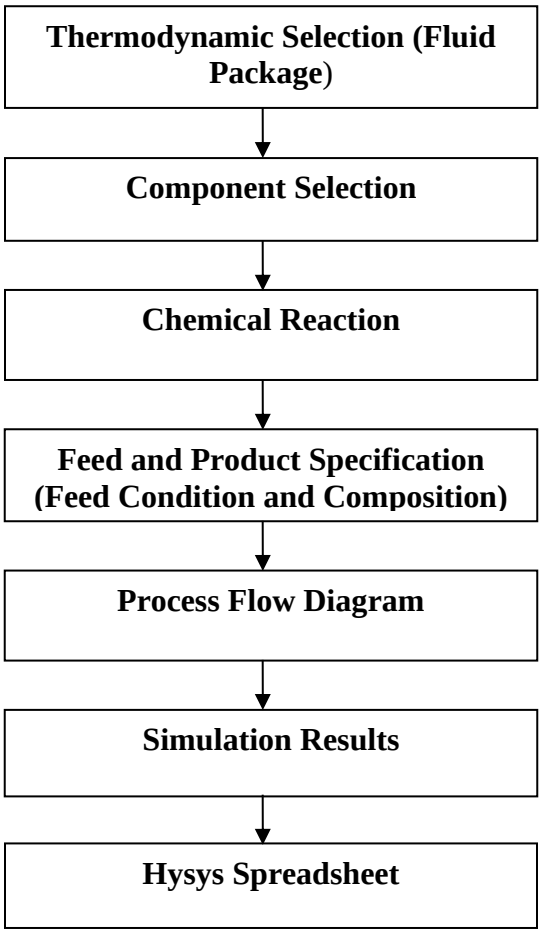

Figure 5. Process Simulation Steps using HYSYS

The minimum approach temperature obtained affected both the capital costs and the operating costs. A low value minimum approach temperature of 20 K means that hot streams approached the temperature of the cold streams more closely. The cold stream thus absorbs more heat from the hot stream. This reduces the utility heating required for the cold stream and also the utility cooling required for the hot stream, as the hot stream exits at a lower temperature after heat exchange with the cold stream. This also reduces the operating costs by lowering the utility costs, but it also increases the capital costs, since the lower approach temperature between the hot and cold streams reduces the Log Mean Temperature Difference (LMTD) in the heat exchanger. The lowered driving force and higher duty of individual heat exchangers resulted in larger heat exchanger areas being required, which increases capital costs. Similarly, a large value of the minimum approach temperature resulted in lower capital costs and higher utility (operating) costs.

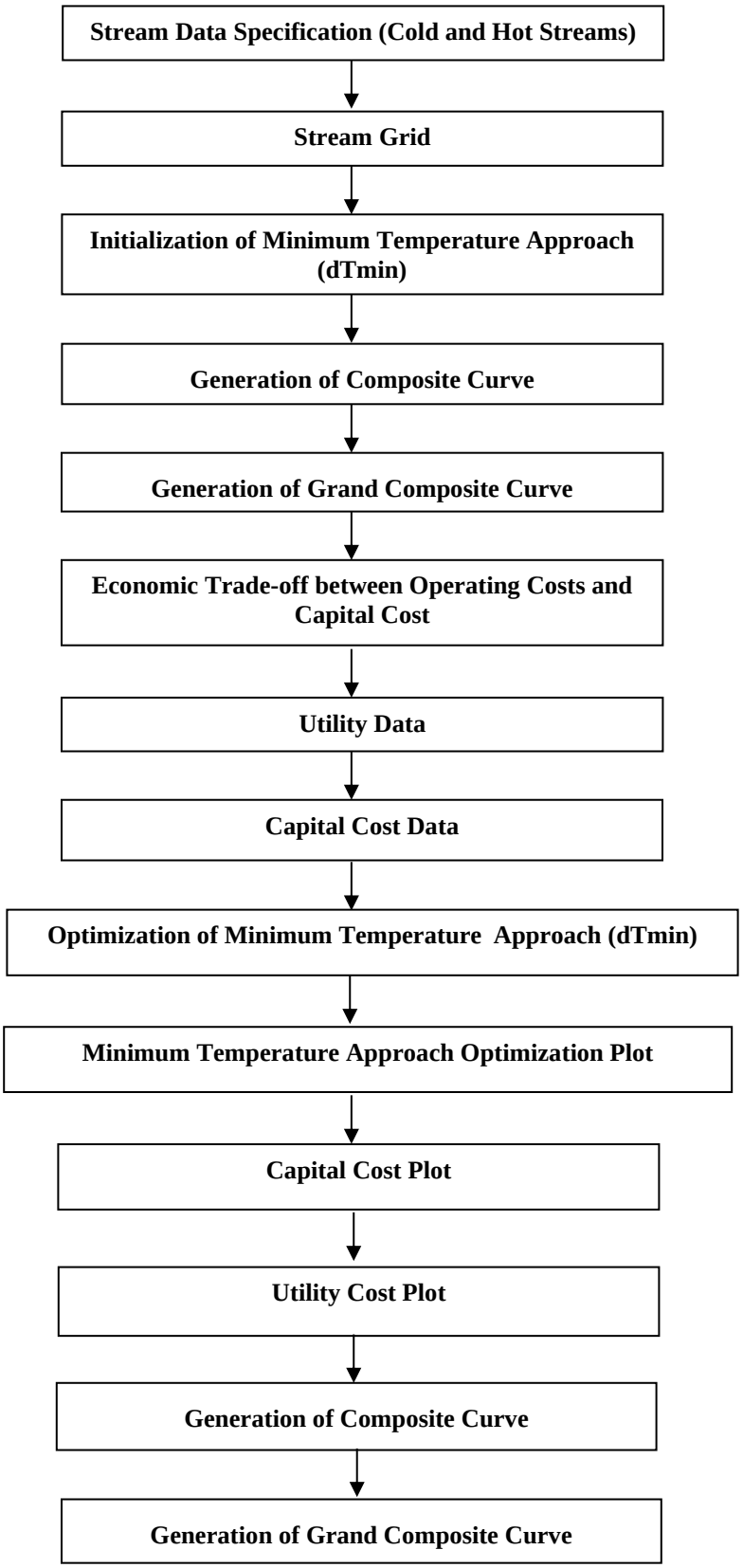

Figure 6. Pinch Analysis Simulation Procedure using Aspen Energy Analyzer

Table 1. Energy Target Values

S/N	Variables	Values
1	Temperature	40 ^{o}C
2	Pressure	33.3 kg/cm^2
3	Mass Flow	1.181 x10^5 kg/hr

Table 2. Data Extracted from Process Flow Diagram

Stream Name	Supply Temperature (°C)	Target Temperature (°C)	Heat Duty (kcal/h)
NHU Reactor Feed	39	293	24160000.000
Effluent Exchanger	370	125	24160000.000
NHU Reactor Effluent Trim Cooler	48	40	520000
NHU Reactor Charge Heater	293	370	6380000
NHU LP Separator Charge Cooler	46	40	350000
NHU Stripper Feed	40	133	6410000.000
Bottom Heat Exchanger	237	133	6410000.000
NHU Stripper OH Condenser	77	48	4390000
NHU Stripper OH Trim Condenser	48	40	560000
NHU Stripper Reboiler Heater	200	237	14700000
NHU Splitter Reboiler	114	137	14700000
NHU Splitter Reboiler	221	190	14700000
NHU Splitter OH Condenser	72	55	5090000
NHU Heavy Naphtha Cooler	137	48	2100000
NHU Heavy Naphtha Trim Cooler	48	40	170000
NHU Light Naphtha Cooler	55	35	230000

Table 3. Hot Minimum Utility Requirement for Traditional Energy Approach and Pinch Analysis of NHU of Kaduna Refining and Petrochemicals Company

Hot Utility (kW) Traditional Energy Approach	Hot Utility (kW) Pinch Analysis	Energy Saving (%)
24,516.0	18,246.1	30.1

Table 4. Cold Minimum Utility Requirement for Traditional Energy Approach and Pinch Analysis of NHU of Kaduna Refining and Petrochemicals Company

Cold Utility (kW) Traditional Energy Approach	Cold Utility (kW) Pinch Analysis	Energy Saving (%)
22,492.4	15,408.4	35.6

Table 5. Experience and Selected ΔTmin Values

Type of heat transfer	Experience ΔTmin values (°C)	Selected ΔTmin values (°C)
Process streams against process streams	30 -40.	35
process streams against steam	10 -20.	15
Process streams against cooling water	10 -20.	10
Process streams against cooling air	15 -25	15

Table 6. Estimated Traditional Hot Utility Energy Requirement of NHU

Stream	Description	H (kW)
1	NHU Reactor Charge Heater	7419.94
2	NHU Stripper Reboiler Heater	17096.1
	Total Heating Duty	**24516**

Table 7. Estimated Traditional Cold Utility Energy Requirement of NHU

Stream	Description	H (kW)
1	NHU Rxtor Effluent Cooler	6896.59
2	NHU Rxtor Eff Trim Cooler	604.76
3	NHU LP Sep Charge Cooler	407.05
4	NHU Stripper OH Condenser	5105.57
5	NHU Stripper OH Trim Condenser	651.28
6	NHU Splitter OH Condenser	5919.67
7	NHU Light Naphtha Cooler	267.49
8	NHU Heavy Naphtha Cooler	2442.3
9	NHU Heavy Naphtha Trim Cooler	197.71
	Total Cooling Duty	**22492.4**

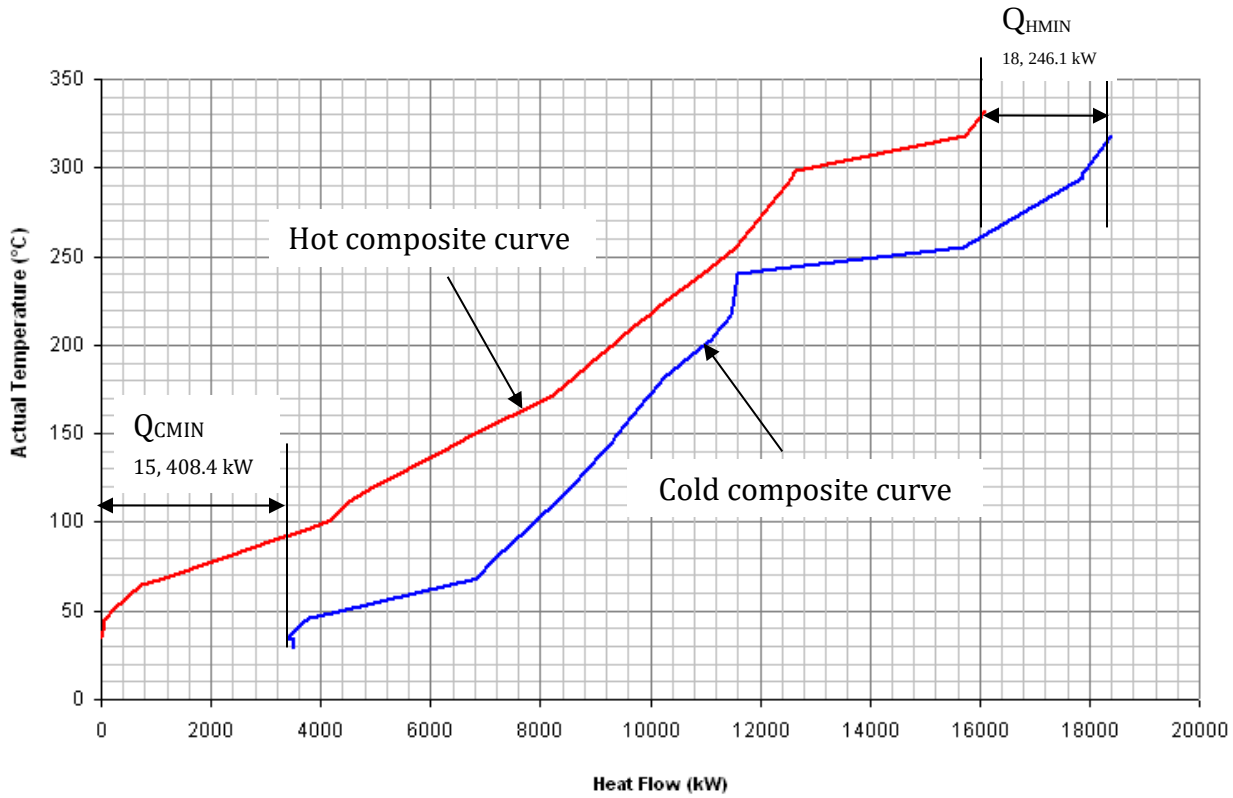

Figure 7. Shifted Composite Curve of NHU

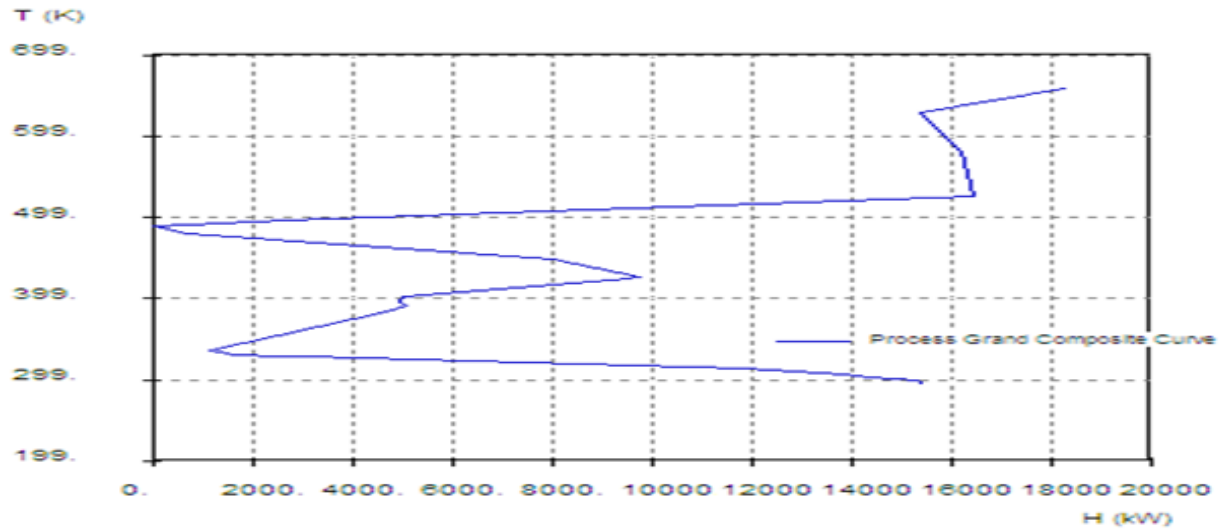

Figure 8: Grand Composite Curve of NHU

Table 6. Optimization Results

Optimum Minimum temperature approach (Optimum ΔT_{min}) (K)	Net Present Cost at ΔT_{min} (million dollars)
10	3.29

4.3 Energy Target Results

Figure 7 is the shifted composite curve (temperature-enthalpy) profile of heat availability in the process (the "hot composite curve") and heat demands in the process (the "cold composite curve") together in a graphical representation. Figure 7, Table 3 and 4 shows that the heat available in the process is 18,246.1 kW while the heat demand in the process is 15,408.4 kW. This shows that more heat is to be removed from the process than heat to be supplied to the system. Figure 8 (Grand composite Curve) shows that the Pinch temperature of the process is 215 ^{o}C (488 K).

The results show that the utility heating of the plant is far less than the utility cooling of the plant. Therefore, any utility heating supplied to the process below the pinch temperature cannot be absorbed and will be rejected by the process to the cooling utility, increasing the amount of cooling utility required, hence waste of energy (cold utilities) by the NHU reactor.

4.4 Energy Saving between the Traditional Energy Approach and Pinch Technology for NHU Main Fractionator

The cold utility requirements of traditional energy approach and pinch analysis obtained in Table 4 are 22,492.4 kW and 15,408.4 kW respectively. The hot utility requirements of traditional energy approach and pinch analysis shown in Table 3 are 24,516.0 kW and 15,408.4 kW respectively. This shows that pinch analysis energy integration saves more energy and utilities cost than the traditional energy approach. This statement is in agreement with literature (Smith, 2005) which states that pinch analysis as an energy integration technique saves more energy than the traditional energy technique.

5. Conclusion

The following conclusions may be drawn from the result of the analysis.

1. Minimum approach temperature 10 ^{o}C was obtained as optimum to determine the energy target.
2. The pinch point was found to be 215 ^{o}C.
3. The utilities targets for the minimum approach temperature were found to be 18,246.1 kW and 15,408.4 kW for hot and cold utilities respectively.
4. Pinch analysis as an energy integration technique saves more energy and utilities cost than the traditional energy technique

Nomenclatures

NHU	Naphtha Hydrotreating
ΔT_{min}	Minimum Temperature Approach
HEN	Heat Exchanger Network
N_{DoF}	Number of Degree of Freedom
N_{ts}	the number of target streams
A	the target area
F_i	the correction factor accounting for non- counter current flow
ΔT_{LM}	The logarithmic mean temperature difference at each interval
i	denotes the i-th enthalpy internal
j	denotes the j-th stream
dT_h	The temperature change for the hot stream at each enthalpy interval
M	The mass flow rate of the stream
C_p	The specific heat capacity of the stream
h	The heat transfer of the stream
dT_c	The temperature change for the cold stream at each enthalpy interval
$N_{u,min}$	The unit target
N_s	The number of process and utility streams
N_{mv}	The number of manipulated variables
N_l	The number of heat exchanger loops
N_i	The number of independent systems
N_s	The number of process and utility streams
N_A	The number of process and utility stream above the pinch
N_B	The number of process and utility streams below the pinch
PFD	Process Flow Diagram

Acknowledgement

The authors wish to acknowledge the funds provided for this research and publication by TETFund Centre of Excellence for Renewable Energy, Kaduna Polytechnic, Kaduna, Nigeria. The funds were provided by the Tertiary Education Trust Fund (TETFUND), Nigeria, under the TETFUND Special Intervention for Establishment of Centres of Excellence (TETF/ES/DS&D/KADPOLY/COE /2021/VOL11).

References

Adefila S. S. (2002). Heat Recovery System: theory and practice, *NSChE International Workshop on Industrial Energy Management*

Akande H. F. (2007). *Energy Integration of Thermal Hydro-dealkylation Plant*, M. Eng. Thesis, FUT Minna, Minna, Nigeria. pp.2.

Chiyoda (1985). *Naphtha Hydrotreating of Toluene Manual*, Chiyoda Engineering Design Comapany, Japan. Pp. 46.

Dayo F. B. (1994). Auditing Energy Use in an Operating Plant, *Industrial Energy Management. pp.34.*

Suleman N. (2011). *Energy Integration of Naphtha Hydrotreating Plant using Heat Integration*, M. Eng. Thesis, FUT Minna, Minna, Nigeria. pp.3.

Linnhoff B. (1983). New Concept of Thermodynamics for better Chemical Process Design, Royal Society Esso Energy Award Lecture, *Chemical Research and Development*. 61: 207-223.

Linnhoff B. and Hindmarch E. (1983). *Pinch Design Method of Heat Exchanger Network, Chemical Engineering Science* 38: (5) pp. 745-763

Linnhoff B. and Parker S. (1984). *Heat Exchanger Network with Process Modification, International Chemical Engineering Annual Research Meeting,* Bath UK

Linnhoff B. and Vredeveld D. R. (1984). *Pinch Technology has come of Age*. *Chemical Engineering Progress* pp 33-40

Nigerian Journal of Renewable Energy Research
Volume 1, Number 1, pp 15-25, 2023

eISSN 1597-8907: pISSN 1597-8877

ASSESSMENT OF KALAMBAINA LIMESTONE FOR QUICKLIME PRODUCTION

[1,2,*]Akande H. F, [3]Nwafulugo F.U., [4]Saka A. S., [4]Kovo A. S., [4]Azeez O. S., [1,2]Mumah S. N. and [4]Onifade, K. R.

[1]TETFund Centre for Renewable Energy, Kaduna Polytechnic, Kaduna, Nigeria
[2]Department of Chemical Engineering, Kaduna Polytechnic, Kaduna, Nigeria
[3]Department of Chemical Engineering, Federal Polytechnic, Oko, Anambra State, Nigeria
[4]Department of Chemical Engineering, Federal University of Technology, Minna, Nigeria

[*]Corresponding author: hassan.akande@kadunapolytechnic.edu.ng
https://doi.org/10.5281/zenodo.11501300
https://www.njrer.org/download/vol_1_No_1_pap_2.pdf

ARTICLE INFORMATION

Article history:
Received 21 May, 2023
Revised 22 Jul, 2023
Accepted 08 Oct, 2023
Available online 30 Dec, 2023

Keywords:
Kalambaina
limestone
characterization, quicklime
ICP-OES, XRD, SEM, ASAP BET

Abstract

Quicklime of high quality is an important mineral for many industries (such as building, agriculture, water treatment, sugar refining, tannery, paper, glass, etc) all over the world. In Nigeria most of the demand for this chemical product is met through importation of quicklime. The Nigerian Kalambaina limestone was subjected to physical, chemical, mineralogical and thermal characterization to determine its suitability for direct use in quicklime production. The physical, chemical, mineralogical and thermal characterization were carried out using Accelerated Surface Area Porosimeter Braunner-Emmet-Teller (ASAP-BET) and Scanning Electron Microscope (SEM), Inductively Coupled Plasma Optical Emission Spectrometer (ICP-OES) and X-Ray Diffractometer (XRD) respectively. The results of the chemical analysis showed that the limestone contains 99.04, 0.894, 0.0414, 0.0085 and 0.006 percents of calcium, magnesium, silicon, iron and aluminum respectively. The XRD result shows that Kalambaina limestone is composed of calcite mineral with small amount of silica. The result of SEM shows that Kalambaina limestone has fine grain of crystals with homogeneous texture. Thermal characterization using TGA shows that weight loss due to release of carbon dioxide from Kalambaina limestone sample is 44.6% and optimum calcination temperature for obtaining quicklime of highest yield in nitrogen atmosphere is 800^{o}C. Also, the physical characterization using ASAP BET method shows that Kalambaina limestone has a surface area of 2.7764 m^2/g. The results of physical, chemical, mineralogical and thermal characterization show that Kalambaina limestone is highly suitable for the production of quicklime making beneficiation treatment little or unnecessary.

1.0 Introduction

Limestone is a naturally occurring mineral that consists principally of calcium carbonate. It generally contains some magnesium carbonate as a secondary component. Limestone is found in many forms and is classified in terms of its origin, chemical composition, structure, and geological formation (Oates, 1998). Thus, limestone may be pure calcite, a mixture of calcite and dolomite or pure dolomite (Benton, 1973).

Large limestone and dolomite occurrences have been reported by Bell (1963), Ola (1977), Gwosdz *et al.*, (1996), RMRDC (2010) and Akande (2015). They are widespread in the sedimentary basin of Nigeria. Nigeria Ministry of Mines and Steel Development reported that Nigeria has an estimated reserve of about 3 trillion tonnes of limestone which are scattered in different states of the country. Those states include Abia, Anambra, Benue, Cross River, Ebonyi, Enugu, Ogun, Sokoto, Gombe, Nassarawa, Edo, Borno, Yobe, Adamawa and Kebbi (RMRDC, 2010).

Kalambaina limestone quarry belongs to the Paleocene marine sediments deposited in the Sokoto Basin during the second phase of sediment deposition when the Tethys Sea moved southwards through the Sahara (Nyong, 1995). The exposed section measured ca.19.5m in thickness. The lower part of the section consists of limestone-shale inter-beds while the upper part is phosphatised shale (Adekeye and Akande, 2002).

Quicklime is a solid material that is produced from thermal decomposition of limestone from which carbon dioxide gas is evolved and upon hydration, forms white powder and releases large amount of heat to form hydrated lime. Hydrated lime is an important industrial mineral because of its physical, chemical and mineralogical properties, as well as its commercial importance and ease of production. Foraminifera (2012) reported that Nigeria has high demand for quicklime based on its wide range of uses. The industries that use quicklime include building, agriculture, water treatment, sugar refining, tannery, paper and glass. The bulk demand for quicklime in Nigeria is for water treatment, soft drink bottling, tannery, breweries and food processing (Foraminifera, 2012).

Quicklime is produced from limestone that varies in properties from one location to another. Dogu (2000) reported that limestone can be obtained from a huge variety of sources and various limestones differ considerably in their chemical composition and physical structure. The chemical reactivity of different limestones shows a large variation due to their differences in crystalline structure and also because of the nature of impurities such as silicon, iron, magnesium, manganese, sodium and potassium present in them (Antonia *et al.*, 2000). There are several references in literature concerning factors that may affect the quality of quicklime. Antonia *et al.*, (2000) reported these factors as characteristics of the limestone, calcination temperature, pressure acquired in kilns, rate of calcination, and fuel quality. The effect of calcination parameters on quicklime produced from various limestone deposits have been reported by the following authors (Khraisha and Dugwell (1989); Rao *et al.*, (1989); Khinast *et al.*, (1996); Dogu and Irfan (2001); Demir *et al.*, (2004); Muaazu *et al.*, (2011); Okonkwo and Adefila (2012) and Rashidi *et al.*, (2012)). Nevertheless, no studies have been reported, to the best of our knowledge, about the suitability of Kalambaina limestone for producing commercial quicklime. Hence, in this study, the characterization of Kalambaina limestone was carried out to determine its suitability for producing commercial quicklime.

2.0 Experimental

2.1 Materials and Procedure
Quicklime was produced from limestone obtained from Kalambaina quarry found in Northern part of Nigeria.

2.2 Analytical methods and techniques
The analytical procedures described below shows the techniques used in characterizing Kalambaina limestone.

2.2.1 Chemical Analysis
ICP-OES was used to determine the metals present in Kalambaina limestone in their elemental form. A mass of 50 g of Kalambaina limestone was dried at temperature of 105^{o}C. 0.5 g subsample of the dried limestone was subsequently digested in 10 ml aqua regia for a period of 1 hr and temperature of 140^{o}C. The digested limestone sample was further heated to temperature of 200^{o}C until the mixture produced a residue. The residue was subsequently dissolved in 2.5 M HNO_3 to form a solution. The solution was filtered and diluted to 50 ml solution. The diluted solution elemental composition was then analyzed using ICP-OES.

2.2.2 XRD Analysis
Kalambaina limestone mineral phases were determined using XRD. The diffractometer was put on and set to a voltage and current of 40kV and 30 mA respectively. The XRD fitted with was also operated at a wavelength of 1.5406. The XRD was scanned at a 2θ range from 20° to 60°. The diffractogram was also scanned at a rate of 3°/min.

2.2.3 Thermal Analysis
Differential thermal and thermogravimetric analyses (simultaneous DTA/TG) were carried out on Kalambaina limestone using Mettler Toledo, TGA/SDTA851 model. 50 mg of the limestone the limestone sample placed in an alumina crucible was weighed. The weighed limestone sample was heated from room temperature to 900°C at a heating rate of 10°C/min and nitrogen flow of 100 mL/min.

2.2.4 SEM Analysis
The texture, shape, and size of the limestone sample was determined using a SEM instrument model, HITACHI, S-3400N. The limestone powder was mounted onto the SEM stubs (layered with sticky carbon tape). 50 mg of the limestone the limestone sample was mounted on SEM stub and placed in a sputter coater (EMITECH, K550X) for five minutes. This is to provide coating with gold so that high reflectivity of the limestone sample during the scanning process. The samples were further heated to temperature of 40°C in an oven before SEM analysis.

2.2.5 Physical Properties Analysis (ASAP-BET-BJH)
Adsorption of nitrogen was performed on the limestone sample to evaluate the specific surface area, total pore volume, and pore size distribution, using a Quantachrome instrument (model Autosorb-1). The physical characterization consisted of three steps, including dehydration, degassing under low vacuum pressure, and nitrogen gas adsorption at 77 K. The isotherm obtained was analyzed using the BET and Barrett-Joyner-Halenda (BJH) methods.

3.0 Results and Discussion

The metals present in Kalambaina limestone sample determined using ICP-OES method is shown in Table 1. The main elements found in it are Ca and Mg, with low levels of Mg and other impurities, such as Fe, Si, K, Na, Al and others. Those impurities either are found in the matrix of the crevices and other strata excavated along with the limestone (Chan *et al.,* 1970). Table 1 shows Kalambaina limestone has Ca content of 99.04%. The 99.04% calcium content of Kalambaina limestone is higher than 98.5% required for limestone used for commercial quicklime production (Oates, 1998). Kalambaina limestone is a higher purity limestone, since it is higher than 98.5% required for higher purity limestone (Cox *et al.,* 1977). The CaO content, i.e., the Ca content (Table 1) less the LOI content (Table 2) for Kalambaina limestone is 54.44%. The 54.44% calcium oxide content of Kalambaina limestone falls within the range of 50% to 65% required for limestone for quicklime production (Plumpton, 1984). The CaO content is also very close to 54.1% determined for limestone to be used for pilot scale iron-making in India. The CaO content of the raw Kalambaina limestone is higher than 43.05% for Indian Salem Madras deposit and is only slightly lower than the flotation concentrate of Salem limestone with 52.9% CaO (Ryemshak *et al.*, 2012). The Kalambaina CaO content is also far higher than 43.44% and 38.68% for low grade raw limestone under consideration for upgrading by Indian Tata Iron and Steel Ltd. and Rhotas Industries, respectively (Ryemshak, 2012).

Table 1. Elemental Chemical Composition of Kalambaina Limestone using ICP-OES

Chemical Compound	Ca	Mg	Si	Fe	Al	Other Oxides
Kalambaina Limestone (% ppm)	99.040	0.8938	0.0414	0.0085	0.006	0.0157
Commercial limestone (% ppm)	98.5	0.5	0.35	0.6	0.2	0.050

The Mg content of 0.474% in the raw Kalambaina limestone is slightly higher than 0.5% standard specified for commercial quicklime production (Oates, 1998). The Mg content which is a function of MgO present in Kalambaina limestone is lower than minimum of 2.48% standard specified for limestone for direct quicklime production (Plumpton, 1984). The MgO content of Kalambaina limestone is lower than 1.0% MgO content for a limestone for pilot scale iron-making in India (Ghandy, 1966). MgO forms the low melting point magnesium silicate with silica during iron-making. These results strongly suggest that the Kalambaina limestone with low Mg content is a high-grade limestone suitable for use in quicklime production as the Mg content which is present as $MgCO_3$ in limestone produces MgO at high calcination temperature and make the quicklime to sinter (Gunasekaran and Anbalagan, 2008). This sintering effect reduces the yield and reactivity of quicklime and this occur because MgO is produced from dolomite at a lower temperature than CaO and so crystallites tend to grow larger and less reactive (Harrison *et al.,* 1998).

The iron content of 0.004% in Kalambaina limestone is lower than 0.6% standard specified for commercial quicklime production (Oates, 1998). The iron oxide content of 0.004% suggest that Kalambaina limestone will produce quicklime of high yield and reactivity as iron present as Fe_2O_3 reacts with produced quicklime at high temperature to form bellite which reduces the yield and reactivity of quicklime.

The 0.006% aluminum content in Kalambaina limestone is lower than 0.6% standard specified for commercial quicklime production (Oates, 1998). Since aluminum present as alumina is a highly refractory oxide, its low content in Kalambaina limestone strongly indicate Kalambaina limestone as a high-grade limestone. Alumina acts as a base or as an acid depending on the conditions imposed. For example, at high temperature, it may form alumina silicates, while in the presence of a strong base like quicklime it may form undesired calcium aluminate that reduces the porosity of quicklime (Ryemshak *et al.*, 2012).

3.1 Thermal analysis

The TG and DTA curves of Kalambaina limestone obtained in nitrogen atmosphere is shown in Figure 1. The trend of the TG curves obtained for Kalambaina limestone sample shown in Figure 1 represents standard TG curves of calcite (Wagner, 2009). It shows that thermal decomposition with the formation of volatile reaction product (CO_2) occurred. Further examination of the TG curves (Figure 1), shows absence of multi-step decomposition which confirms calcite as the predominant mineral phase present in Kalambaina limestone (Wagner, 2009). This result is also in agreement with XRD, ICP and SEM analysis of the limestone samples. The DTA curve of Kalambaina limestone, shown in Figure 1, presents one endothermic peak at temperature above 750 °C. This confirms calcite as the predominant mineral phase present in the limestone. The typical TG curves of Figure 1 show that Kalambaina limestone presented a weight loss of 2.5% below temperature of 300°C. The weight loss detected in the temperature range of 100–300°C can be attributed to the chemically bound water (Gunasekaran and Anbalagan, 2008). This was followed by a weight loss attributed to the decomposition of carbonates. The thermal curves representing the carbonate mineral are characterized by endothermic peaks caused by the evolution of carbon dioxide. DTA curve of calcite shows one endothermic peak (Harrison *et al.*, 1998).

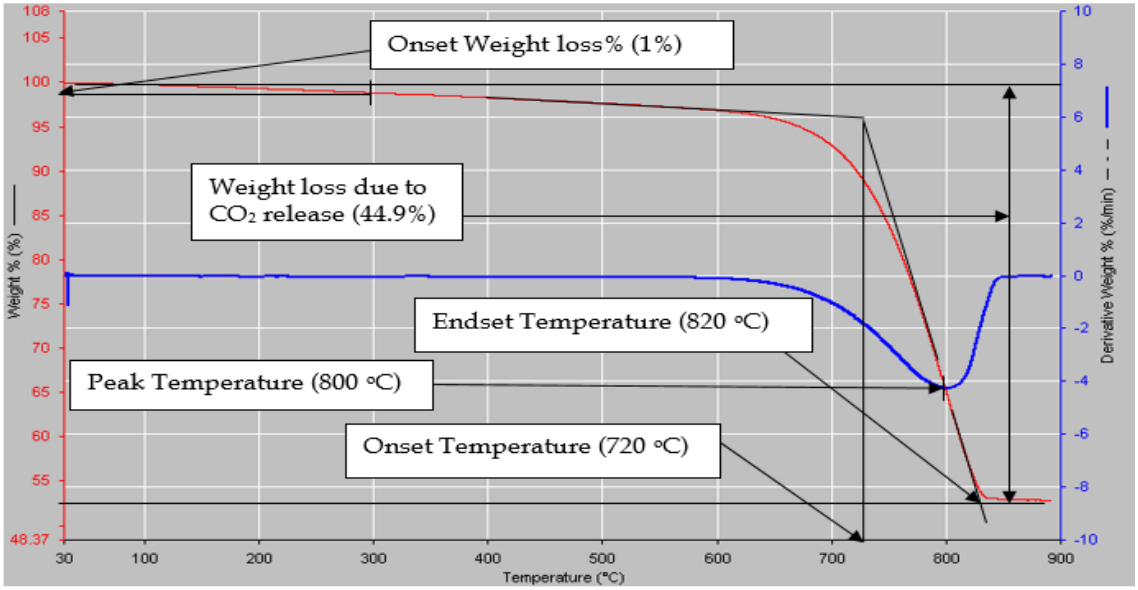

Figure 1. Thermogravimetry and Differential Thermal Analysis of Kalambaina limestone at heating rate of 20°C/minutes from 30°C to 900°C.

The calcination of Kalambaina limestone as shown in Figure 1 and Table 2 begins at 720^{o}C, reaches a peak at 800^{o}C and ends at 820^{o}C. The presence of one peak temperature and absence of peak at lower temperature represents the decomposition of calcite and absence or non-significant yield of dolomite (Anthony *et al.,* (2001); Gunasekaran and Anbalagan, (2008); Chan *et al.,* (1970); Harrison *et al.,* (1998) and Kilic and Mesut (2006)). The result of the TGA shows that optimum temperature for obtaining quicklime of highest yield in nitrogen atmosphere is 800^{o}Cas indicated in the peak temperature obtained in TGA plot of Figure 1.

Table 2. Thermogravimetric Analysis Parameters of Kalambaina Limestone

Limestone Type	Onset Temperature (^{o}C)	Peak Temperature (^{o}C)	Endset Temperature (^{o}C)	Onset Weight (%)	Weight Loss due to CO_2 release (wt%)
Kalambaina	720	800	820	99	44.6

Table 2 and Figure 1 show that weight loss due to release of carbon dioxide from Kalambaina limestone samples is 44.6%. Furthermore, it is observed that the percentage of carbon dioxide of Kalambaina limestone is higher than the theoretical one (44%). This fact might be ascribed to the presence of a high content of dolomite in Kalambaina limestone (Antonia *et al.,* 2000). Gunasekaran and Anbalagan (2008) also reported that the weight loss of calcite is attributed to the decomposition of carbonates. For pure calcite, the expected mass decrease in one step (at 900 ^{o}C) is 44.6% (Gunasekaran and Anbalagan, 2008). A value of LOI higher than 44%, are indications for the presence of metallic impurities in the limestone sample which is higher in Kalambaina (44.6%) limestone sample (Gunasekaran and Anbalagan, 2008). Additionally, the case of presence of low quartz (silica) present in Kalambaina limestone, as observed in XRD result (Figure 3) and ICP result (Table 1) leads to no fluctuation in Kalambaina DTA curve, at temperature of 360 - 680 ^{o}C (Gunasekaran and Anbalagan, 2008).

3.2 SEM analysis

The scanning electron microscopy (SEM) image of Kalambaina limestone is presented in Figure 2. The SEM image also show there may be presence of Oolites cemented by different types of calcites as observed in Kalambaina and Kalambaina limestones. The SEM analysis confirmed the granulometric characteristic of the calcite as microcalcite and syntaxial calcite in the core of the oolites. The SEM images also show that the crystal shapes of Kalambaina limestone are distributed homogeneously throughout the mass and the crystal size are fine grain, compact and homogeneous texture (Akande, 2015).

SEM image of Figure 2 shows that Kalambaina limestone with fine grain and homogeneous texture of crystals will produce quicklime with bigger surface area and high reactivity due to a fine-grained rock is relatively quick-burning as carbon dioxide diffuses rapidly through the large number of internal pores between small limestone crystals (Harrison, 1993). Kalambaina limestone with fine grain and homogeneous texture of crystals when decomposed, the limestone front will reach the core of the chippings faster and a quicklime product containing burnt carbonate as well as high reactive quicklime will be produced (Harrison *et al.,* 1998).

3.3 XRD analysis

The XRD spectrum of Kalambaina limestone is shown in Figure 3. The horizontal axis caption, 2θ in the figures is doubled Bragg angle in XRD analysis while the vertical axis shows the peak intensity. Analyzing the diffractograms (Figure 3) and peak matching with JCPDS (Joint Committee for Powder Diffraction Standards) data, the crystal phase predominant on the samples was calcite. As can be seen from Figure 3, the main peak of the XRD spectrum appears for calcite at $2\theta = 29.5^{o}$and minor peaks appear at $2\theta = 26.6^{o}$, 29.5^{o}, 31.4^{o}, 36.0^{o}, 39.4^{o}, 43.2^{o}, 47.2^{o}, 47.5^{o} and 48.5^{o}, respectively. The mineral phase of limestone identified in Kalambaina limestone is similar to that obtained by the following authors (Navarro *et al.*, 2009; Soares *et al.*, 2008)

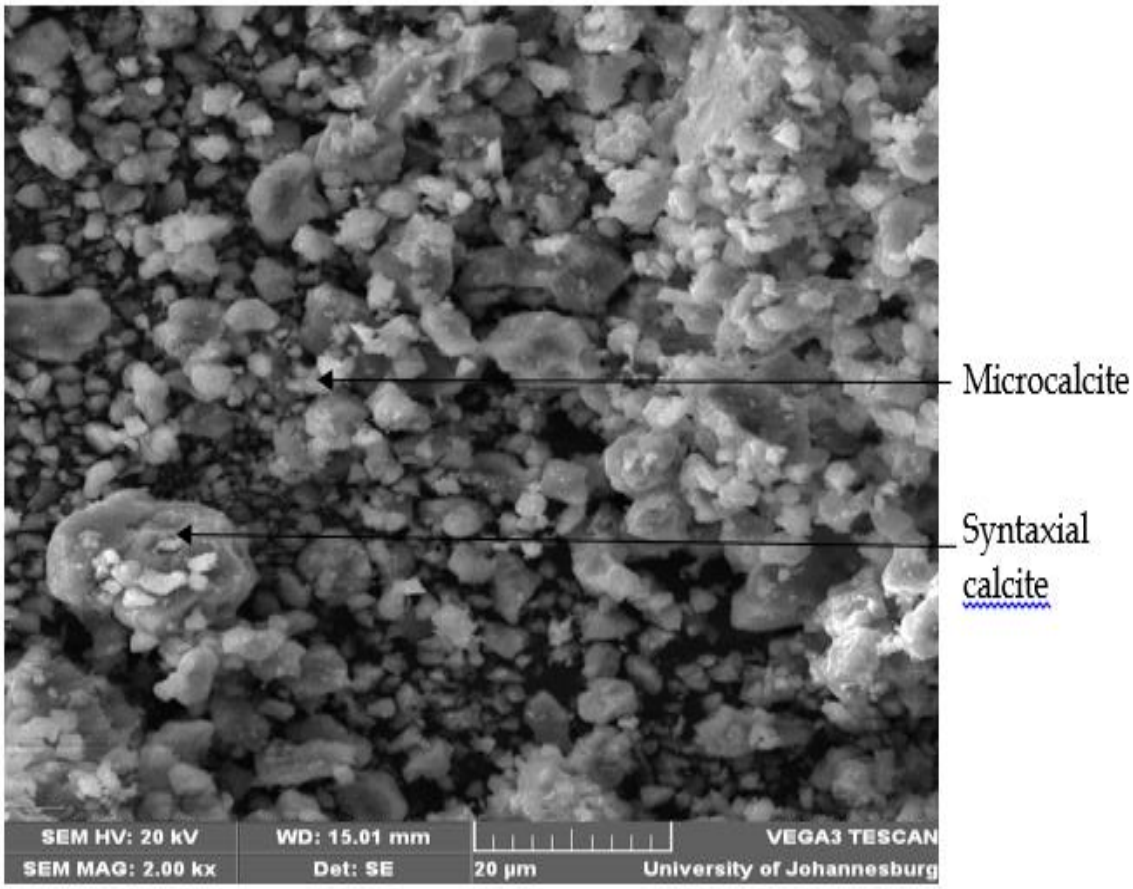

Figure 2. Scanning Electron Microscopic (SEM) Image of Kalambaina Limestone

Table 3 present the crystallinity parameters of limestone samples obtained from XRD analysis. By XRD examination using d-values spacing of $^{o}2\theta$values obtained above, the main constituent of the limestone samples is calcite. The XRD result shown in Figure 3 shows that Kalambaina limestone sample has small yield of quartz. This is corroborated by the silica level determined by ICP-OES (Table 1).

Table 3 shows that Kalambaina limestone has variable grain size of 428.19 *nm* respectively. This shows that Kalambaina has a high coherent scattering domain with perfect arrangement of unit cells at d-spacing (2θ) of 29.5^{o} (Chen *et al.*, 2007). Further examination of the diffractograms of Kalambaina shows that it has a calcitic strain of 0.18%. This shows that Kalambaina limestone is

crystalline. The results of crystallite strain show that Kalambaina will produce quicklime of high reactivity and tendency to decrepitate during calcination is low (Harrison *et al.*, 1998). Decrepitation decreases the porosity of the bed, retarding the flow of heat and reducing efficiency of the calciner (Harrison *et al.*, 1998). Also, Kalambaina fine-grained rock is relatively quick-burning as carbon dioxide diffuses rapidly through the large number of pores between small lime crystals (Harrison *et al.*, 1998).

Table 3. Crystallinity Parameters of Limestone Samples Analyzed Using XRD

LimestoneType	Crystallite Size		Strain (%)	
	Calcite	Quartz	Calcite	Quartz
Kalambaina	428.9	-	0.16	-

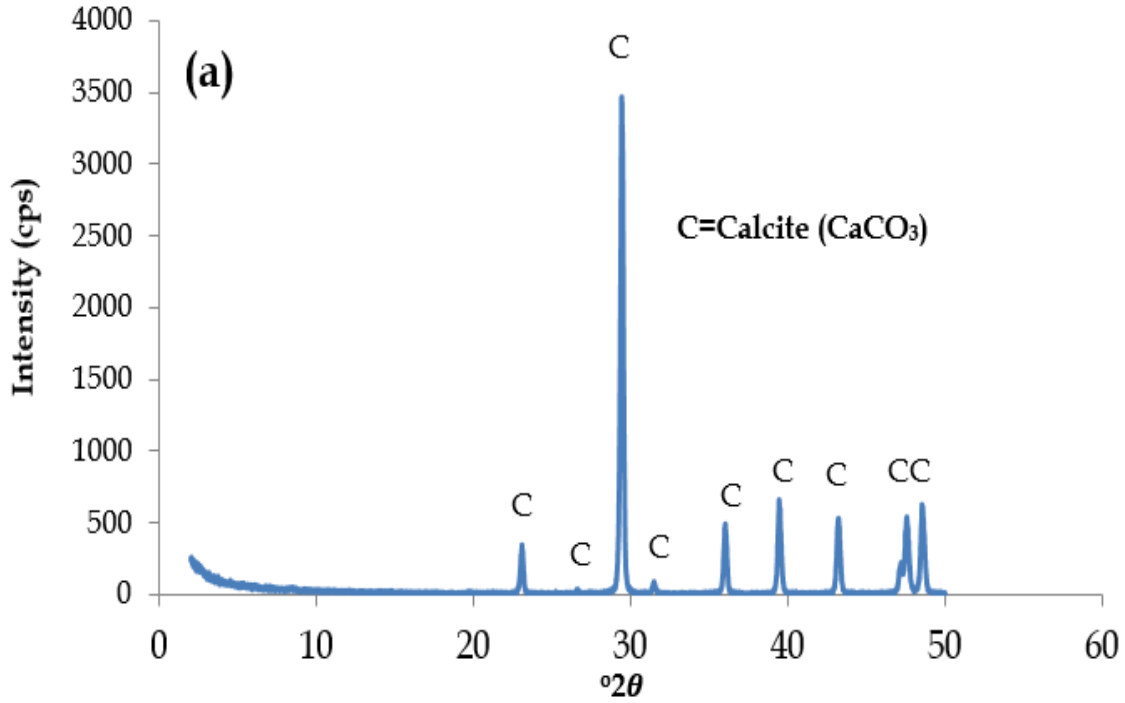

Figure 3, XRD pattern of Kalambaina Limestone

3.4 Surface area analysis using BET

The BET surface area, BJH adsorption cumulative surface area of pores, BJH desorption cumulative surface area of pores and pore volume are 2.7764m^2/g, 3.095m^2/g and 3.424m^2/g and 0.011328 cm^3/g respectively. The BET surface area of 2.7764 m^2/g in the raw Kalambaina limestone is higher than minimum of 1 m^2/g standard specified for limestone (Stanmore and Gilot, 2005). This high surface area greater than minimum shows that Kalambaina will produce more reactive quicklime as the calcination process is under the kinetics reaction control and therefore, the reaction rate is proportional to the BET surface area (Borgwardt, 1985). In addition, the high surface area of the sample will significantly improve the heat distribution within them and thus, accelerates better decomposition process (Mustakimah *et al.*, 2012).

Table 4. Surface Area, BJH Adsorption cumulative surface area of pores, BJH Desorption cumulative surface Area of pores and Pore Volume of Kalambaina limestone

BET Surface Area (m^2/g)	BJH Adsorption Cumulative Surface Area of Pores (m^2/g)	BJH Desorption Cumulative Surface Area of Pores (m^2/g)	Pore Volume (cm^3/g)
2.7764	3.095	3.424	0.011328

4.0 Conclusion

This work has demonstrated the characterization of Kalambaina limestone using analytical techniques in order to determine its suitability for production of commercial quicklime. The following conclusions were obtained:

1. Kalambaina limestone has a calcitic mineral with fine grain homogeneous texture of crystals.
2. Kalambaina limestone is suitable for production of quicklime from limestone.
3. The optimum temperature for producing quicklime of highest yield in nitrogen atmosphere is 800^{o}C.
4. Kalambaina limestone has LOI due to release of carbon dioxide of44.6%.

Acknowledgement

The authors wish to acknowledge the funds provided for this research and publication by TETFund Centre of Excellence for Renewable Energy, Kaduna Polytechnic, Kaduna, Nigeria. The funds were provided by the Tertiary Education Trust Fund (TETFUND), Nigeria, under the TETFUND Special Intervention for Establishment of Centre of Excellence (TETF/ES/DS&D/KADPOLY/COE /2021/VOL11).

References

Adekeye, O. A. and Akande, S. O. (2002). Depositional Environment of the Albian Asu River Group around Yandev, Middle Benue Trough, Nigeria. Journal of Mining and Geology, 38, 2, pp 91 – 101.

Akande, H. F. (2015). Multiple Response Optimization of Quicklime Production from Limestone Using Design of Experiment: PhD Thesis Federal University of Technology Minna, Nigeria.

Antonia, M., Bakolas, A., and Aggelakopoulou, E. (2000). The effects of limestone characteristics and calcination temperature to the reactivity of the quicklime. *Cement and Concrete Research*, 3-5.

Bell, J. P. (1963). A Summary of the Principal Limestone and Marble Deposits of Nigeria. *Geological Survey, 11*, 92.

Borgwardt, R. H. (1985). Calcination Kinetics and Surface Area of Dispersed Limestone Particles. *AIChE Journal*, 31 (1), 103-111.

Benton, W. (1973). Encyclopedia Britannica, 15th Edition, 10: 980-982

Chan, R. K., Murthi, K. S., and Harrison, D. (1970). Thermogravimetric Analysis of Ontario Limestones and dolomites I. Calcination, surface area, and porosity. *Canadian Journal of Chemistry*, 48, 2972-2978.

Chen, C., Zhao, C., Liang, C., and Pang, K. (2007). Calcination and Sintering Characteristics of Limestone under O_2/CO_2 Combustion Atmosphere. *Fuel Processing Technology 88*, 171–178.

Cox, F C, McC Bridge, D and Hull, J H, (1977). Procedures for the assessment of limestone resources. Miner Assess Rep Znst *GeolSci*, No 30.

Demir, F., Donmez, B., Okur, H., and Sevim, F. (2004). Calcination Kinetic of Magnesite from Thermogravimetric Data. *Trans IChemE, Vol 81*, 618-622.

Dogu, G. and Irfan, A. (2000). Calcination Kinetics of High Purity Limestones. *Chemical Engineering Journal*, 1-2.

Foraminifera (2012). Hydrated Lime Production from Limestone in Nigeria How Viable. Retrieved from http://www.foramfera.com/index.php/investment-opportunities-in-nigeria/item/420.

Ghandy, J.J. (1966). "*Annual Report*". National Metallurgical Laboratory: Delhi, India. 1965-1966. 32-33, 152-153.

Gwosdz, W., Lorenz, J., Markwich, R. W., and Wolf, F. (1996). Limestone and Dolomite Resources of Africa. *Geology*, 102:326-327.

Gunasekaran, S., and Anbalagan, G. (2008). Thermal Decomposition of Natural Dolomite. *Indian Academy of Sciences,* 30 (4), 339-344.

Harrison, D J, (1993). Industrial minerals laboratory manual: Limestone. *British Geological Survey Technical Report* WG/92/29.

Harrison, D J, Hudson, J M and Cannell, B, (1998). Appraisal of high purity limestones in England and Wales. A study of resources, needs, uses and demands. Part 1 Resources. British Geological Survey Technical Report WF/90/10.

Khinast, J., Krammer, G. F., Brunner, C., and Staudinger, G. (1996). Decomposition of Limestone; The Influence of $CO_2$and Particle Size on the Reaction Rate. *Chem. Eng. Sci. 51*, 623–634.

Khraisha, Y. H., and Dugwell, D. R. (1989). Thermal Decomposition of Couldon Limestone In A Thermogravimetric Analyser. *Chem. Eng. Res. Des. 67*, 48–51.

Kilic, O., and Mesut, A. (2006). Effects of Limestone Characteristics Properties and Calcination Temperature on Lime Quality. *Asian Journal of Chemistry*, 18(1), 655-666.

Muaazu, K., Abdullahi, M., and Akuso, A. S., (2011). Kinetic Studies of Jakura Limestone using Power Rate Law Model. NIgerian *Journal of Basic and Applied Science Vol. 19, No. 1.*, 116-120.

Mustakimah, M., Nor-Adilla, R, Suzana, Y., Lee, K. T., Umer, R., Razol M. A. (2012). Effects of experimental variables on conversion of cockle shell to calcium oxide using thermal gravimetric analysis. *Australian Journal of Basic and Applied Sciences*, 5(9): 1566-1577.

Navarro, R., Ruiz-Agudo, E., Luque, A., Navarro, A.B., and Ortega-Huertas, M. (2009). Thermal Decomposition of Calcite: mechanism of Formation and Textural Evolution of CaO nanocrystal. *Am Mineral.* 94, 578-593.

Nyong, E. E. (1995). *Geological Excursion Guide book to Calabar Flank and Oban Massif*. In the 31st Annual conference of the Nigerian Mining and Geosciences Society, Calabar, March 12 -16.

Oates, J. H. (1998). *Lime and Limestone: Chemistry and Technology, Production and Uses.* Weinheim: Wiley-VCH.

Okonkwo, P. C., and Adefila, S. S. (2012). The Kinetics of Calcination of High Calcium Limestone. *International Journal of Engineering Science and Technology*, 391-400.

Ola, S. A. (1977). Limestone Deposits and Small Scale Production of Lime in Nigeria. *Engineering Geology, 11*, 128.

Plumpton, A.J. (1984). *Production and Processing of Fine Particles.* Third Edition. Pergamon Press: New York, NY.605.

Rashidi, N. A., Mohamed, M., and Yusup, S. (2012). The Kinetic Model of Calcination and Carbonation of Anadara Granosa. *International Journal of Renewable Energy Research,* 2 (3), 497-503.

Ryemshak, S. A., Adeleke, A. A., andSalami, S. (2012). Characterization of Ubo Limestone for Direct Burnt Lime Production. *The Pacific Journal of Science and Technology, 13*(1), 661-668.

RMDC. (2010). *Multi-Disciplinary Committee Report of the Techno- Economic Survey on Non Metallic Minerals Sector.* Abuja: RMDC.

Soares, B. D., Hori, C. E., Batista, E. A., and Henrique, H. M. (2008). Optimization of the Production of Quicklime by Calcination in Rotary. *Materials Science Forum*, 1-5.

Stanmore, B. R., and Gilot, P. (2005). Review-Calcination and Carbonation of Limestone during Thermal Cycling for CO_2 Sequestration. *Fuel Processing Technology 86*, 1707-1743.

Wagner, M. (2009). *Thermal Analysis in Practice*. Mettler Toledo, Usercom.

Nigerian Journal of Renewable Energy Research
Volume 1, Number 1, pp 26-54, 2023
 eISSN 1597-8907: pISSN 1597-8877

REVIEW OF THE SELECTION AND PERFORMANCE EVALUATION PROCEDURES FOR JAW CRUSHERS

[1,2,*]Mumah, S.N., [3]Kuye, A.O and [4]Okpara, K.O.

[1]TETFund Centre of Excellence for Renewable Energy, Kaduna Polytechnic, Kaduna Nigeria
[2]Department of Chemical Engineering, Kaduna Polytechnic, Kaduna, Nigeria
[3]Department of Chemical Engineering, University of Port Harcourt, P.M.B 5323, Port Harcourt, Nigeria
[4]Department of Chemical Engineering, Federal University of Technology, PMB 1526, Owerri, Nigeria

*Corresponding author: mumahsndoyi@kadunapolytechnic.edu.ng
https://doi.org/10.5281/zenodo.11501462
https://www.njrer.org/download/vol_1_No_1_pap_3.pdf

ARTICLE INFORMATION

Article history:
Received 13 Apr, 2023
Revised 23 Aug, 2023
Accepted 07 Oct, 2023
Available online 30 Dec, 2023

Keywords:
crushing
jaw crushers
Selection
performance
design

Abstract

Crushing and grinding of rocks and other particles has many important applications, including coarse crushing mined ore and quarry rock, fine grinding of coal for power station boilers, and for production of paint, ceramics, cement and other materials. Crushing and grinding of rocks and other particles are governed by the laws of physics involving mass, velocity, kinetic energy, gravity, etc. As crushing and grinding activities evolves in the mining industry, the issue of optimization becomes paramount. Crushing plants operate under very harsh conditions and in most cases involve very abrasive materials. Multiple factors therefore influence the performance of crushers.

This paper examines the procedure for selecting and evaluating the performance of jaw crushers. It is however important to note that it is impractical to reduce the process of selecting and sizing a crusher to a series of formulas. The selection process is largely based on experience and testing with actual field applications and laboratory tests that show how a given material will be reduced by a given crusher type. The paper examines the critical design parameters of jaw crushers. Crushers encounter considerable difficulties concerning external loads acting on their mechanical joints which make it almost impracticable to use theoretical calculations for design and performance evaluation. It is therefore necessary to use experimental studies to verify any theoretical methods used for these purposes. It should be noted however that considering the variety of applications as well as rock materials, minerals and ores, a truly optimal performance of a crushing application must be based on an optimized crusher design as well as a continuously optimized crusher operation.

1.0 Introduction

Jaw crushers are one of the most commonly used crushers in the world. They can easily be distinguished by the presence of two plates. One plate is fixed where the other opens and closes. This process ensures that the materials are trapped and crushed. Three types of jaw crushers are presently widely used. They are the Blake, Dodge, and Universal jaw crushers. The classification is based on the location of the pivot point of the swinging jaw. The Blake crusher is most commonly used of the three and it was designed and patented by Eli Whitney Blake in 1858 (Weiss, 1985). Jaw crushers have found wide use in quarries, mining, ore crushing and metallurgical plants, where the material physical condition varies from dry to slightly wet, not sticky. The single toggle jaw crusher has found wide used because of its higher capacity and much lower cost when compare to other types of jaw crushers (Donovan, 2003). Jaw crushers are very suitable for rocks that has the hardness index of medium-hard to very-hard and so are very common in quarries that requires the primary crushing of blasted rockpile. They can be applied to rocks or ore with edge lengths of more than 2,000 mm (Donovan, 2003).

2.0 Description of the Double Toggle and the Single Toggle Jaw Crusher

A noted characteristic of single toggle jaw crushers is that the swing jaw is suspended on the eccentric drive shaft (Figure 1) and the toggle plate that is placed against the crusher frame supports the swing jaw. The whole arrangement results in a motion that results in a higher capacity than that achieved by the double-toggle jaw crushers (Figure 2). The characteristics of different feeds have influenced the variation in design of the single-toggle jaw crushers by rock hardness.

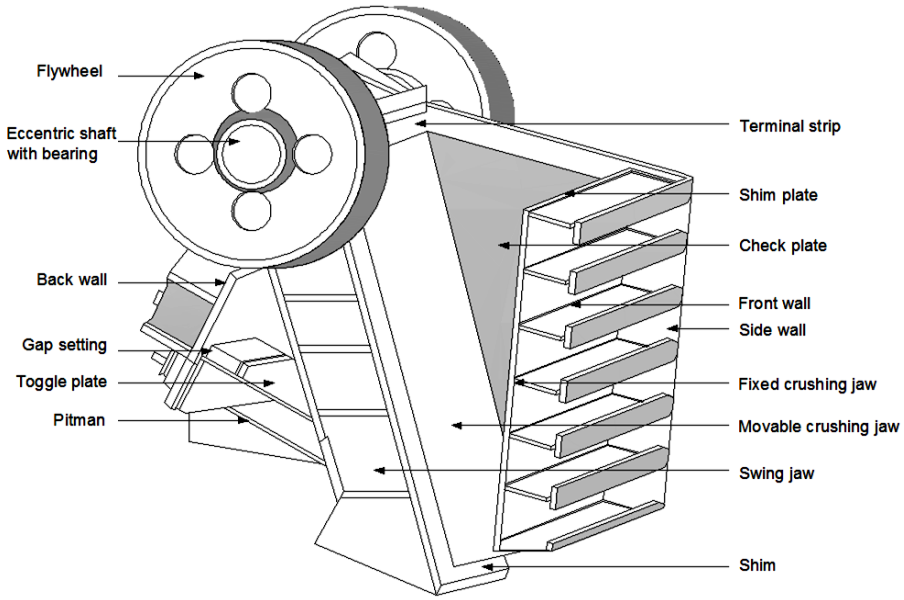

Figure 1. The various parts of a single-toggle jaw crusher *(adapted from www.thyssenkrupp-industrial-solutions.com/backenbrecher_en.pdf)*

Double-toggle jaw crushers are fitted with a system of toggle levers which upward and downward movement is effected by a pitman by means of an eccentric shaft (Figure 3). The resultant effect of the upward and downward movement is the oscillating motion of the swing jaw. The ores or rocks to be crushed are fed to the crusher by allowing them fall by gravity and the necessary pressure to crush the material is achieved when the crushing chamber is narrowed by the movement of the swing jaw. To increase the crushing effect, the crushing jaw lining is toothed. The retraction

of the swing jaw allows the crushed materials to leave the crusher. The crusher is designed in such a way that as crushed materials exits the crusher, new uncrushed materials enter concurrently (Figure 4). The transmission of the required power to the relevant parts of the crusher is effected by the toggle lever system which makes this type of crusher the equipment of choice for the crushing of very hard, toughest and abrasive materials.

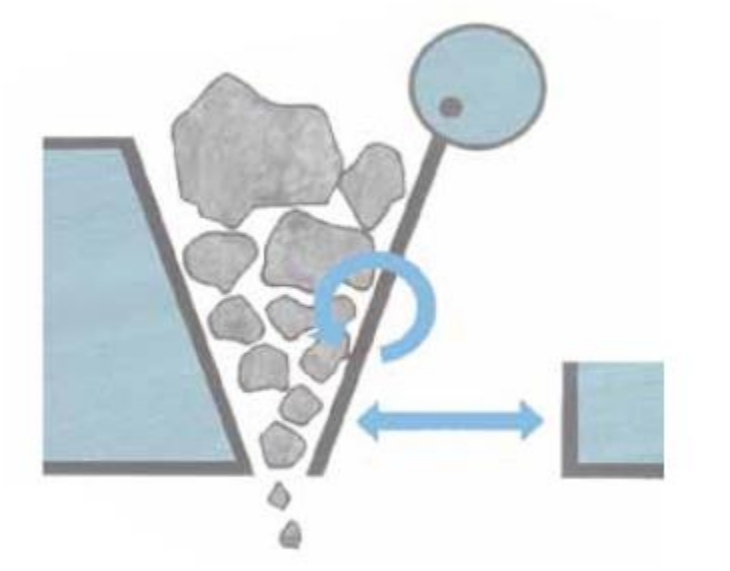

Figure 2. How a single-toggle jaw crusher with the toggle system operates *(www.thyssenkrupp-industrial-solutions.com/backenbrecher_en.pdf)*

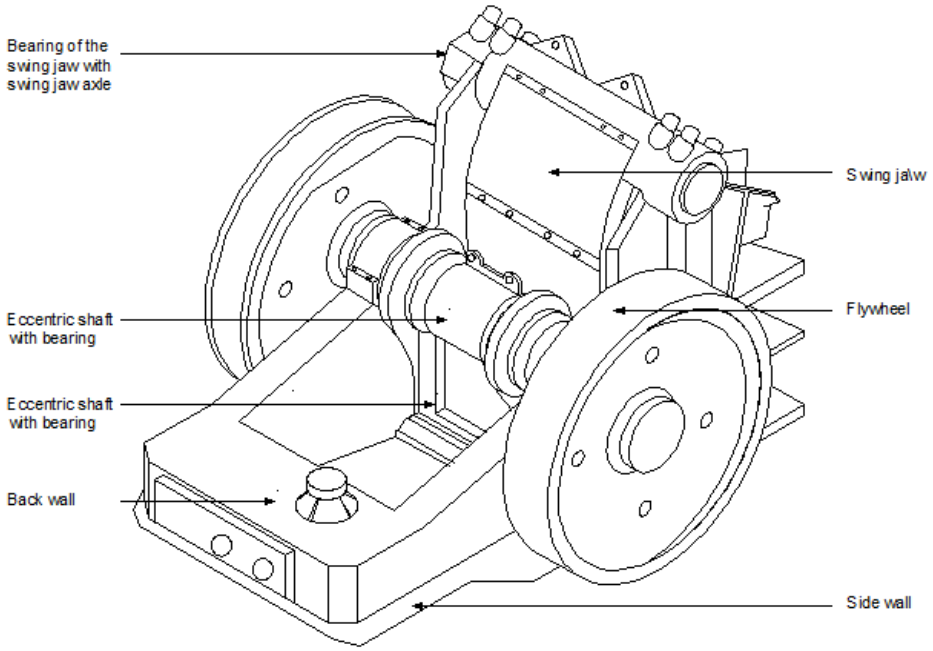

Figure 3: Double-toggle jaw crusher with its main components *(Adapted from www.thyssenkrupp-industrial-solutions.com/backenbrecher_en.pdf)*

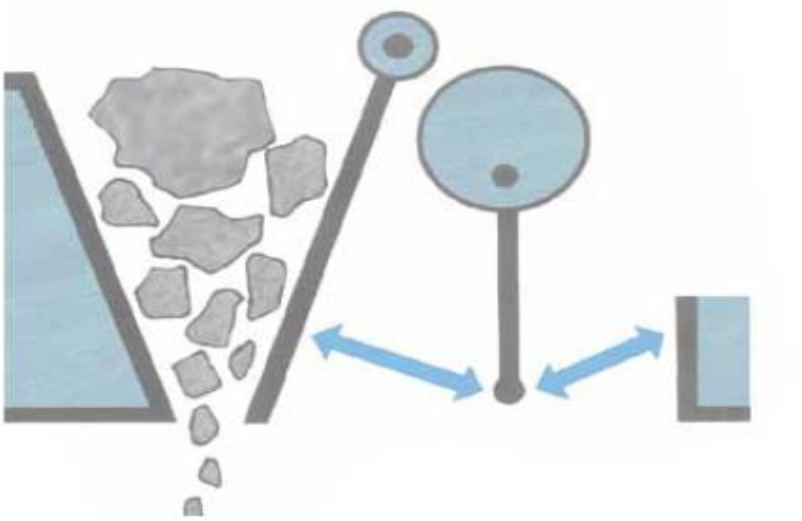

Figure 4. The Operating mechanism of a double-toggle jaw crusher with the toggle-lever system *(www.thyssenkrupp-industrial-solutions.com/backenbrecher_en.pdf)*

Table 1 shows the materials that the various parts of a jaw crusher are made. The selection of the materials is to ensure the jaw crusher last for long time even subject to very hard ore.

Table 1. Material for components of jaw crusher (Garnaik, 2010)

S/No	Component	Material / Function
1.	Body	Made from high quality steel plates and ribbed heavily in welded steel construction
2.	Swing jaw Plate	Manganese steel
3.	Fixed jaw plate	Manganese steel
4.	Pitman	Crushers have a light weight pitman having white-metal lining for bearing surface
5.	Toggle	Double toggles, for even the smallest size crushers give even distribution of load
6.	Flywheel	high grade cast iron
7.	Tension Rod	Pullback rods helps easy movement, reduces pressure on toggles and machine vibration
8.	Hinge plate	Strong hinge pin made from steel are used for crushing without rubbing
9.	Shaft and bearings	Massive rigid eccentric shafts made from steel along with roller bearing ensures smooth running.
10.	Diaphragm	Flexible diaphragm seals opening in oil chamber and protects components from dust

One of the trends in design solutions of crushers ensuring the crushing ratio of about 30 involves the application of the vibratory-impulse action to the material to be crushed. Crushers utilizing these effects are referred to as vibratory crushers. During the vibratory crushing the material to be disintegrated is subjected to the action of fast changing shearing forces, which leads to the material being crushed either by applied impulses or by fatigue action, unlike conventional crushers where the structure of the material is damaged by the applied pressure (Wolny, 2013).

3.0 Dimensions and Operating Parameters

Feed characteristics are important parameters when designing or selecting a jaw crusher for a specific job (Napier-Munn *et al.*, 1999). The feed particle sizes of interest are those of the ore or rock that enters the crusher, the particle that can be nipped, particle that can fall through the chamber, and the particle that can fall through the chamber when the jaws are wide open (Donovan, 2003). The dimensions defined by these particle sizes include the gape which is the distance between the jaws at the feed opening, the Closed Side Set (CSS) which is the minimum opening between the jaws during the crushing cycle (minimum discharge aperture), the Open Side Set (OSS) which is the maximum discharge aperture, and the throw – the stroke of the swing jaw and the difference between OSS and CSS. Figure 5 shows a schematic of crusher dimensions (Donovan, 2003)

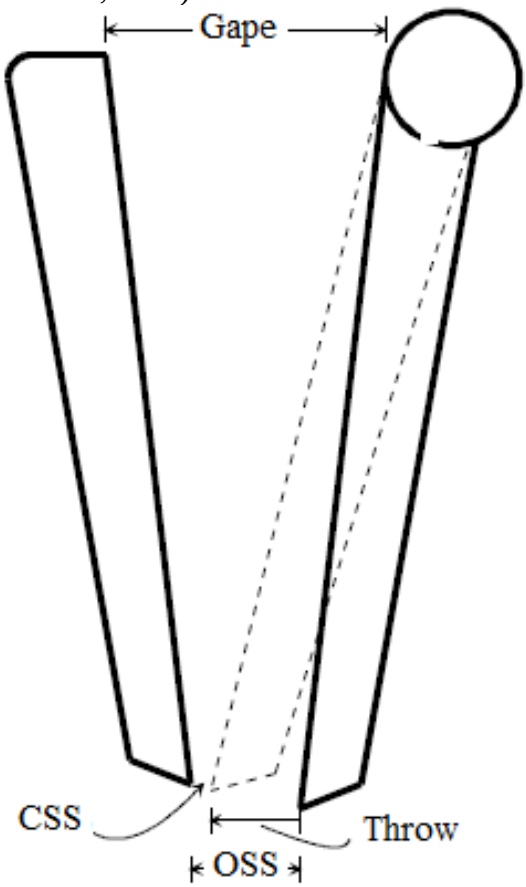

Figure 5. Schematic of crusher dimensions (Donovan, 2003)

The rating of jaw crushers is determined by the maximum dimensions of their feed opening, defined by the gape and the width of the plates. The fed openings of jaw crushers are known to vary from 250 mm by 500 mm to 1524 mm by 2032 mm. The largest particle size of the rock to be crushed should not be more than 80% of the rated gape (Weiss, 1985). The size of rectangular or square opening at the top of the jaws crusher defines the size the crusher. Therefore a 30 x 40 jaw crusher has an opening of 30" by 40". Primary jaw crushers generally come with square opening design while secondary jaw crushers have the rectangular opening design (Garnaik, 2010).

4.0 Selection of Crushers

The main factor that ensures effective control of the crushing process is proper selection of the crushing equipment. The principal factors that should be considered while selecting jaw crushers include (Donovan, 2003);

a. The petrographic nature of the rock
b. The abrasion index of the aggregate
c. The mechanical strength of the rock
d. The work index, or impact crushability, of the rock
e. The brittleness of the rock
f. The flakiness of the rock
g. The feed size
h. The desired product size (or reduction ratio)
i. The throughput to be crushed (tons per hour)
j. The capital cost
k. The long-term operating costs.
l. Project location, Operational considerations (e.g capacity per hour or day)
m. Climatic conditions,
n. Safety and environment,
o. Life of mine/expansion plans and Maintenance requirements.

The petrographic nature of the rock and its resistance to crushing forces (characterized by strength, work index, etc.) are used first to determine what type of crusher is needed and then in part to determine the power requirement of the crusher. When a jaw crusher is selected outright, the physical properties of the rock can be used to determine the mechanical features of the jaw crusher, but for the most part they are used along with the feed size and desired throughput to determine the size of the jaw crusher and its power requirement.

Usually, the feed size range or the desired throughput dictates the selection of specific jaw crusher. The current trend is to go to the largest feed opening that is economically feasible in order to avoid as much secondary breakage as possible (Donovan, 2003). Once a crusher is selected it can be determined whether or not the crusher will provide the desired reduction ratio or product size distribution. As was noted previously the size of a jaw crusher's discharge opening controls the product size distribution. Thus, determining whether a specific jaw can produce the desired product is dependent upon whether or not that crusher can have its discharge opening set to the required dimension. Table 2 shows the capacities for various Nordberg series jaw crushers.

Screen analysis graphs (Figure 6) and capacity charts (Table 2) have greatly simplified the task of selecting a crusher for a specific task. This been applied extensively in the selection of Nordberg C Series jaw crushers (Donovan, 2003; Metso Minerals, 2003) where computer program has been developed to speed up the process. The program known as the *Bruno* program requires inputs such as rock type, feed gradation, and the desired crusher to simulate expected capacities and product size distribution curves (Metso Minerals, 2003). The use of crusher efficiency index number based on crusher manufacturer's published data and the crushability factor of the rock has been proposed by Wagner (1990) to assist in crusher selection. However, the use of information based on standard rock size such as those presented in graphs, charts, etc, may be inaccurate because of the inhomogeneous nature of many rock types (Bearman, Barley and Hitchcock (1990). To carry out

a selection that may be consider accurate will therefore necessitate the need to fully characterize the rock which may require a lot of laboratory tests and experiments.

Table 2. Capacities for various Nordberg C Series jaw crushers (After Metso Minerals, 2003, Donovan, 2003)

CSS* mm	***C63*** 440 × 630	***C100*** 760 × 1000	***C110*** 850 × 1100	***C140*** 1070 ×1400	***C160*** 1200 ×1600	***C200*** 1500 ×2000
40	40					
50	55					
60	65					
70	80	150	190			
80	95	170	210			
90	110	190	235			
100	120	215	255			
125		265	310	385		
150		315	370	455	455	520
175		370	425	520	595	760
200		420	480	590	675	855
225				655	750	945
250				725	825	1040
275					900	1130
300					980	1225

Capacities in metric tons per hour

**CSS stands for closed side set (CSS) - the minimum opening between the jaws during the crushing cycle (minimum discharge aperture)*

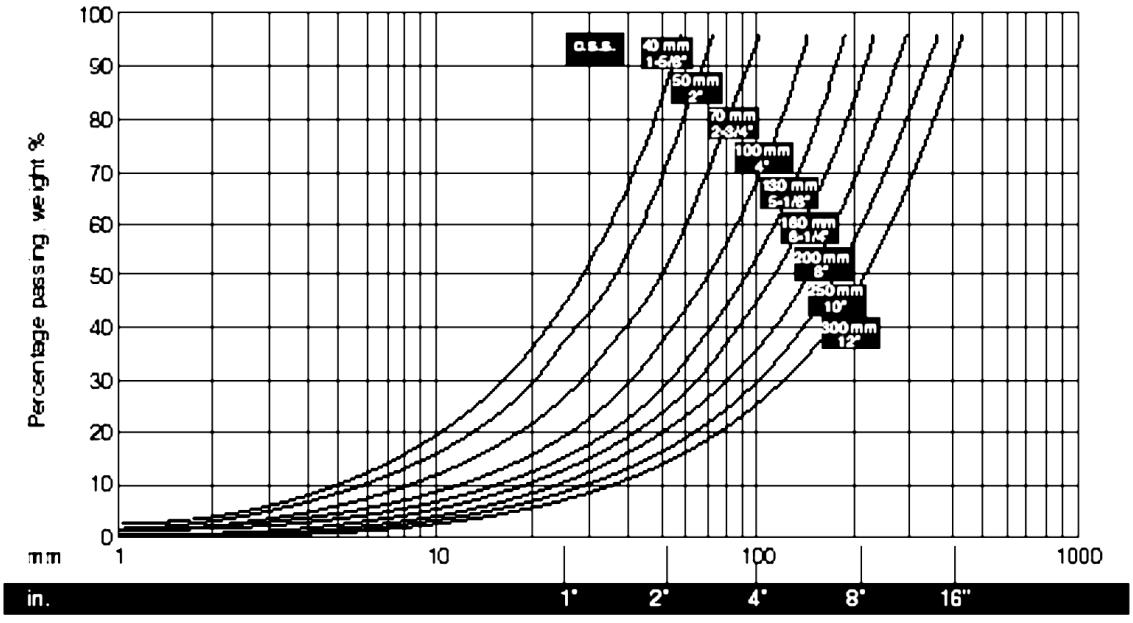

Figure 6. Product size distributions based on CSS (From Metso Minerals, 2003; Donovan, 2003)

For jaw crushers, a lot of considerations should be analysed such as (*Peter mayo; http:/www.quarry.com.au*):

a. The particle size of the should not be greater than 80% of the 'gape';
b. The crusher's operating setting (close side setting);
c. Maximum product particle diameter which normally is 1½ times the close side setting of the machine. This those not follow for slappy materials;
d. It is normally considered that 50% - 60% of the crushed product will pass the close side setting;
e. Jaw crushers reduction ratio are normally 6:1
f. When selecting a jaw crusher as a primary crusher, it should be noted that its output should exceed the average capacity of the plant, as primary feed to the plant is generally of a cyclical nature, relying on trucks or loaders in most cases.
g. For jaw crushers to operate optimally, all feed with particle size smaller than the closed side setting is removed to bypass the jaw crusher;
h. Generally, maximum feed size is critical in the selection of jaw crushers and not required capacity. This is because putting too fine a feed into a jaw crusher normally leads to equipment failure because of overload.

A lot of dynamic forces are present during a crushing process. These forces and the load also affect the supporting structures and foundations. It is therefore very important to consider how these forces and load affect the crusher structures and the outcome incorporated in the design (Rusiński, 2013).

5.0 Energy and Size Reduction

Crushing theory is concerned with the relationship between the amount of energy put into a rock or particle of a known size and the reduced particle size after the comminution process has taken place. The amount of energy required to do this work is referred to as the 'Work Index' and it is an expression of the resistance that a material has to crushing (or grinding). It is a measurement of how hard the ore is. Therefore 'Work Index' can be defined as *(http://gravel.gravelwasher.com/metalliferous-mining-processing-resource-book-crushing.html)*:

The amount of energy (work) required to break a rock from one size to another.

Each rock has a characteristic Work Index. For example, more energy is required to break quartz than sandstone so quartz will have a higher work index. Numerically the work index is known as the kilowatt-hours per tonne or kWh/t. A kilowatthour is the number of kilowatts consumed in an hour. For example, if you ran a 20kW motor for an hour, you would expend 20kWh. If you used that motor to do work to 2 tonnes of rock you would have used 20kWh/2 tonne, which is 10kWt/h. The higher the Work Index, the more work required to break the rock, hence the harder the rock. Whereas Work Index refers to the size fraction when rocks are reduced in size, Specific energy input refers to the amount of energy required to treat a certain tonnage. In simple terms if you crush 100t of rock from your feed size to your product size and it takes 180kWh, your specific energy input is 180kWh/100t = 1.8kWh/t.

The concepts of Work Index and Specific Energy make it clear that a certain (calculable) amount of energy is required to break a rock from one size to another. Experience has shown that to break a rock from coarse and medium size should require less energy per unit mass than to break a rock from coarse to fine, i.e. the smaller you want to break a rock, from a given starting size, the more

energy you require. Because we are talking about specific energy, i.e. energy per tonne of ore, it also follows that a given amount of energy spread out over a larger number of rocks will produce less breakage*(http://gravel.gravelwasher.com/metalliferous-mining-processing-resource-book-crushing.html)*. This can be demonstrated by looking at the numbers:

For example: Say it takes 100kWh to break 50t of rock from 50mm to 10mm. Then the Specific Energy Input from 50mm to 10mm is 100kWh/50t = 2kWh/t. If we then tried to use that same 100kWh to break 100t of rock, we would only be putting in 100kWh/100t or 1kWh/t.

Now, we know that to break a rock finer we need to increase the energy input, so a Specific Energy Input of 1kWh/t will produce a much coarser product than a Specific Energy Input of 2kWh/t.

6.0 Mechanisms of Particle Fracture

A size reduction process is analyzed by looking at the entire size distribution of its feed and product material. However, as each particle breaks as a result of the stresses applied to it and it alone, it is of value to look at single particle fracture. For a particle to fracture, a stress high enough to exceed the fracture strength of the particle is required. The manner in which the particle fractures depends on the nature of the particle, and on the manner in which the forcer is applied. There are three main generalized mechanisms of single particle fracture and they are*(http://gravel.gravelwasher.com/metalliferous-mining-processing-resource-book-crushing.html)*.

6.1 Abrasion

Abrasion fracture occurs when insufficient energy is applied to cause significant fracture of the particle. Rather, localised stressing occurs and a small area is fractured to give a distribution of very fine particles. This type of breakage occurs predominantly in ball mills.

6.2 Cleavage

Fracture by cleavage occurs when the energy applied is just sufficient to fracture the particle. Only a few particles result and their size is comparatively close to the original particle. Typically, this situation occurs under conditions of slow compression where the fracture immediately relieves the loading on the particle. This is the main type of fracture found in jaw crushers.

6.3 Shatter

Fracture by shatter occurs when the applied energy is well in excess of that required for fracture; under these conditions many areas in the particle are overloaded and the result is a comparatively large number of particles with a wide size distribution. In practice these events do not occur in isolation, rather breakages involve a combination of fracture mechanisms.

7.0 Predicting Jaw Crusher Performance

Comminution concerns the breakage of brittle particles under conditions of applied compressive stress. The nature of the failure mechanisms is governed by material properties of the particulate material and by the nature of the stress field around and within individual particles. The response of the particulate material to the stress field is largely elastic but significant non-elastic behavior occurs, particularly at the tips of growing cracks where large quantities of energy are dissipated when the criteria for fracture are met. The dissipation at the crack tip of the stored elastic energy in the particle turns out to be of critical interest in industrial comminution machines where energy

efficiency is of major consequence because of its economic importance. Industrial comminution processes are typically inefficient in their use of energy in the sense that considerably more energy is consumed by the operating equipment than is actually required to break the particles. In spite of the importance of this observation, it has not been possible to calculate precisely how much energy is actually required (Umucu *et al.,* 2013).

Specific fracture energy of the particles is not the only fundamental property that is important. The particle strength also plays a significant role in determining the overall comminution properties of the material. A particle will be broken only if it is stressed beyond its strength which is determined by the intrinsic properties of the material, the presence of micro flaws which act as stress raisers when the particle is under load and the state of stress that is experienced by the particle (Umucu *et al.,* 2013).

The performance of jaw crusher is mainly determined by the kinetic characteristic of the liner during the crushing process. The practical kinetic characteristic of the liners which are located in certain domain of the coupler plane are computed and discussed by Jinxi *et al.,* (2007) and Shrivastava (2012).

The performance of a jaw crusher is most aptly defined using the product size, the capacity or throughput, and the power consumption. The main object of size reduction in the aggregate industry is to generate a well-shaped product within a specified size range with a minimum of fines. It is also desirable to maintain target production rates and to crush the rock material as efficiently as possible.

There are various methods for the prediction of crusher performance. As noted previously in the discussion of crusher selection, technical literature provided by crusher manufacturers can be used to determine capacities and product size. Adjustments can be made to account for physical variations in feed materials using the aforementioned laboratory tests. When the actual performance of a jaw crusher is difficult to determine or unclear to the manufacturer, laboratory tests using small-scale jaw crushers are sometimes conducted in order to predict the performance of full capacity machines. The normal procedure is to test crush a representative sample of the feed material and determine the product size distribution. Comparison of the product distribution and associated properties of the feed material to other materials is used to estimate overall crushing performance, power requirements, and to detect characteristics that may require special design considerations. These tests provide an opportunity to evaluate the effects of various crusher settings, speeds, feeding methods, and the physical characteristics of the material (Pennsylvania Crusher Corporation, 2003).

In addition to charts, graphs, and lab-scale crushing tests, jaw crushers can also be evaluated using mathematical modeling techniques. Mathematical techniques are usually derived from laboratory data and can be used to predict crusher performance and possibly improve selection and design procedures (Rimmer *et al.,* 1986). Models/equations are typically used to determine the product size, power draw, and capacity of crushers. The advantage of models is that they reduce complex operations to a few numbers or parameters and can provide guidance to improved performance and decision making (Napier-Munn *et al.,* 1999).

7.1 Estimating capacity

The capacity of a jaw crusher is dependent upon the machine characteristics, the feed, and the nature of the rock material. The volumetric capacity of a jaw crusher can be estimated from the following equations (Sastri, 1994):

$$V = 60Nw\ (CSS + 0.5T)\ \left(\frac{DT}{G-(CSS+T)}\right) \text{ at low speeds}$$

$$V = 60Nw\ (CSS + 0.5T)\ \left(\frac{450g}{N^2}\right) \text{ at high speeds} \quad (1)$$

where N is the speed of the crusher in rpm
w is the width of the jaws in m
CSS is the closed side set in m
T is the throw in m
D is the vertical depth between the jaws in m
G is the crusher gape in m, and
g is gravitational acceleration in m/s^2.

Equation 1 gives volumetric capacity under ideal conditions. At low crusher speeds the material falls down the chamber due to gravity flow, and the distance of the fall is dependent on the geometry of the machine. At higher speeds there is less time between strokes/revolutions and movement of material down the chamber is constricted and controlled by the speed of the machine (Hersam, 1923).

In order to determine the actual capacity of a jaw crusher, Equation (1) needs to be corrected by accounting for the feed size, the degree of compaction resulting from vibration, and the nature of the material. Equation (2) gives the estimated capacity using these parameters (Sastri, 1994):

$$V = 60Nw\ (CSS + 0.5T)\ \left(\frac{DT}{G-(CSS+T)}\right)\ K_1\ K_2\ K_3 \text{ at low speeds}$$

$$V = 60Nw\ (CSS + 0.5T)\ \left(\frac{450g}{N^2}\right)\ K_1\ K_2\ K_3 \text{ at high speeds} \quad (2)$$

with

$$K_1 = 0.85 - \left(\frac{F_{avg}}{G}\right)^{2.5}$$

$$K_2 = 1.92\ \times\ 10^{\frac{-6.5T}{G}} \quad (3)$$

where, F_{avg} is the average feed size in m, and K_3 is a parameter related to the nature of the material. The parameter K_3 does not have a suggested value but is considered to increase with increasing hardness or toughness.

7.2 Product Size Distribution for Crushers

Specific fracture energy of the particles is not the only fundamental property that is important. The particle strength also plays a significant role in determining the overall comminution properties of the material. A particle will be broken only if it is stressed beyond its strength which is determined by the intrinsic properties of the material, the presence of micro flaws which act as stress raisers when the particle is under load and the state of stress that is experienced by the particle.

For impact breakage mechanism, many stakeholders are using the model of the percentage of broken product passing 1/10 the original particle size, t_{10}. The parameter t_a is defined as one tenth of t_{10} as follows (Napier-Munn *et al.*, 1996):

$$t_a = \frac{t_{10}}{10} \quad (4)$$

The abrasion breakage parameter, t_a, is determined by performing a tumbling test. A lower value of t_{10} (hence a lower t_a value) indicates that there is a lower percentage of material passing 1/10th the original particle size, or greater resistance to abrasion breakage.

Equation (5) relates t_{10} to E_{CS} which is specific energy of comminution (Napier-Munn *et al.*, 1996):

$$t_{10} = A\,(1 - e^{-bE_{cs}}) \quad (5)$$

where: t_{10} = percentage passing 1/10th of the initial mean size,
E_{cs} = specific comminution energy (kWh/kg)
A, b = ore impact breakage parameters.

The impact breakage parameters, namely A and b, are determined using a high energy impact breakage device called JK Drop Weight Tester. Specific energy of comminution, E_{cs}, in Equation (5) can be calculated according to experimental setup data, as follows (Napier-Munn *et al.*, 1996):

$$E_{cs} = \frac{0.0272 M_d (h_i - h_f)}{\bar{m}} \quad (5a)$$

Where, M_d is drop weight mass (kg), m is the medium mass of per particle size class; (g), h_i is initial height of drop weight above the anvil (cm) and h_f is final height of drop weight above the anvil (cm).

It is noted that A is the maximum t_{10} value achieved. This is significant for higher energy breakage. The parameter b is related to the overall slope of t_{10} versus E_{cs} curve at the lower energies. A and b are interdependent, since the value of one will directly affect the other. Parameters A and b are related and usually are reported by $A.b$ as a single value to indicate the ore hardness in terms of impact breakage. The $A.b$ parameter is the slope of the t_{10} vs. E_{cs} curve at its origin and it is a measure of breakage of the ore at lower energy levels.

Napier-Munn *et al.*, indicate a possible correlation between the impact ($A.b$) and abrasion (t_a) parameters and the Bond ball mill work index given by the equations (Hasani *et al.*,; 2009):

$$A \times b = -3.5 W_i + 117 \quad (6)$$

$$t_a = 19.7{W_i}^{-1.34} \quad (7)$$

Narayanan (1983), Pauw and Mare (1988), Bourgeois (1993) and King (2002), King (2002) proposed breakage distribution model as (Soni *et al.*, 2013):

$$t_n = 1 - (1 - t_{10})^{\left[\left\{\frac{9}{(n-1)}\right\}^{\propto}\right]} \quad (8)$$

Where, t_n= cumulative fraction passing from 1/nth of the feed size
t_{10}= cumulative fraction passing from 1/10th of the feed size
α = a material characteristic

The t_n versus t_{10} relationships can then be used to predict the product size distributions at different grind times (Sand and Subasinghe, 2004).

King (2002) proposed the relationship of t_{10} to the specific comminution energy by the equation:

$$t_{10} = t_{10(max)} \left[1 - e^{\frac{\beta E_{CS}}{E_{50}}}\right] \quad (9)$$

where, E_{CS} = specific comminution energy (Kwh/ton).

The coefficient β and E_{50} (median impact energy at fracture) were considered as material characteristics by (Narayanan, 1987), (Napier-Munn, 1996) and (Weedon, 2001).

Umucu *et al.,* (2013) proposed a different size distribution relation for t_n values of crushing products obtained from different laboratory scale crushers (jaw, roller and hammer). The following equation was used to predict the cumulative percentage passing (t_n), depending on the Crushing Engine Power *(CEP)* and feed particle size (X) before crushing:

$$t_n = \left(\frac{56.12}{n^{1.168\ CEP^{-1.274}}}\right) X^{0.30} \quad (10)$$

The relationship has however not been tested on industrial crushers.

Narayanan (1986) used a novel procedure for estimation of breakage distribution functions of ores from the t-family of curves. In this method, the product size distribution can be represented by a family of curves using marker points on the size distribution defined as the percentage passing (t) at a fraction of the parent particle size. Thus, t_2 is the percentage passing an aperture of half the size of the parent particle size, t_4 is one quarter and t_{10} is one-tenth of parent particle size. Narayanan and Whiten (1988) have proposed empirical equations for relating the reference curve data t_{10} with the impact energy.

7.3 Product Size Models

Csoke *et al.,* (1996) developed an empirical method for determining the product size of "preliminary" crushers, i.e. jaw crushers and gyratory crushers. The product size resulting from

breakage of the material larger than the CSS of the crusher can be modeled using the following function:

$$P\,(d) = \left(\frac{r}{r_{max}}\right)^{m} \tag{11}$$

With $r = \frac{d_p}{Gap}$ (12)

$$r_{max} = \frac{d_{PMAX}}{Gap} \tag{13}$$

where,
m is exponent describing the product size distribution
d_p is the particle size
d_{pMAX} is the largest size in the product (OSS), and

G_{ap} is the CSS (CSS is closed side set (CSS) - the minimum opening between the jaws during the crushing cycle (minimum discharge aperture)) of the crusher.

Based on operating data found in the literature, Equation (11) fits the product size of a jaw crusher with r_{max} equal to 1.223 and m of 0.842.

King (2001) outlined a model for the prediction of product size based on data from a crusher manufacturer. The main concept is that the size distribution of the product is characterized by the particle size relative to the OSS and by the product type, P_t, which is the fraction of the product smaller than the OSS. P_t is related to the nature of the material and is distinguished by the work index and a qualitative description of the material. The size distribution given by this model is determined from the following equations:

$$P\,(d) = 1 - e^{\left(-\left[\frac{r}{K_u}\right]^{1.5}\right)} \qquad \text{for r > 0.5}$$

$$P\,(d) = 1 - e^{\left(-\left[\frac{r}{K_l}\right]^{0.85}\right)} \qquad \text{for r < 0.5} \tag{14}$$

With

$$r_i = \frac{D_i}{OSS} \tag{15}$$

$$K_u = \left[In\left(\frac{1}{1-P_1}\right)\right]^{-0.67} \tag{16}$$

$$K_1 = 0.5\left[In\left(\frac{1}{1-P_b}\right)\right]^{-1.18} \tag{17}$$

$$P_b = 1 - e^{\left(-\left(\frac{0.5}{K_u}\right)^{1.5}\right)} \quad (18)$$

Equation (14) should only be used when the size at which half of the feed material passes is greater than the OSS.

Other product size models of note is the one developed by Whiten in 1972 (Donovan, 2003).

First the classification and breakage could be illustrated by Figure 7.

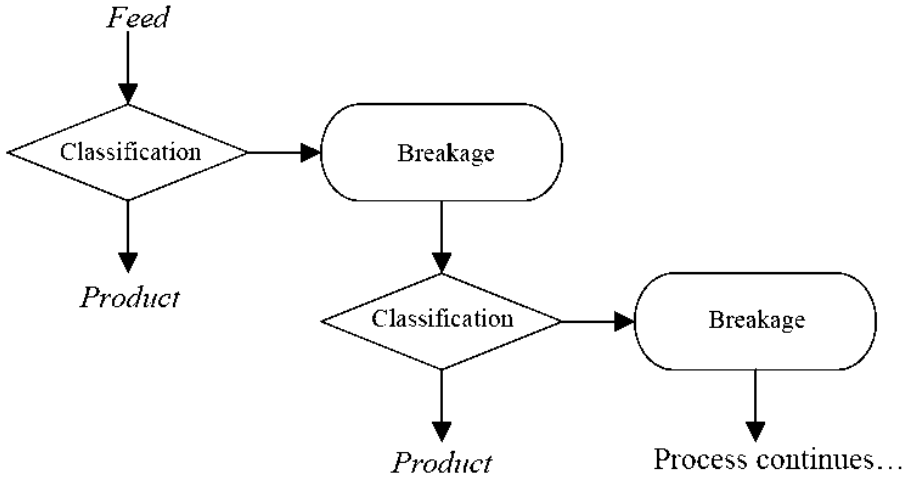

Figure 7. Flowchart of classification and breakage process (Donovan, 2003)

If the classification and breakage of particles in a jaw crusher is considered as a closed circuit process, Figure 7 can be represented by Figure 8, a representation of the Whiten crusher model (Donovan, 2003).

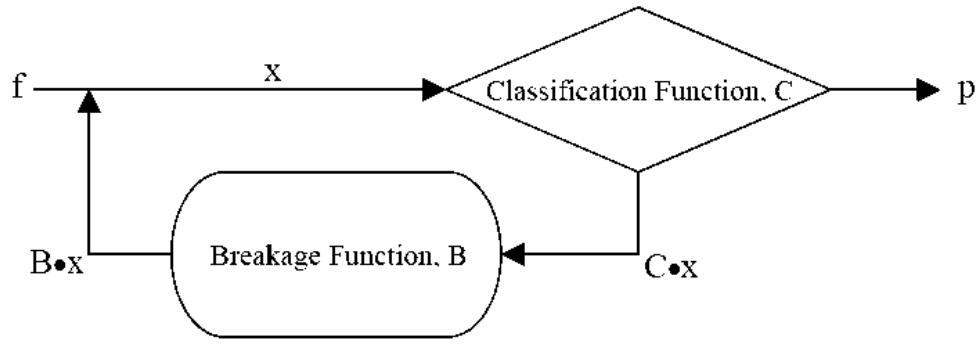

Figure 8. Whiten crusher model (Donovan, 2003)

The Mass balance equations written about each node of Figure 8 describe the repetitive process of classification and breakage and are expressed as (Kojovic *et al.*, 1997, Donovan, 2003):

$$X = f + Bx \quad (19)$$

$$X = p + Cx \qquad (20)$$

where, *x* is a vector representing the amount in each size fraction entering the crusher
f is the feed size distribution vector
p is the product size distribution vector
C is the classification (diagonal) matrix
B is the breakage distribution (lower triangular) matrix.

The classification matrix describes the proportion of particles in each size interval entering the crushing zone. The breakage distribution matrix gives the relative distribution of each size fraction after a breakage event. Equations (19) and (20) can be combined resulting in the Whiten crusher model equation (Whiten, 1972):

$$P = (I - C).(I - BC)^{-1} . f \qquad (21)$$

where, *I* is the unit matrix. Equation (21) can be used to determine the product size of a jaw crusher given the feed size, classification function, and the breakage function (Donovan, 2003).

7.4 Power Models for Jaw Crushers

The classical comminution theories, which were derived by Rittinger, Kick and Bond (Lee, 2012) respectively, aim to describe the relation between energy and size reduction for a given feed size. The three theories, which are usually referred to as the first, second and third theory of comminution, are formulated in Equations (22) to (24) (Asbjörnsson, 2013; Lee, 2012).

$$E_{Rittninger} = C_{Ritt} \left(\frac{1}{p_{80}} - \frac{1}{f_{80}}\right) \qquad (22)$$

Where $E_{Rittinger}$ is the energy input, C_{Ritt} is a material constant, p_{80} is the size which 80 % of the product passes, and f_{80} is the size which 80 % of the feed passes (Asbjörnsson, 2013; Lee, 2012).

$$E_{Kick} = -C_{Kick}\, In \left(\frac{p_{80}}{f_{80}}\right) \qquad (23)$$

where E_{Kick} is the energy input and C_{Kick} is a material constant.

Rittinger's and Kick's laws lack precision in describing the shape of a size distribution curve as only a single point is used (Lee, 2012).

The third and final classical relationship was proposed by Bond in 1952. According to his theory, the energy input is proportional to the length of the produced crack tip and is equal to the difference in energy represented by the product and the feed, and is expressed as (Lee, 2012):

$$E_{Bond} = C_{Bond} \left(\frac{1}{\sqrt{p_{80}}} - \frac{1}{\sqrt{f_{80}}}\right) = W_1 \left(\frac{10}{\sqrt{p_{80}}} - \frac{10}{\sqrt{f_{80}}}\right) \qquad (24)$$

where *p* and *f* are in microns. W_I is the Bond´s *work index* which expresses the resistance of a material to crushing or grinding. This constant is a function of material properties and the

efficiency of the crusher. A lower efficiency in a crusher will give a higher work index (Asbjörnsson, 2013; Lee, 2012).

The above classical laws of comminution have not been found to accurate in many cases and others have worked to improve them with varying degree of success. Hukki in 1975 (Lee, 2012) suggested that all three relationships were in fact applicable but in different and relatively narrow size ranges (Will and Napier-Munn,2005; Morrel (2004). Based on Hukki's work, Morrell (2004) later successfully proposed a modification of Bond's equation. Unfortunately, as pointed out by Lindqvist (2008), Morrell's modified energy model still lacks precision due to the sole use of f_{80} and P_{80}. Egbe *et al.,* (2013) presented procedures for determining the Bond's work index of some Nigerian ores. An alternative approach to calculate the energy cost to produce a given product size distribution from a given feed size distribution was suggested by Lindqvist (2008) and Lee (2012).

However, there is generally little confidence in the model results and it is also suspected that all these underlying ideas are incorrect and that the energy–size reduction relationship does not suitably define the process of size reduction (Napier-Munn, 1996, Lynch, 1977). Bond's "law" is an empirical law that only fits experimental data over a limited range of variables and only in certain cases (Choi, 1982). It can be corrected for other operating conditions but even with this correction it has been shown that the power consumption of a jaw crusher can be as much as 240% greater than the expected consumption based on Bond's equation (Eloranta, 1997). Rose and English have suggested a relationship for power consumption based on Bond's work index but take into account the material density and machine characteristics, i.e., gape, throw, CSS, etc. (Lowrison, 1974).

A more recent approach for predicting power consumption in crushers was presented Andersen and Napier-Munn (1988) and Morrell *et al.,* 1992. In this case, they used using a single regression equation relating the power actually drawn by the industrial machine in producing a particular product size distribution, to the calculated power required to achieve the same size reduction in a laboratory test (Sabic and Forlin, 2002, Donovan, 2003).

$$P_c = AP_p + P_n \tag{25}$$

where P_c is the power drawn by the crusher under load in kW and P_p is the pendulum power in kW expressed as

$$P_p = \sum_{i-1}^{j} E_{cs} t_{10i} C_i \; x_i \tag{26}$$

P_n is the power drawn by the crusher under no load in kW.

This power model provides a means of comparing the power efficiency of different patterns and types of crushers, in terms of efficiency constant A, and has been found to provide satisfactory predictions for several crusher types. However, as the regression coefficients are not valid for all crushers, the tests must be repeated for some crusher types (Sabic and Forlin, 2002).

Today the energy-size relation in the comminution process is usually presented in the form of the differential equation proposed by Walker *et al.*, (1937) and revised by Hukki (1962). This is represented by Equation (27) (Asbjörnsson, 2013):

$$dE = -C \frac{dx}{x^{f(x)}} \quad (27)$$

The most common mathematical model used today for expressing the crusher performance is the empirical Selection-Breakage model proposed by Whiten (1972). This model is however empirically fitted to data from drop weight tests, which is more suitable for mills than compressive crushers and does not predict capacity.

More detailed analytical models based on the mechanical properties of the crusher have been proposed by Evertsson (2000) and Briggs (1997). These models can provide more accurate information from the process but require detailed information about crusher geometry, breakage behaviour and require considerable simulation time (Asbjörnsson, 2013).

7.5 Size Reduction Relationships

The general size reduction equation is as follows (Morrell, 2004):

$$W_i = M_i\, 4\left(x_2^{f(x_2)} - x_1^{f(x_1)}\right) \quad (28)$$

Where:
W_i = Specific comminution (kWh/tonne);
M_i = Work index related to the breakage property of an ore (kWh/tonne);
x_2 = 80% passing size for the product (microns)
x_1 = 80% passing size for the feed (microns)
$f(x_j)$ is calculated from the relationship: ((Morrell, 2006):

$$f(xj) = -(0.295 + xj \times 10^{-6}) \quad (29)$$

For grinding from the product of the final stage of crushing to a P_{80} of 750 microns (coarse particles) the index is labeled M_{ia} and for size reduction from 750 microns to the final product P_{80} normally reached by conventional ball mills (fine particles) it is labeled M_{ib}. For conventional crushing, M_{ic} is used and for High Pressure Grinding Rolls, (HPGRs), M_{ih} is used.

For coarse particle grinding in tumbling mills Equation (28) is written as:

$$W_a = K_1 M_{ia}\, 4\left(x_2^{f(x_2)} - x_1^{f(x_1)}\right) \quad (30)$$

where K_1 = 1.0 for all circuits that do not contain a recycle pebble crusher and 0.95 where circuits do have a pebble crusher; $x_1 = P_{80}$ in microns of the product of the last stage of crushing before grinding; x_2 = 750 microns and M_{ia}= Coarse ore work index and is provided directly by Semi-autogenous Mill Comminution (SMC) Test.

For fine particle grinding Equation (28) is written as:

$$W_b = M_{ib}\, 4\left(x_3^{f(x_3)} - x_2^{f(x_2)}\right) \quad (31)$$

where x_2 = 750 microns; $x_3 = P_{80}$ of final grind in microns; M_{ib} is provided by data from the standard Bond ball work index test using the following equation (Morrell, 2006):

$$M_{ib} = \frac{18.18}{P_1^{0.295}(Gbp)\left(p_{80}^{f(p_{80})} - f_{80}^{f(f_{80})}\right)} \quad (32)$$

where M_{ib} = fine ore work index (kWh/tonne); P_1 = closing screen size in microns; Gbp = net grams of screen undersize per mill; P_{80} = 80% passing size of the product in microns and f_{80} = 80% passing size of the feed in microns. Note that the Bond ball work index test should be carried out with a closing screen size which gives a final product P_{80} similar to that intended for the full scale circuit.

Equation (28) for conventional crushers is written as:

$$W_c = S_c K_2 M_{ic}\, 4\left({x_2}^{f(x_2)} - {x_1}^{f(x_1)}\right) \quad (33)$$

Where S_c = coarse ore hardness parameter which is used in primary and secondary crushing situations. It is defined by Equation (34) with K_s set to 55; K_2 = 1.0 for all crushers operating in closed circuit with a classifying screen; $x_1 = P_{80}$ in microns of the circuit feed; $x_2 = P_{80}$ in microns of the circuit product and M_{ic} = Crushing ore work index and is provided directly by SMC Test. If the crusher is in open circuit, eg pebble crusher in an Autogenous/Semi Autogenous, AG/SAG circuit, K_2 takes the value of 1.19.

The coarse ore hardness parameter (S) makes allowance for the decrease in ore hardness that becomes significant in relatively coarse crushing applications such as primary and secondary cone/gyratory circuits. In tertiary and pebble crushing circuits it is normally not necessary and takes the value of unity. In full scale HPGR circuits where feed sizes tend to be higher than used in laboratory and pilot scale machines the parameter has also been found to improve predictive accuracy. The parameter is defined by Equation (34);

$$S = K_s(x_1 x_2)^{-0.2} \quad (34)$$

Where K_s = machine-specific constant that takes the value of 55 for conventional crushers and 35 in the case of HPGRs; $x_1 = P_{80}$ in microns of the circuit feed and $x_2 = P_{80}$ in microns of the circuit product.

High Pressure Grinding Rolls (HPGR)

Equation (28) for HPGR's crushers is written as:

$$W_h = S_h K_3 M_{ih}\, 4\left(x_2^{f(x_2)} - x_1^{f(x_1)}\right) \quad (35)$$

Where S_h = coarse ore harness parameter as defined by Equation 2.34 and with K_s set to 35 K_3 = 1.0 for all HPGRs operating in closed circuit with a classifying screen. If the HPGR is in open circuit, K_3 takes the value of 1.19. Also $x_1 = P_{80}$ in microns of the circuit feed; $x_2 = P_{80}$ in microns

of the circuit product; M_{ih} = HPGR ore work index and is provided directly by SMC Test.

Specific Energy Correction for Size Distribution (Ws)

It should be noted that the feed and product size distributions are usually different (an assumption that was made in arriving in the above specific energy requirement) and so allowances for additional specific energy. However, for the purposes of this approach it has been assumed that the additional specific energy for ball milling is the same as the difference in specific energy between open and closed crushing to reach the nominated ball mill feed size. This assumes that a crusher would provide this energy. However, in this situation the ball mill has to supply this energy and it has a different (higher) work index than the crusher (that is, the ball mill is less energy efficient than a crusher and has to input more energy to do the same amount of size reduction). Hence from Equation (33), to crush to the ball mill circuit feed size (x_2) in open circuit requires specific energy equivalent to:

$$W_c = 1.19^* M_{ic}\, 4\left(x_2^{f(x_2)} - x_1^{f(x_1)}\right) \quad (36)$$

closed circuit crushing the specific energy is:

$$W_c = 1^* M_{ic}\, 4\left(x_2^{f(x_2)} - x_1^{f(x_1)}\right) \quad (37)$$

The difference between the two (Equation (36) and Equation (37)) has to be provided by the milling circuit with an allowance for the fact that the ball mill, with its lower energy efficiency, has to provide it and not the crusher. Thus Ws (specific energy correction for size distribution) is represented by:

$$W_s = 0.19^* M_{ia}\, 4\left(x_2^{f(x_2)} - x_1^{f(x_1)}\right) \quad (38)$$

It should be noted that in Equation (38), M_{ic} has been replaced with M_{ia}, the coarse particle tumbling mill grinding work index.

7.6 Sizes of aggregate produced by jaw crushers

Even though the setting of the discharge opening of a crusher will determine the maximum size of aggregate produced, the aggregate sizes will range from slightly greater than the crusher setting to fine dust. For any given setting for jaw or roll crushers, approximately 15% of the total amount passing through the crusher will be larger than the setting. If the opening of the screen which receives the output from such crusher are the same size as the crusher setting, 15% of the output will not pass through the screen.

Figure 9 (Assakkaf, 2003) provides the percentage of material passing or retained on screens having the size opening indicated for jaw and roll crushers. To read the chart:

a. Select the vertical line corresponding to the crusher setting
b. Then go down this line to the number which indicate the size of screen opening
c. From the size of the screen opening, proceed horizontally to the left to determine the percent of material passing through the screen or the right to determine the percentage of material retained on the screen.

Example 1 (Assakkaf, 2003)
A jaw crusher with a closed setting of 3½ in produces 60 tons per hour of crushed stone. Determine the amount of stone produced in tons per hour within the following size range: in excess of 1 in; between 1 and ½ in; between ½ and ¼ in.

It can be seen from Figure 9 that the amount retained on a 1-in screen is 71% of 60, which is 42.6 tons per hr. Also, details for each of the size range have been determined and calculations made as shown on Table 3:

Table 3. Sizes of aggregate produced by jaw crushers

Size Range (in)	% Passing Screen	%in Size Range	Crusher's Total Output (ton/hr)	Amount Produced in Size Range (ton/hr)
Over 1	100 – 29	71	60	42.6
1 – ½	29 – 17	12	60	7.2
½ – ¼	17 – 11	6	60	3.6
¼ - 0	11 – 0	11	60	6.6
Total		100%		60.0 tph

Examples 2 (Adapted from; Using The Smc Test® to Predict Comminution Circuit Performance (http://www.smctesting.com/documents/ Using_the_SMC_Test.pdf))

Calculate the overall specific energy to mill a rock in a primary crusher from a P_{80} of 110 mm to a product with a P_{80} of 116 microns for the following three circuit SAB mill crusher, SABC, HPGR/ball mill *and Conventional crushing/ball mill. SMC Test and Bond ball work index test on a similar sample has generated the following details: SMC Test:* M_{ia} *= 20.2 kWh/t,* M_{ic} *= 8.2 kWh/t,* M_{ih} *= 14.8 kWh/t Bond test carried out with a 160-micron closing screen:* M_{ib} *= 19.7 kWh/t.*

Solution

SABC Circuit

Coarse particle tumbling mill specific energy
Since it has a pebble crusher in the circuit, $k_1 = 0.95$. Also, 110mm = 110,000 microns.
Combining Equations (29) and (30):

$$W_a = 0.95 * 20.2 * 4 * \left(750^{-(0.295+750 \times 10^{-6})} - 110{,}000^{-(0.295+110{,}000 \times 10^{-6})}\right)$$

= 10.14 kWh/t

Fine particle tumbling mill

specific energy

Combining Equations (29) and (31):

$$W_b = 19.7 * 4 * \left(116^{-(0.295+116\times10^{-6})} - 750^{-(0.295+750\times10^{-6})}\right)$$

= 8.27kWh/t

Pebble crusher specific energy

The assumption for this circuit is that the feed to the pebble crusher has a P_{80} of 60mm. Normally, this value is calculated by assuming that it is 0.75 of the nominal pebble port apertures which is 80mm in this case. The setting of the pebble crusher produces a product with P_{80} of 14mm. The feed rate of the pebble crusher feed rate is estimated to be 30% of new feed tph. Combining Equations (29) and (33):

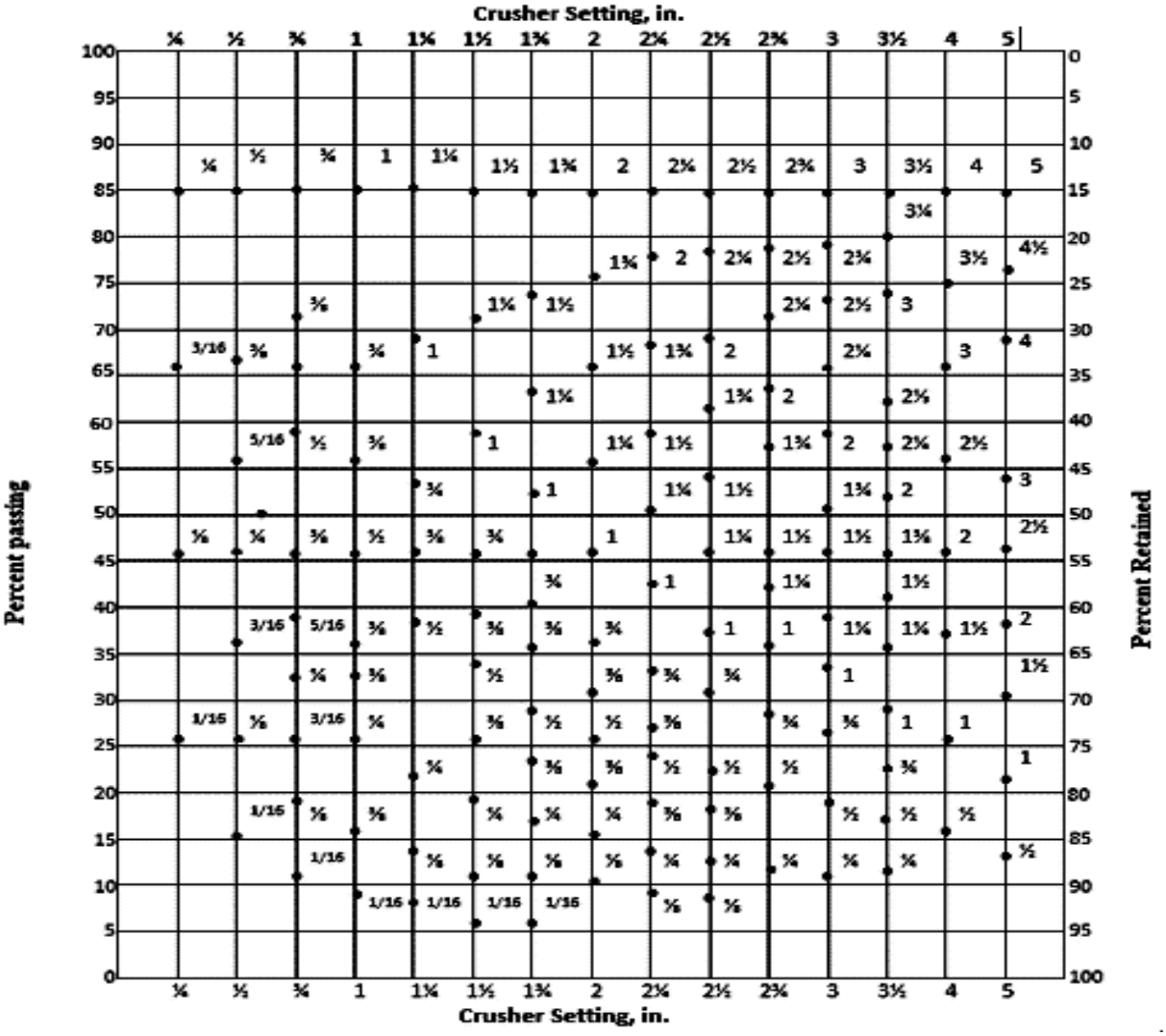

Figure 9. Analysis of the size of aggregate by jaw crushers

$$W_c = 1.19 * 8.2 * 4 * \left(14000^{-(0.295+14000\times10^{-6})} - 60000^{-(0.295+60000\times10^{-6})}\right)$$

= 1.26 kWh/t when expressed in terms of the crusher feed rate

= 1.26* 0.30 kWh/t when expressed in terms of the SABC circuit new feed rate

= 0.38kWh/t of SAG mill circuit new feed

Total net comminution specific energy:

W_T = 10.14+ 8.27+ 0.38 kWh/t

= 18.79kWh/t

HPGR/Ball Milling Circuit

The assumption in the circuit is that the primary crusher product is reduced to a HPGR circuit feed P_{80} of 38 mm by a closed-circuit secondary crushing. The HPGR is also considered to be in the closed circuit and reduces the 38 mm feed to a circuit product P_{80} of 6 mm. after this, the product is feed to a closed-circuit ball mill which takes the crushing down to a P_{80} of 116 microns.

Secondary crushing specific energy

Combining Equations (29), (33) and (34):

$$W_c = 1 * 55 * (38000 * 110000)^{-0.2} * 8.2 * 4 * \left(38000^{-(0.295+38000 \times 10^{-6})} - 110{,}000^{-(0.295+110{,}000 \times 10^{-6})}\right)$$

= 0.446kWh/t

HPGR specific energy

Combining Equations (29) and (34):

$$W_c = 1 * 35 * (6000 * 38000)^{-0.2} 14.8 * 4 * \left(6000^{-(0.295+6000 \times 10^{-6})} - 38000^{-(0.295+38000 \times 10^{-6})}\right)$$

= 1.90kWh/t

Coarse particle tumbling mill specific energy

Combining Equations (29) and (30):

$$W_a = 1 * 20.2 * 4 * \left(750^{-(0.295+750 \times 10^{-6})} - 6000^{-(0.295+6000 \times 10^{-6})}\right)$$

= 5.50kWh/t

Fine particle tumbling mill specific energy

Combining Equations (29) and (31):

$$W_b = 19.7 * 4 * \left(116^{-(0.295+116 \times 10^{-6})} - 750^{-(0.295+750 \times 10^{-6})}\right)$$

= 8.25kWh/t

Total net comminution specific energy:

W_T = 0.45+ 1.90+ 5.50+8.25 kWh/t

= 16.1 kWh/t

Conventional Crushing/Ball Milling Circuit

The assumption in this circuit is that the primary crusher product is reduced in size to P_{80} of 6.8 mm via a secondary/tertiary crushing circuit (closed) which is then fed to a closed-circuit ball mill which reduces the product to a P_{80} of 116 microns.

Secondary/tertiary crushing specific energy

Combining Equations (29) and (33):

$$W_c = 1 * 8.2 * 4 * \left(6800^{-(0.295+6800 \times 10^{-6})} - 110{,}000^{-(0.295+110{,}000 \times 10^{-6})}\right)$$

= 1.99kWh/t

Coarse particle tumbling mill specific energy

Combining Equations (29) and (30):

$$W_a = 1 * 20.2 * 4 * \left(750^{-(0.295+750 \times 10^{-6})} - 6800^{-(0.295+6800 \times 10^{-6})}\right)$$

= 5.76 kWh/t

Fine particle tumbling mill specific energy

Combining Equations (29) and (31):

$$W_b = 19.7 * 4 * \left(116^{-(0.295+116 \times 10^{-6})} - 750^{-(0.295+750 \times 10^{-6})}\right)$$

= 8.27 kWh/t

Size distribution correction

$$W_s = 0.19 * 20.2 * 4 * \left(6800^{-(0.295+6800 \times 10^{-6})} - 110{,}000^{-(0.295+110{,}000 \times 10^{-6})}\right)$$

= 0.93kWh/t

Total net comminution specific energy:

W_T = 1.99+ 5.76+ 8.27+ 0.93 kWh/t = 16.95 kWh/t

Worked Example 3: Feed Size

For a roll crusher, the diameter of the roll is directly proportional to the maximum particle diameter of the rock or ore that can be fed into it. This therefore means that very large diameter particles cannot be gripped by the rollers, and if they are too small, they simply fall through with size reduction.

For roll crusher that has an angle of nip, B, of 18.86^0, the maximum particle size that can be crushed by the roll crusher is calculated as follows:

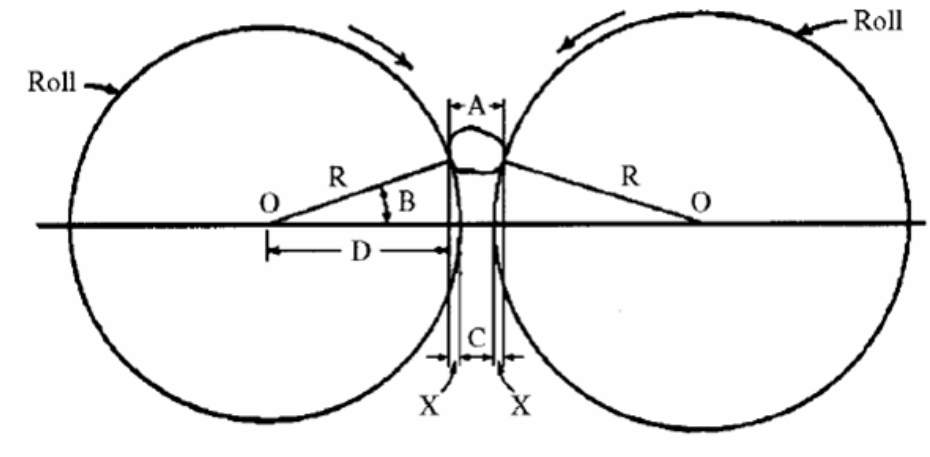

Figure 9. Crushing Rocks between two rolls

Let
R = radius of rolls
B = angle of nip
$D = R \cos B = R \cos (18.86) = 0.9463$ R
A = maximum particle size of the feed
C = roll setting which also equals the size of finished product
$X = R - D = R - 0.9463R = 0.0537R$
$A = 2X + C = 2\ (0.0537R) + C = 0.1074R + C$

∴ Maximum size Feed (A) = 0.1074R + C

Therefore, if we are to estimate the maximum particle size of rock or ore that can be crushed by a roll crusher with a roll of diameter, 80 cm, and a roll setting of 2.0 cm, then:

Maximum particle size of the feed (A) = 0.1074R + C
A = 0.1074(80) +2 = 10.59cm

8.0 Conclusion

This paper reviews the selection process as well as the theoretical performance evaluation procedures for jaw crushers. It is however important to note that Crushers encounter considerable difficulties concerning external loads acting on their mechanical joints which make it almost impracticable to use theoretical calculations for design and performance evaluation. It is therefore necessary to use experimental studies to verify any theoretical methods used for these purposes.

Acknowledgement

The authors wish to acknowledge the funds provided for this research and publication by TETFund Centre of Excellence for Renewable Energy, Kaduna Polytechnic, Kaduna, Nigeria. The funds were provided by the Tertiary Education Trust Fund (TETFUND), Nigeria, under the

TETFUND Special Intervention for Establishment of Centre of Excellence (TETF/ES/DS&D/KADPOLY/COE /2021/VOL11).

References

Assakkaf, I. (2003); Construction planning equipment and methods; Chapter 14, sixth edition, McGraw Hill.

Asbjörnsson, G. (2013); Modelling and Simulation of Dynamic Behaviour in Crushing Plants; Thesis for Licentiate of Engineering; Chalmers University of Technology

Andersen, J.S. and Napier-Munn, T.J. (1988); Power Prediction for Cone Crushers, 3rd Mill Operators Conference, AusIMM, Cobar, Australia

Aleksandar Sabic & Forlin Zhang (2002); Predicting Gyracone crusher performance using dynamic model (www.agg.net.com/resources/articles/).

Bearman, R.A., Barley, R.W., and Hitchcock, A. (1990); The Development of a Comminution Index for Rock and The Use of an Expert System to Assist the Engineer in Predicting Crushing Requirements, Minerals Engineering, Vol. 3, No. 1-2, pp. 117-127).

Bourgeois, F.(1993); Micro-scale Modelling of Comminution Processes. Thesis, University of Utah.

Briggs, C.A., A Fundamental Model of a Cone Crusher (1997); PhD thesis from University of Queensland: Brisbane, Australia.

Bond, F.C. (1952); The Third Theory of Comminution, Transactions of AIME/SME, Vol. 193, pp. 4884-494).

Bond, F.C. (1961); Crushing and grinding calculations, Part I-II. Br. Chem. Eng., vol. 6, 1961. pp. 378–385, pp. 543–548).

Choi, Woo-Zin (1982); Comminution and Liberation Studies of Complex Sulfide Ores, MS Thesis – Virginia Tech, Blacksburg, VA.

Csöke B., S. Petho J. Foldesi and L Meszaros (1996); Optimization Of Stone-quarry Technologies; International Journal of Mineral Processing - Vol. 44-45 - 1996 - pp. 447-459.

Donovan, James G. (2003); Fracture toughness-based models for the prediction of power consumption, product size and capacity of jaw crusher, Ph.D. thesis, U.S.A, Virginia Polytechnic Institute and state University.

Eloranta, J. (2006); Crushing and Screening Handbook, Sept 2006] [Http://www.infominerals.com/impact-crusher.html].

Egbe, E.A.P., E. Mudiare, O.K. Abubakre (2013); Determination Of The Bond's Work Index Of Baban Tsauni (Nigeria) Lead-Gold Ore; European Scientific Journal April 2013 edition Vol.9, No.12.

Evertsson, C.M. (1972); Cone Crusher Performance, in Department of Machine and Vehicle Systems. 2000, PhD thesis from Chalmers University of Technology: Gothenburg.

Garnaik, Sobhan Kumar (2009); Computer Aided Design of Jaw crusher, B.Tech Thesis, National Institute of technology, Rourkela, 2010.

Hasani, S., Dehghani, A., Khosravi, M. (2009); Determination of Work Index by abrasion mill and drop weight apparatus, 3rd Conference of Iran Mining Engineering, pp. 1786(http://www.maden.org.tr/resimler/ekler/ 3a8b724132b8e3d_ek.pdf).

Hasani, S., Dehghani, A., Khosravi, M. (2009); Breakage experiments for modeling of the AG and SAG mills; 3rd Conference of Iran Mining Engineering, pp. 1778 (http://www.maden.org.tr/resimler/ekler/ 3a8b724132b8e3d_ek.pdf).

Hersam, E.A. (1923); Factors Controlling the Capacity of Rock Crushers, Transactions AIME, Vol. 68, pp. 463-476

Hukki, R.T. (1962); Proposal for a Solomonic Settlement between the Theories of von Rittinger, Kick and Bond; AIME Transaction, 223: pp. 403-408

Jinxi Cao, Qin Zhiyu, Wang Guopeng, Rong Xingfu, Yang Shichun (2007); Investigation on Kinetic Features of Multi-Liners in Coupler Plane of Single Toggle Jaw Crusher" by, IEEE, College of Mechanical Engineering, Taiyuan University of Technology, Taiyuan.

King, R.P.(2002); Modeling and Simulation of Mineral Processing Systems, first ed. Butterworth-Heinemann Publishers, NY.

King, R.P., ed. (2001); Modelling and simulations of mineral processing systems, Butterworth-Heinemann.

Kojovic, T., Napier-Munn, T.J., and Andersen, J.S. (1997); Modeling Cone and Impact Crushers Using Laboratory Determined Energy-Breakage Functions, Comminution Practices, ch. 25, (edited by S. Komar Kawatra), SME, Littleton, CO.

Lee E. (2012); Optimization of Compressive Crushing; PhD Thesis; Department of Product and Production Development, Chalmers University of Technology, Göteborg, Sweden.

Lindqvist, M. (2008); Energy considerations in compressive and impact crushing of rock. Minerals Engineering, 21: p. 631-641.

Lowrison, G.C. (1974); Crushing and Grinding, CRC Press, Cleveland, Ohio.

Lynch, A.J., ed. (1977); Mineral Crushing and Grinding Circuits - Their Simulation, Optimisation, Design and Control. Developments in Mineral Processing. Vol. 1, Elsevier Scientific Publishing Company.

Morrell, S. (2004); An alternative energy–size relationship to that proposed by Bond for the design and optimisation of grinding circuits. International Journal of Mineral Processing, 74(1–4): p. 133-141.

Morrel, S., Napier-Munn, T.J., and Andersen, J.S. (1992); The Prediction of Power Drawfor Comminution Machines, Communition – Theory and Practice, (edited by S. Komar Kawatra), AIME, pp. 405-426.

Metso Minerals (2003); Nordberg C Series Jaw Crushers, Technical publication).

Morrell, S. (2004); An Alternative Energy-Size Relationship to that Proposed by Bond for the Design and Optimisation of Grinding Circuits; International Journal of Mineral Processing, 74, 133-141), (http://www.smctesting.com/documents/Using_the_SMC_Test.pdf)

Morrell, S. (2006); Rock Characterisation for High Pressure Grinding Rolls Circuit Design, Proc International Autogenous and Semi Autogenous Grinding Technology, Vancouver, vol IV pp 267-278.

Narayanan, S.S., Whiten W.J. (1983); Breakage characteristics of ores for ball mill modeling. Proceedings of AusIMM, 286, June, pp.31-39.

Napier-Munn, N., Morrell, S., Morrison, R.D., Kojovic, T. (1996); Mineral Comminution Circuits: Their Operation and Optimization, JKMRC, Brisbane, pp.413.

Napier-Munn, T.J., Morrell, S., Morrison, R.D., Kojovic, T. (1999); Mineral Comminution Circuits – Their Operation and Optimization, Julius Kruttschnitt Mineral Research Center, Queensland.

Pauw, O.G., Mare, M.S. (1988); The determination of optimum impact-breakage routes for an ore. Powder Technology, Vol 54, pp.3-13.

Pennsylvania Crusher Corporation (2003); Crusher Selection, Handbook of Crushing - http://penncrusher.com/1sol1_3.html.

Rimmer, H.W., Swaroop, S., Flavel, M.D., Leverance, N.C. (1986); Equipment Sizing and Process Design Procedures for Crushing and Screening Circuits, Advances in Mineral Processing, (edited by P. Somasundaran), SME/AIME, pp. 575-593.

Rusiński, E. Przemysław Moczko, Damian Pietrusiak, Grzegorz Przybyłek (2013); Experimental and Numerical Studies of Jaw Crusher Supporting Structure Fatigue Failure, Journal of Mechanical Engineering, 59(2013)9, 556-563.

Sand, G. W. and Subasinghe, G. K. N. (2004); A novel approach to evaluating breakage parameters and modeling batch grinding. Miner. Eng., 17 (11-12), 1111-16.

Sastri, S.R (1994); Capacities and Performance Characteristics of Jaw Crushers, Minerals and Metallurgical Processing, Vol. 11, No. 2, pp. 80-86.

Shrivastava Ashish Kumar, Avadesh k. Sharma; A Review on Study of Jaw Crusher (2012); International Journal of Modern Engineering Research (IJMER) www.ijmer.com Vol.2, Issue.3, May-June; pp-885-888

Soni, R.K, C. Eswaraiah and B.K. Mishra; (2013); Analysis of model parameters dependency on breakage characteristics (www.researchgate.net/.../235997803

Umucu, Y, Vedat Deniz, Nazmi Unal (2013); An Evaluation of a Modified Product Size Distribution Model Based On T-Family Curves for Three Different Crushers; Physicochem. Probl. Miner. Process. 49(2), 2013, 473−480.

Wagner, W.J. (1990); Rating Crushers by Formula, Rock Products, February, pp. 48-51.)

Walker, William H.; Lewis, Warren K.; McAdams, William H.; Gilliland, Edwin R. (1937); Principles of chemical engineering. 1937: McGraw-Hill Book Company, inc.

Weedon, D.M. (2001); A perfect mixing matrix model for ball mills. Minerals Engineering, Vol 14, No.10, pp.1225-1236.

Weiss, N.L. (1985); Jaw Crushers, SME Mineral Processing Handbook, ch. 3B-1, (edited by N.L. Weiss), SME/AIME, New York.

Whiten, W.J. (1972); The simulation of crushing plants with models developed using multiple spline regression; Journal of the South African Institute of Mining and Metallurgy, May 1972.

Wills, B.A. and Napier-Munn, T. (2005); Comminution, in Wills' Mineral Processing.

Technology (Seventh Edition), Butterworth-Heinemann: Oxford. p. 108-117.

Wolny, S. (2013); Dynamic Behaviour of a Vibrating Jaw Crusher for Disintegration of Hard Materials; Archives of metallurgy and Materials; Volume 58, Issue 3.

Nigerian Journal of Renewable Energy Research
Volume 1, Number 1, pp 55-65, 2023
 eISSN 1597-8907: pISSN 1597-8877

UTILISING THE INNOVATIVE PROPORTIONAL NODES CURVE FITTING TECHNIQUE TO ESTABLISH CORRELATIONS FOR THE DYNAMIC VISCOSITY OF AMMONIA-WATER SOLUTION

[1,2,*]Mumah S. N., [3]Nwafulugo F.U., Akande H.F.[1,2] and S. Alexander[4]
[1]TETFund Centre of Excellence for Renewable Energy, Kaduna Polytechnic, Kaduna, Nigeria
[2]Department of Chemical Engineering, Kaduna Polytechnic, Kaduna, Nigeria
[3]Department of Chemical Engineering, Federal, Polytechnic, Oko, Anambra State, Nigeria
[4]Department of Marketing, Kaduna Polytechnic, Kaduna, Nigeria

[*]Corresponding author: *mumahsndoyi@kadunapolytechnic.edu.ng*
https://doi.org/10.5281/zenodo.11501500
https://www.njrer.org/download/vol_1_No_1_pap_4.pdf

ARTICLE INFORMATION

Article history:
Received 28 Jun, 2023
Revised 26 Sep, 2023
Accepted 03 Oct, 2023
Available online 30 Dec, 2023

Keywords:
Correlations
Proportional nodes
Curve fitting
dynamic viscosity
ammonia-water solution

Abstract

This work employed a novel curve fitting technique called the "Proportional Nodes Method" to correlate data for the dynamic viscosity of an ammonia-water solution. This methodology combines polynomial equations that are produced at different temperatures with those that are computed at certain mole fraction nodes. The dynamic viscosity changes at various temperatures at particular mole fractions are taken into consideration by these scaling factors, or nodes. With R^2 values ranging from 0.999663 to 0.99985, the polynomial equations offered a high degree of fitting accuracy. Once the proportional nodes equation was determined, it was combined with equations of the boundary data to form a strong and very accurate polynomial model. The model demonstrated a high degree of predictive accuracy by displaying low average percentage deviation between the anticipated and real viscosity values. Academic and industrial research can both benefit greatly from the Proportional Nodes Method. It offers a more accurate and flexible model for estimating the dynamic viscosity of ammonia-water solutions, which is essential for developing and optimising a range of industrial applications, such as refrigeration systems.

1.0 Introduction

When evaluating the limitations of the data, data fitting provides the user with a mathematical function that most closely matches a set of data points. An equation that fits a given set of data points so that the departure of the points from the equation is as small as possible is found using a process called curve fitting. Polynomial regression is a technique for fitting two or three-dimensional data. Efficient design, simulation, and optimisation of chemical processes need the establishment of accurate data correlations. Many correlation-generating techniques are available for data fitting. However, they differ in terms of accuracy and complexity.

This paper presents the 'Proportional Nodes Method,' a unique curve-fitting technique, and assesses its efficacy. Mumah (2021) introduced us to the proportional nodes approach. The method is used to determine the ammonia-water solution's dynamic viscosity. For refrigeration system design and optimisation, one important component that is required is the dynamic viscosity of the ammonia-water solution. Based on temperature and composition, the viscosity of such a solution has already been described by polynomial equations in previous research (Kumar and Gardas, 2010). When it comes to temperature variations, these models, however, are not very flexible, which could result in inaccurate predictions.

2.0 Methods

The usefulness of the Proportional Nodes Method is illustrated in this work by the use of data for the dynamic viscosity of ammonia-water solution at different temperatures and mole fractions, as reported by Conde-Petit (2006). This method combines polynomial equations that are derived at any temperature with those that are calculated at certain mole fraction nodes. These scaling factors, or nodes, take into consideration differences in the dynamic viscosity at various temperatures and mole fractions.

In order to account for changes in dynamic viscosity at various temperatures for a given mole fraction, these proportional nodes function as scaling factors. This work fills a major vacuum in the literature by presenting a technique that provides more accurate and temperature-adaptive predictions for the ammonia-water solution's dynamic viscosity. This study, which makes a substantial contribution to the academic community as well as relevant companies, verifies the robustness and high dependability of the proposed model by reaching R^2 values very near to 1 and minor variations between anticipated and actual values.

3.0 Results

The dynamic viscosity values of an ammonia-water solution, as reported by Conde-Petit (2006), were used in this investigation. For different mole fractions, they are presented in Table 1 and clearly show a decrease in dynamic viscosity as the temperature rises. This is a typical characteristic seen in fluids, where a rise in temperature tends to lower the viscosity by lowering the internal resistance to flow (Lide, 2005).

Table 1. Dynamic Viscosity of Ammonia-Water Solution for various temperatures and mole fraction

T (K)	Mole fraction (-)										
	0	**0.1**	**0.2**	**0.3**	**0.4**	**0.5**	**0.6**	**0.7**	**0.8**	**0.9**	**1**
273.15	1.749E-03	2.122E-03	2.363E-03	2.301E-03	1.970E-03	1.500E-03	1.027E-03	6.492E-04	3.971E-04	2.478E-04	1.631E-04
283.15	1.328E-03	1.596E-03	1.771E-03	1.728E-03	1.490E-03	1.147E-03	7.982E-04	5.152E-04	3.233E-04	2.073E-04	1.367E-04
293.15	1.012E-03	1.201E-03	1.326E-03	1.297E-03	1.128E-03	8.811E-04	6.258E-04	4.144E-04	2.678E-04	1.769E-04	1.168E-04
303.15	7.819E-04	9.134E-04	1.002E-03	9.834E-04	8.651E-04	6.878E-04	5.004E-04	3.411E-04	2.274E-04	1.547E-04	1.023E-04

Although published publications typically do not show data in two versions, we have done so for specific reasons. Figure 1 illustrates how the dynamic viscosity of an ammonia-water solution varies for different mole fractions and temperatures.

Making polynomial equations for every curve is the next stage. Figures 2 to 5 display them. R^2 values that are extremely close to 1 suggest that the polynomial equations and coefficient of determination, R^2, produced by Microsoft Excel, as displayed in Table 2, offered a high degree of fitting accuracy. These R^2 values, which vary from 0.999663 to 0.99985, show that, for a given temperature, variations in the mole fraction of ammonia in the solution can account for more than 99.96% of the variance in dynamic viscosity. This excellent match is in line with earlier research on the viscosity of mixes of ammonia and water (Kumar and Gardas, 2010).

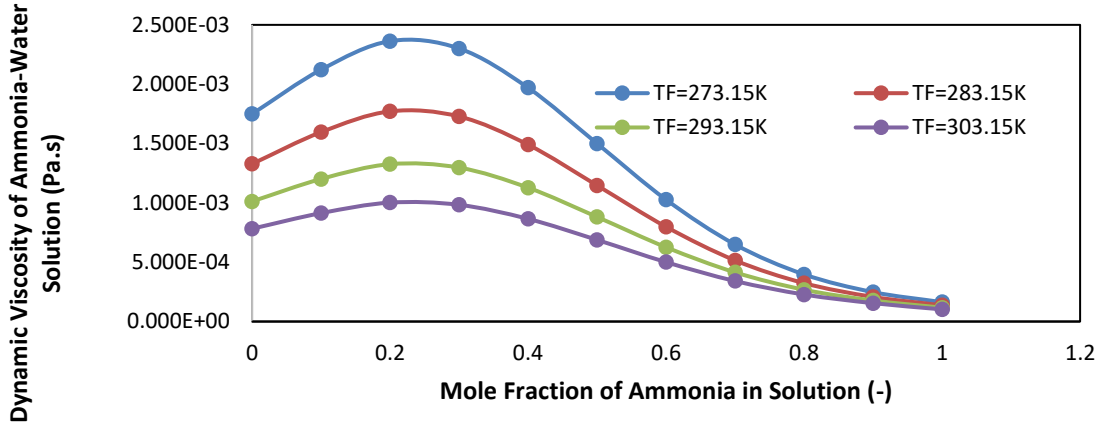

Figure 1. Variation of dynamic viscosity of ammonia-water solution for various mole fraction and temperatures

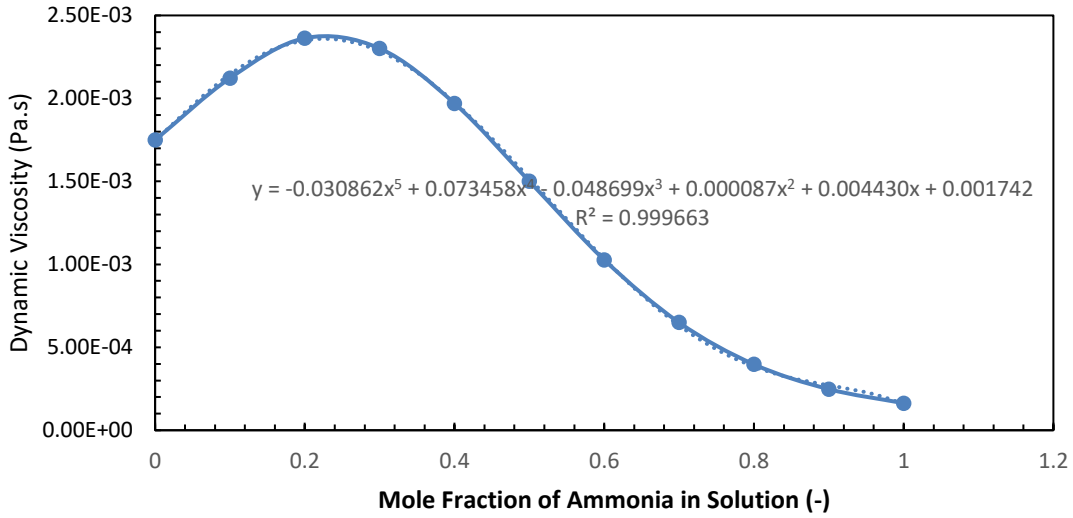

Figure 2. Equation at T = 273.15K

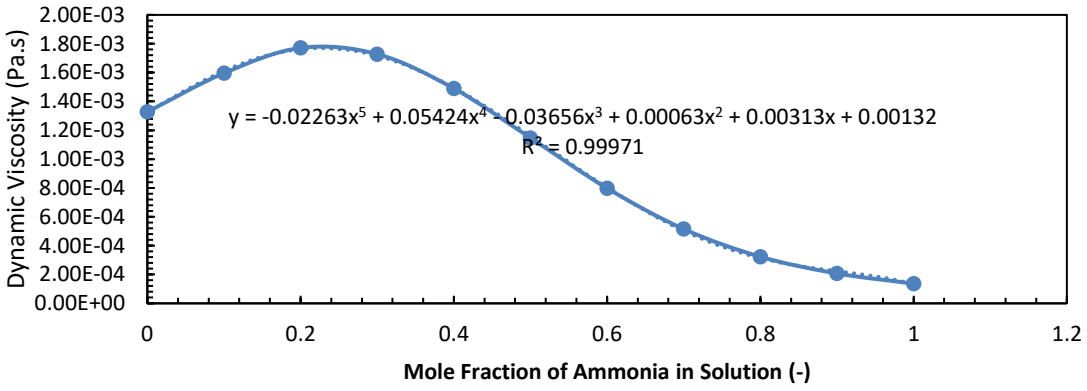

Figure 3. Equation at T = 283.15K

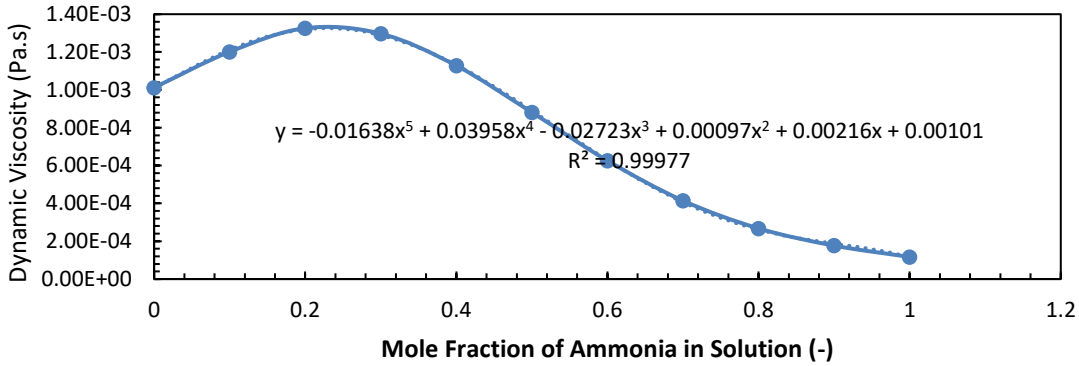

Figure 4. Equation at T = 293.15K

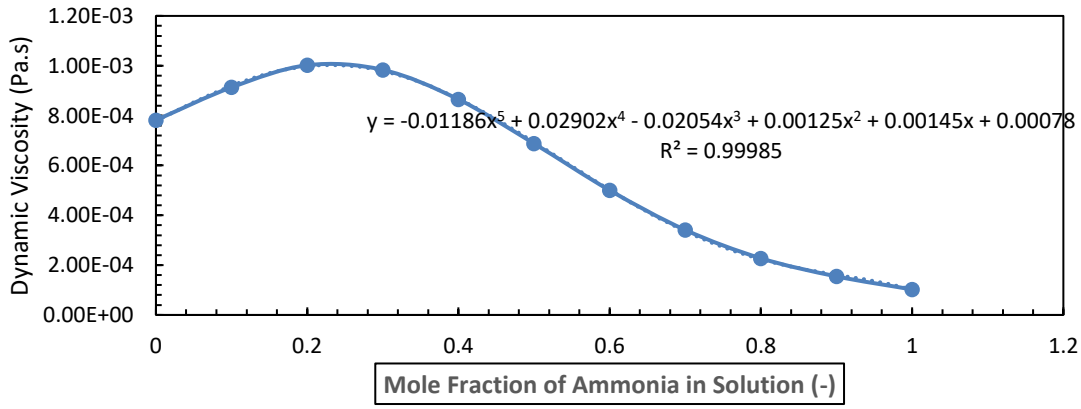

Figure 5. Equation at T = 303.15K

A fifth-order polynomial was employed to fit the data, as indicated by the equations produced at each temperature. The analysis's R2 values serve as a reference for selecting a fifth-order polynomial that remains constant at various temperatures. Observations show that the coefficients

of the polynomials vary with temperature, which makes sense given that temperature is a primary factor influencing viscosity.

To account for differences in the dynamic viscosity of the ammonia-water solution at different temperatures, the innovative concept of 'proportional nodes' was introduced in this study. This method was demonstrated by looking at the mole fraction that had the largest variation in dynamic viscosity, which was imagined to be 0.2 moles for demonstration reasons. It is for this reason that a pictorial illustration is required. To find the precise mole fraction, a computer programme can usually be created. Table 3 shows that the dynamic viscosity constantly decreases with increasing temperature, confirming the inverse relationship between temperature and viscosity that is frequently seen in fluid dynamics (Holman and Gajda, 2001).

Table 2. Equations and coefficient of determination for dynamic viscosity at each temperature

Mole Fraction of Ammonia in Solution	0	0.1	0.2	0.3	0.4	0.5	0.6	0.7	0.8	0.9	1
273.15K	1.749E-03	2.122E-03	2.363E-03	2.301 E-03	1.970 E-03	1.500 E-03	1.027 E-03	6.492 E-04	3.971 E-04	2.478 E-04	1.631 E-04
Generated Equation 1 and R^2 from Microsoft Excel	$\eta = -0.030862x^5 + 0.073458x^4 - 0.048699x^3 + 0.000087x^2 + 0.004430x + 0.001742$ $R^2 = 0.999663$										
283.15K	1.328E-03	1.596E-03	1.771E-03	1.728 E-03	1.490 E-03	1.147 E-03	7.982 E-04	5.152 E-04	3.233 E-04	2.073 E-04	1.367 E-04
Generated Equation 2 and R^2 from Microsoft Excel	$\eta = -0.02263x^5 + 0.05424x^4 - 0.03656x^3 + 0.00063x^2 + 0.00313x + 0.00132$ $R^2 = 0.99971$										
293.15K	1.012E-03	1.201E-03	1.326E-03	1.297 E-03	1.128 E-03	8.811 E-04	6.258 E-04	4.144 E-04	2.678 E-04	1.769 E-04	1.168 E-04
Generated Equation 3 and R^2 from Microsoft Excel	$\eta = -0.01638x^5 + 0.03958x^4 - 0.02723x^3 + 0.00097x^2 + 0.00216x + 0.00101$ $R^2 = 0.99977$										
303.15K	7.819E-04	9.134E-04	1.002E-03	9.834 E-04	8.651 E-04	6.878 E-04	5.004 E-04	3.411 E-04	2.274 E-04	1.547 E-04	1.023 E-04
Generated Equation 4 and R^2 from Microsoft Excel	$\eta = -0.01186x^5 + 0.02902x^4 - 0.02054x^3 + 0.00125x^2 + 0.00145x + 0.00078$ $R^2 = 0.99985$										

Table 3. Dynamic Viscosity Values of Ammonia-water Solution at 0.2 wt fraction for Various Temperatures

Temperature (K) (y Value)	Dynamic Viscosity (Pa.s) (x value)
273.15	2.363E-03
283.15	1.771E-03
293.15	1.326E-03
303.15	1.002E-03

The procedure for calculating the proportional nodes for each temperature is shown in Table 4.

The equation of the proportional nodes is gotten by applying Microsoft Excel. The details are extracted from Table 4 and is shown in Table 5.

Table 4. Procedure for calculating the proportional nodes

Temperature (K) (y value)	Dynamic viscosity (Pa.s) (X value)	Values of proportional nodes (x values)	
273.15=E	2.363E-03 =A	(A-A)/(A-D)	0.0000
283.15=F	1.771E-03 = B	(A-B)/(A-D)	4.35E-01
293.15=G	1.326E-03 = C	(A-C)/(A-D)	7.62E-01
303.15=H	1.002E-03 = D	(A-D)/A-D)	1.0000

Table 5. Proportional nodes data

Temperature (K)	Nodes
273.1500	0.0000
283.1500	4.35E-01
293.1500	7.62E-01
303.1500	1.0000

The Microsoft Excel plot of Table 5 is shown in Figure 6.

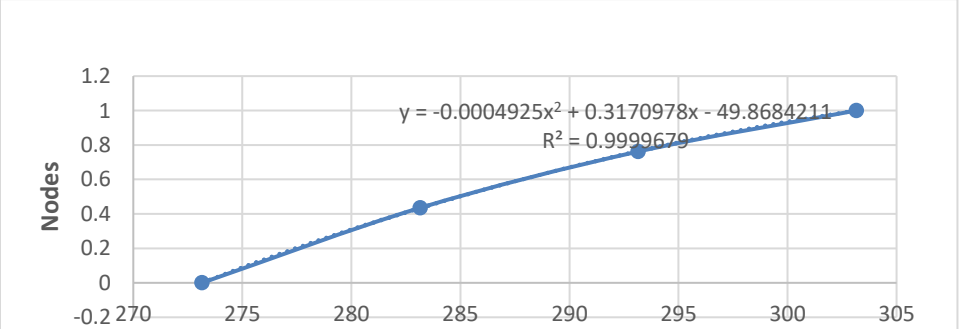

Figure 6. Plot of Nodes data

$$Nodes = -0.0004925\,T^2 + 0.3170978\,T - 49.8684211 \quad (1)$$
$$R^2 = 0.9999679$$

Table 4 describes the systematic process that was used to compute the proportional nodes. Equation (1), which shows the remarkable R^2 value of 0.9999679, illustrates how these nodes were used to create a second-degree polynomial. For a given mole fraction, this polynomial serves as a scaling factor by illustrating how the viscosity varies with temperature.

We have the proportional nodes equation and the equations for each line, as displayed in Table 2.

The importance of maintaining the polynomial's power at each temperature cannot be overstated while using this strategy. Furthermore, each process should continue to use the Microsoft Excel Trendline Option.

Therefore, Equation (2) gives the dynamic viscosity at any position within the temperature range.

η (Pa.s)= (Equation of enthalpy at point where nodes =0) - [(Equation of enthalpy at point where nodes =1) – (Equation of enthalpy at point where nodes =0)] x Nodes Equation* (2)

* Please note that the sign is minus and not plus because dynamic viscosity decreases as temperature increases.

The dynamic viscosity of ammonia water solution can be represented by;

$$\eta\ (Pa.s) = y = (-0.030862X^5 + 0.073458X^4 - 0.048699X^3 + 0.000087X^2 + 0.00443X + 0.001742)-((-0.030862X^5 + 0.073458X^4 - 0.048699X^3 + 0.000087X^2 + 0.00443X + 0.001742)-(-0.01186X^5 + 0.02902X^4 - 0.02054X^3 + 0.00125X^2 + 0.00145X + 0.00078))x\ Nodes \quad (3)$$

or

$$\eta\ (Pa.s)=(-0.030862X^5 + 0.073458X^4 - 0.048699X^3 + 0.000087X^2 + 0.00443X + 0.001742)-((-0.030862X^5 + 0.073458X^4 - 0.048699X^3 + 0.000087X^2 + 0.00443X + 0.001742)-(-0.01186X^5 + 0.02902X^4 - 0.02054X^3 + 0.00125X^2 + 0.00145X + 0.00078))\ (-0.0004925T^2 + 0.31709775T - 49.868421081) \quad (4)$$

Simplifying;

$-0.030862x^5 + 0.073458x^4 - 0.048699x^3 + 0.000087x^2 + 0.004430x + 0.001742$

-

There is a bracket here

$-0.030862x^5 + 0.073458x^4 - 0.048699x^3 + 0.000087x^2 + 0.004430x + 0.001742$ - $(-0.01186x^5 + 0.02902x^4 - 0.02054x^3 + 0.00125x^2 + 0.00145x + 0.00078)$	* $(-0.0004925T^2 + 0.31709775T - 49.868421081$

Subtracting first the coefficients in the bracket;

-0.030862	0.073458	-0.048699	0.000087	0.004430	0.001742
-					
-0.01186	0.02902	-0.02054	0.00125	0.00145	0.00078
=					
-0.01900	0.04444	-0.02816	-0.00116	0.00298	0.00096

Thus

$-0.030862x^5 + 0.073458x^4 - 0.048699x^3 + 0.000087x^2 + 0.004430x + 0.001742$
-
There is a bracket here

$-0.01900x^5 + 0.04444x^4 - 0.02816x^3 -0.00116x^2 + 0.00298x + 0.00096$	$* (-0.0004925T^2 + 0.31709775T - 49.868421081)$

Or;

$$\eta\ (Pa.s) = (-0.030862x^5 + 0.073458x^4 - 0.048699x^3 + 0.000087x^2 + 0.004430x + 0.001742) - (-0.01900x^5 + 0.04444x^4 - 0.02816x^3 - 0.00116x^2 + 0.00298x + 0.00096) * (-0.0004925T^2 + 0.31709775T - 49.868421081) \quad (5)$$

The average percentage difference (Sum of Percentage Difference/Number of Points) is calculated from these values in order to demonstrate that this equation satisfactorily represents the data. The percentage difference for values from correlation and actual values is calculated as $[(\eta_{actual} - \eta_{calculated})/ \eta_{actual}] * 100.0]$. Table 6 summarises the values.

Table 6. Percentage difference for dynamic viscosity values from correlations and actual values

Mole Fraction of ammonia in Ammonia in Solution	0	0.1	0.2	0.3	0.4	0.5	0.6	0.7	0.8	0.9	1
273.15K	1.749E-03	2.122E-03	2.363E-03	2.301E-03	1.970E-03	1.500E-03	1.027E-03	6.492E-04	3.971E-04	2.478E-04	1.631E-04
Calculated value from Proportional Nodes Method 273.15	0.001741086	0.002143045	0.002348	0.002283	0.001975	0.001517	0.001032	0.000632	0.000383	0.00027	0.000156
Percentage Difference $[(\eta_{actual} - \eta_{calculated})/ \eta_{actual}]*100.0$	0.452487	-0.99175	0.634786	0.782269	-0.25381	-1.13333	-0.48685	2.649415	3.550743	-8.95884	4.353158
Generated Equation 1 and R^2 from Excel	$\eta = -0.030862x^5 + 0.073458x^4 - 0.048699x^3 + 0.000087x^2 + 0.004430x + 0.001742$ $R^2 = 0.999663$										
Mole Fraction of Ammonia in Solution	0	0.1	0.2	0.3	0.4	0.5	0.6	0.7	0.8	0.9	1
283.15K	1.328E-03	1.596E-03	1.771E-03	1.728E-03	1.490E-03	1.147E-03	7.982E-04	5.152E-04	3.233E-04	2.073E-04	1.367E-04
Calculated value from Proportional Nodes Method 283.15K	0.001326272	0.001615056	0.001766	0.00172	0.001497	0.001162	0.000803	0.000504	0.000314	0.000223	0.000132
Percentage Difference $[(\eta_{actual} - \eta_{calculated})/ \eta_{actual}]*100.0$	0.13012	-1.19398	0.282326	0.462963	-0.4698	-1.30776	-0.60135	2.173913	2.876585	-7.57356	3.438186
Generated Equation 2 and R^2 from Excel	$\eta = -0.02263x^5 + 0.05424x^4 - 0.03656x^3 + 0.00063x^2 + 0.00313x + 0.00132$ $R^2 = 0.99971$										
Mole Fraction of Ammonia in Solution	0	0.1	0.2	0.3	0.4	0.5	0.6	0.7	0.8	0.9	1

293.15K	1.012E-03	1.201E-03	1.326E-03	1.297E-03	1.128E-03	8.811E-04	6.258E-04	4.144E-04	2.678E-04	1.769E-04	1.168E-04
Calculated value from Proportional Nodes Method 293.15K	0.001006214	0.001207676	0.001316	0.001286	0.001128	0.000887	0.000627	0.000406	0.000261	0.000186	0.000113
Percentage Difference $[(\eta_{actual} - \eta_{calculated})/\eta_{actual}]*100.0$	0.571739	-0.55587	0.754148	0.848111	0	-0.66962	-0.19175	2.027027	2.539208	-3135.16	3.253425
Generated Equation 3 and R^2 from Excel	$\eta = -0.01638x^5 + 0.03958x^4 - 0.02723x^3 + 0.00097x^2 + 0.00216x + 0.00101$ $R^2 = 0.99977$										
Mole Fraction of Ammonia in Solution	0	0.1	0.2	0.3	0.4	0.5	0.6	0.7	0.8	0.9	1
303.15K	7.819E-04	9.134E-04	1.002E-03	9.834E-04	8.651E-04	6.878E-04	5.004E-04	3.411E-04	2.274E-04	1.547E-04	1.023E-04
Calculated value from Proportional Nodes Method 303.15K	0.000780914	0.000920907	0.001	0.00098	0.000868	0.000694	0.000503	0.000337	0.000224	0.000161	0.0001
Percentage Difference $[(\eta_{actual} - \eta_{calculated})/\eta_{actual}]*100.0$	0.126103	-0.82187	0.199601	0.345739	-0.33522	-0.90142	-0.51958	1.201994	1.495163	-4.0724	2.248289
Generated Equation 4 and R^2 from Excel	$\eta = -0.01186x^5 + 0.02902x^4 - 0.02054x^3 + 0.00125x^2 + 0.00145x + 0.00078$ $R^2 = 0.99985$										

The average percentage difference for the surface (Sum of percentage deviation/Number of points) is calculated from values in Table 6 and presented in Table 7.

Table 7. Values of percentage deviation for various temperatures and mole fractions

	Mole Fraction										
Temp (K)	**0**	**0.1**	**0.2**	**0.3**	**0.4**	**0.5**	**0.6**	**0.7**	**0.8**	**0.9**	**1.0**
273.15	0.452487	-0.99175	0.634786	0.782269	-0.25381	-1.13333	-0.48685	2.649415	3.550743	-8.95884	4.353158
283.15	0.13012	-1.19398	0.282326	0.462963	-0.4698	-1.30776	-0.60135	2.173913	2.876585	-7.57356	3.438186
293.15	0.571739	-0.55587	0.754148	0.848111	0	-0.66962	-0.19175	2.027027	2.539208	-5.14415	3.253425
303.15	0.126103	-0.82187	0.199601	0.345739	-0.33522	-0.90142	-0.51958	1.201994	1.495163	-4.0724	2.248289
										Average percentage difference for the surface	±0.2614293

Equation (5) satisfactorily provides the final equation for determining the dynamic viscosity of the ammonia-water solution at any given temperature and mole fraction for the defined temperature range, as demonstrated by the very low average percentage difference for the surface.

4.0 Discussion

The correlation for determining the dynamic viscosity of the ammonia-water solution at any given temperature and mole fraction for the chosen temperature range is satisfactorily represented by Equation (5). Together with the proportional nodes equation, it includes the polynomial equations for the two extreme temperatures, 273.15K and 303.15K. In addition to being simpler, the derived

equation provides a reliable and extremely accurate model for estimating the dynamic viscosity of an ammonia-water solution under various circumstances.

Every created equation (as seen in Table 6) has R^2 values that range from 0.999663 to 0.99985, all of which are consistently very close to 1. This demonstrates how well the model can predict the dynamic viscosity of an ammonia-water solution under various circumstances. The obtained model's validity and dependability are further supported by these R^2 values, which demonstrate the model's good agreement with empirical observations (Motulsky and Ransnas, 1987). According to our findings, temperature and viscosity have an inverse connection, which is in line with previous fluid dynamics research (Bergman *et al.*, 2011). It is known, for instance, that rising temperatures typically cause viscosity to decrease because of the molecules' higher kinetic energy, which lowers internal resistance to flow (Incropera and DeWitt, 2002).

Table 7 tabulates the average percentage deviations between the calculated and real dynamic viscosity values over a range of temperatures and mole fractions. The strong agreement between the model's predictions and the actual observed data is confirmed by the normally very small percentage differences. The variances, which are noteworthy for not being systematic and varying about zero, suggest that the model's predictions are not biassed in any way.

5.0 Conclusion

The dynamic viscosity of an ammonia-water solution at different temperatures and mole fractions can be predicted using a thorough and extremely accurate model that is provided by this work. The model's remarkable predictive power and dependability are shown by the R^2 values, which are near to 1, and the small percentage variations between estimated and actual values under different scenarios. In summary, this research significantly advances our knowledge of and ability to compute the correlation for the dynamic viscosity of ammonia-water mixes. It also holds promise for a number of applications where such data arrangement for mixtures exists.

Acknowledgement

The authors wish to acknowledge the funds provided for this research and publication by TETFund Centre of Excellence for Renewable Energy, Kaduna Polytechnic, Kaduna, Nigeria. The funds were provided by the Tertiary Education Trust Fund (TETFUND), Nigeria, under the TETFUND Special Intervention for Establishment of Centre of Excellence (TETF/ES/DS&D/KADPOLY/COE /2021/VOL11).

References

Bergman, T. L., Lavine, A. S., Incropera, F. P., & DeWitt, D. P. (2011). Fundamentals of Heat and Mass Transfer (7th ed.). John Wiley & Sons.

Cheng, N. S. (2008). Formula for the viscosity of a glycerol-water mixture. *Industrial & Engineering Chemistry Research*, 47(9), 3285-3288. https://doi.org/xxxxxxx

Conde-Petit, M. (2006). Thermophysical Properties of NH_3/H_2O Mixtures for the Industrial Design of Absorption Refrigeration Equipment. A formulation for Industrial Use. M. Conde Engineering, Zurich, Switzerland

Holman, J. P., & Gajda, W. J. (2001). Experimental Methods for Engineers (7th ed.). McGraw-Hill.

Incropera, F. P., & DeWitt, D. P. (2002). *Introduction to Heat Transfer* (4th ed.). John Wiley & Sons.

Kumar, A., & Gardas, R. L. (2010). Viscosity of aqueous ammonia solution at high pressures. *Journal of Chemical Engineering Data*, 55, 3983-3986. https://doi.org/xxxxxxx

Lide, D. R. (2005). CRC Handbook of Chemistry and Physics (86th ed.). CRC Press.

Motulsky, H., & Ransnas, L. (1987). Fitting curves to data using nonlinear regression: A practical and nonmathematical review. *FASEB Journal*, 1(5), 365-374. https://doi.org/xxxxxxx

Mumah, S.N. (2022). Introduction of a novel curve fitting approach: The use of Proportional Nodes [Unpublished Research and Innovation Report].Kaduna Polytechnic, Kaduna, Nigeria

Nigerian Journal of Renewable Energy Research
Volume 1, Number 1, pp 66-81, 2023
 eISSN 1597-8907: pISSN 1597-8877

PERFORMANCE EVALUATION OF AN ACTIVE SOLAR STILL UNDER FORCED CIRCULATION MODE

[1,2]Tanimu Garba Ibrahim, [1,3,*]S. N. Mumah, [4]Nwafulugo F.U, [1,3]H.F. Akande and [5]Abdullahi Ismail Belli[3]

[1]TETFund Centre of Excellence for Renewable Energy, Kaduna Polytechnic, Kaduna, Nigeria
[2]Department of Mechanical Engineering, Kaduna Polytechnic, Kaduna, Nigeria
[3]Department of Chemical Engineering, Kaduna Polytechnic, Kaduna, Nigeria
[4]Department of Chemical Engineering, Federal Polytechnic, Oko, Anambra State, Nigeria
[5]Department of Electrical & Electronics Engineering, Kaduna Polytechnic, Kaduna, Nigeria

[*]Corresponding author: *mumahsndoyi@kadunapolytechnic.edu.ng*
https://doi.org/10.5281/zenodo.11501394
https://www.njrer.org/download/vol_1_No_1_pap_5.pdf

ARTICLE INFORMATION

Article history:
Received 21 Jun., 2023
Revised 24 Sep., 2023
Accepted 13 Oct., 2023
Available online 20 Oct., 2023

Keywords:
Solar Still
Forced Circulation
Design
Performance Evaluation

Abstract

Water is essential to human survival and well-being on Earth. In Nigeria, getting access to clean water is a big problem for many rural and urban people. The increasing population of Nigeria coupled with evident socio-economic issues would pose a persistent difficulty for communities to supply clean water to suit the needs of their entire populace. There is an urgent need to build self-sustaining systems in order to meet the growing demand for freshwater resources. The solar distillation technique appears to be a viable option among the traditional distillation methods for meeting the current freshwater demand. This is particularly true in places like the artisanal mining districts of Northern Nigeria where the water table is already tainted or polluted. This effort was done with the intention of designing and building a solar water distillation system that can clean water from different sources. These sources include runoff from residential structures and plants, streams, rivers, and tainted wells and boreholes. By using solar water distillation, contaminants including salts and heavy metals like lead, arsenic, and mercury are removed, along with microbiological organisms. The country's rural areas face issues with portable water and electricity, which led to the design and construction of a Solar Still. The polluted water in the basin is heated by the sun's incoming radiation, which causes the water to evaporate and condense into pure drinking water. A double slope active solar still of the basin type was designed, built, and its performance assessed in this paper. to ascertain the still's efficiency.

1.0 Introduction

The necessity of maintaining good health has led to an increase in the requirement for clean drinking water over time. Pressure on the quantity and quality of water resources is rising as a result of rapid economic growth and climate change, particularly in tropical and developing

nations. There is usually enough water available, but it needs to be treated because it is brackish and saline. In Nigeria, the majority of people lack access to clean drinking water. This is especially true in places where artisanal mining is widespread.

Toxic compounds are emitted into the environment throughout many of the methods employed by artisanal miners, posing a serious risk to the health of the miners, their families, and the neighbouring populations. For example, the amalgamation of mercury used in gold mining processes to extract gold from ores makes them extremely hazardous. In addition, these substances end up in the water table, contaminating other water sources including wells. Because of the associated costs, most State governments find remediation to be quite expensive.

Because they have a tendency to bioaccumulate, heavy metals are harmful. When a chemical's concentration in a biological organism rises over time relative to its concentration in the environment, this is referred to as bioaccumulation. Damage to the blood composition, lungs, kidneys, liver, and other essential organs, as well as diminished or impaired mental and central nervous system function, can all be consequences of heavy metal poisoning. Prolonged exposure can cause slowly developing neurological, musculoskeletal, and physical degenerative processes that resemble multiple sclerosis, Parkinson's disease, Alzheimer's disease, and muscular dystrophy. According to the International Occupational Safety and Health Information Centre (1999), exposure to certain metals or their compounds over an extended period of time can lead to allergies and even cancer. The two most damaging elements to the growing brain are lead and mercury (http://www.purewaterservices.co.nz/contaminants/other-contaminants-issues/heavy-metals):

1. Early lead exposure increases the risk of attention deficit disorder and lowers reading and learning abilities in children compared to peers.
2. Learning disabilities are observed in children exposed to mercury at above-average levels.
3. According to recent research, arsenic may also be harmful to the growing brain.
4. These metals are known to have numerous other negative health impacts.

While it can be more affordable, emerging distillation technology powered by renewable energy is seen as a viable alternative for supplying water. It also has the potential to significantly improve the lives of those who live in tiny towns in isolated and rural locations.

Numerous academics have conducted studies on the architecture, manufacturing processes, and performance evaluation of solar distillation. According to Kabeel and El-Agouz's (2011) investigation, preheating the water in the collector can result in a 33% improvement in the distillate production. This system is an active system of a traditional solar still integrated with a flat plate collector operating in thermosiphon mode. Mink *et al.* (1998) have presented an air-blown, multiple effect solar still with heat energy recycle to boost yield. By simulating the relationship between the distillate yield and the evaporation area, Kwatra (1996) demonstrated that a larger evaporation area results in a higher yield. In their 1999 study, Khalifa *et al.* examined the impact of feed water preheating on solar stills with single and double slopes, and they found that preheating improved the solar still's yield output and efficiency. The convective mass transfer relation for a double condensing chamber solar still was derived by Sethi and Dwivedi (2013). Regression analysis was used to find the values of C and n in the relation Nu = C(GrPr)n for a variety of temperature ranges. It was discovered that the values of C and n suggested by Dunkle

(1961) are only true for lower temperature ranges; for higher temperature ranges, the values of C and n vary. A novel empirical methodology for calculating mass flow rates in single slope solar stills is proposed by Rubio *et al.* (2000), after they assessed the distillate production for a double-slope solar still under controlled settings for basin water and collector temperatures within typical operating ranges. In order to forecast the productivity of a single-slope solar still, Nafey *et al.* (2001) investigated the several factors influencing solar still performance and created an equation linking the dependent and independent variables.

Tripathi and Tiwari (2005) constructed thermal models to establish the energy balance equations of both active and passive solar stills, and they validated the theoretical results with experimental data. The effects of sponge cube were researched by Abu-Hijleh *et al.* (2003), who demonstrated a significant improvement in the daily production of solar still. The efficiency and fresh water production rate of a stepped solar still with integrated latent heat storage improved, according to Radhwan's 2005 study. In their 2009 study, El-Sebaii *et al.* (2009) investigated an analytical solution of the energy-balance equations for the thermal performance of a triple-basin solar still and discovered that, during the day, the bottom basin's productivity is greater than the upper basins' productivity. Exergetic efficiencies for solar-powered distillers are less than 4% for single-effect systems, 17–20% for double-effect systems, and 19–26% for triple-effect systems, according to research done by Sow *et al.* (2005). By building a plastic solar still and examining how water depth affects mass and heat transmission, Stephen *et al.* (2012) discovered that distillate output of 2.1 L/m2/day could be attained in a still basin with a water depth of 0.02 m. According to Lindblom (2010), utilising black granite gravel in a single slope solar still can increase efficiency to a maximum of 52%, which is 8% more than in a traditional single slope solar still. A new mass and heat transfer model for a tubular solar still was proposed by Ahsan and Fukuhara (2009, 2010). It included different mass and heat transfer coefficients and took into consideration the humid air qualities inside the still.

Stephen *et al.,* (2012) investigate how a double slope sun still's production is affected by its direction and the depth of the water in its basin, contrasting it with that of a single slope solar still. The authors replaced the traditional collectors with GI plate sandwiched collectors in their work on a new solar collector design, and they compared the steady state outlet temperature and efficiency.

2.0 Importance of Solar Stills

The results of mathematical and practical models have demonstrated that full insulation, minimum wind speed, and high insulation intensity are necessary for solar-powered systems to operate at their peak efficiency. Nigeria's climate satisfies these requirements. There is an urgent need to build self-sustaining systems to fulfil the growing demand for freshwater resources. The solar distillation technique appears to be a viable option among the traditional distillation methods for meeting the current freshwater demand. Microbiological organisms and contaminants like salts and heavy metals are eliminated using solar water distillation. One may classify the water generated by the procedure as pharmaceutical grade.

The most promising method for using solar energy to purify water from contaminated wells, polluted water sources contaminated by crude oil, and salty seawater is to use solar stills. This method essentially removes impurities from these contaminated sources, such as dirt,

microorganisms, salt, and crude oil and its related constituents, to produce purified water. It is among the most crucial ways to obtain drinkable water. The utilisation of solar energy in renewable energy-based solar stills is not only infinite, clean, and readily available, but it is also far more cost-effective than using fossil fuels (Stephen *et al.*, 2012). An enhanced solar still that can generate purified water from several sources has been created and assessed in order to justify the usage of this energy source in water purification techniques. It is suggested to use two solar heat gathering systems. We anticipate that this setup will increase the still's overall effectiveness. Furthermore, the entire apparatus on the constructed rig will run on solar power, enabling installation in remote areas without access to electricity.

In this work, distillate output and instantaneous thermal efficiency at various water depths were computed, and a double slope active solar still operating in forced circulation mode was developed and built.

3.0 Design View/ (Isometric Sketch)

The isometric, Orthographic Projections and exploded view are shown in Figures 1a to 1f.

4.0 Design Assembly

The Complete Design Assembly is presented in Figure 2.

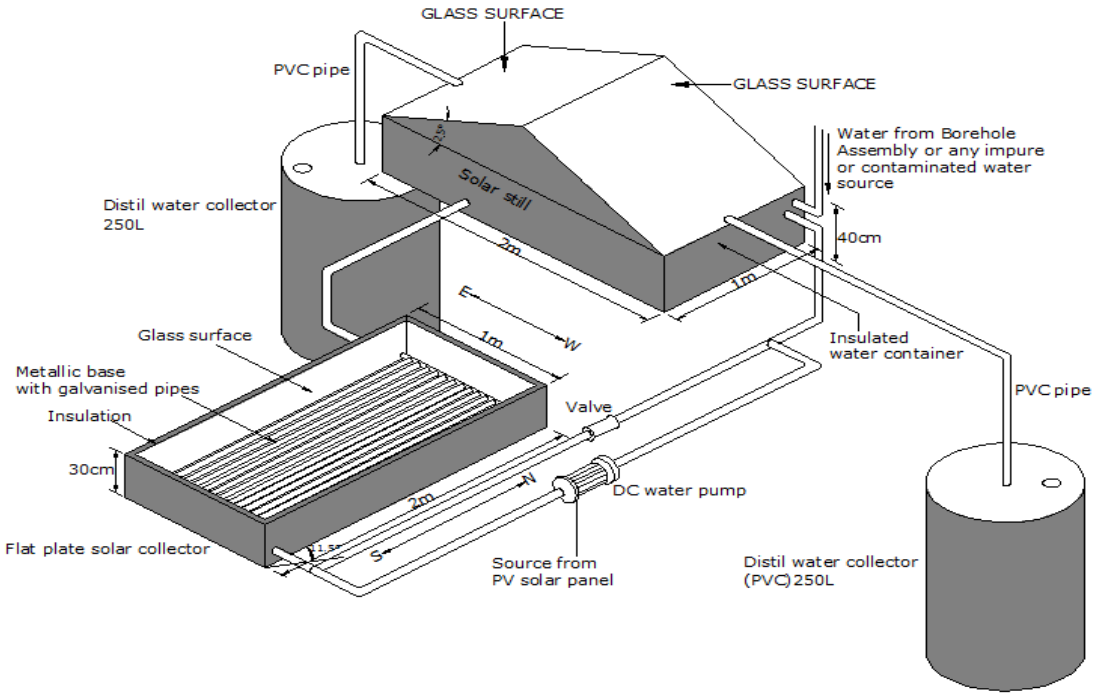

Figure 1a. Isometric Sketch of key components (solar Still and Flat Plat Solar Collector)

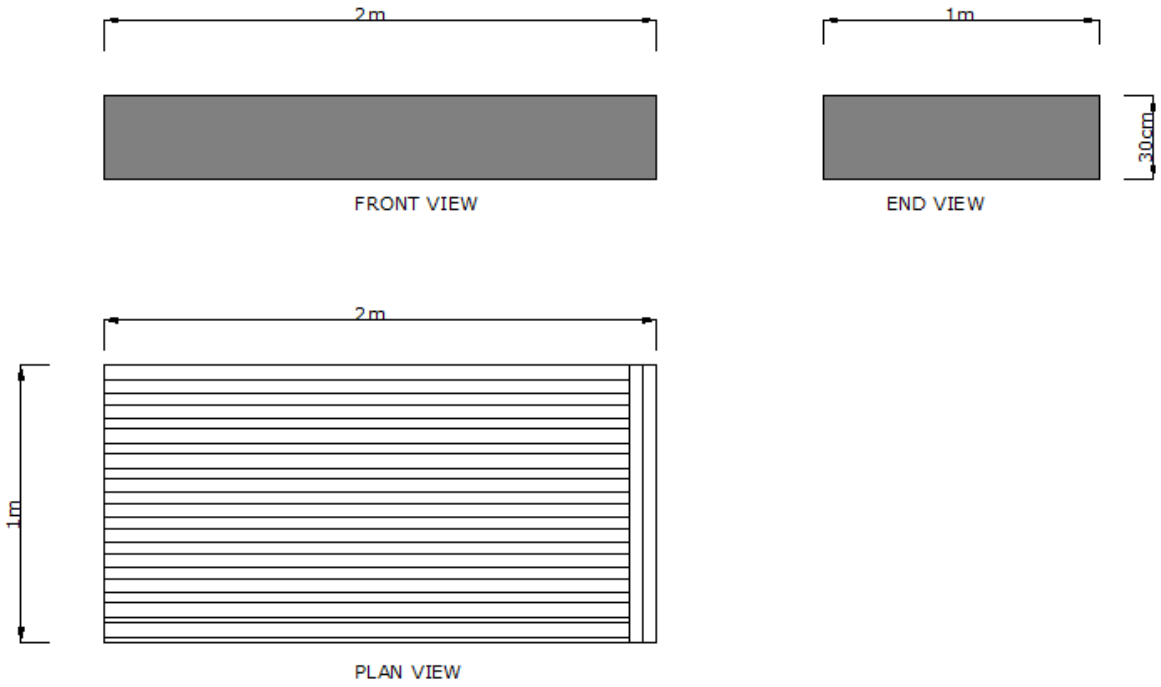

Figure 1b. Orthographic Projection of Solar Collector

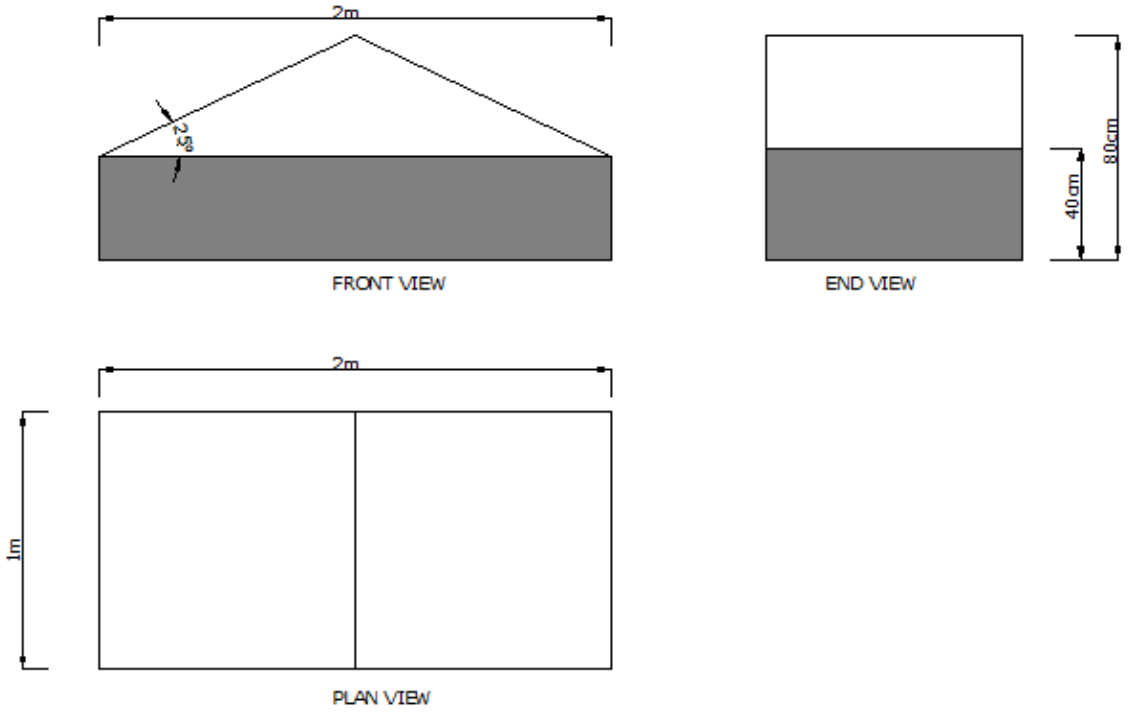

Figure 1c. Orthographic Projection of Solar Still

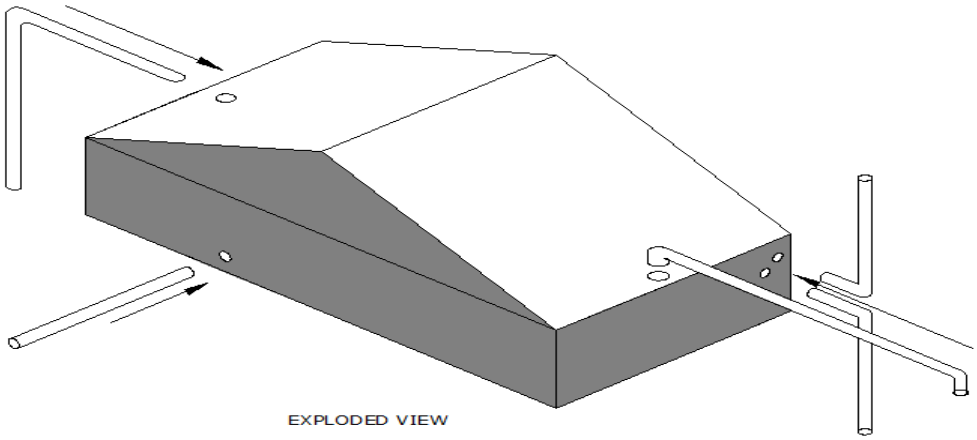

Figure 1e. Exploded Diagram for Solar Still

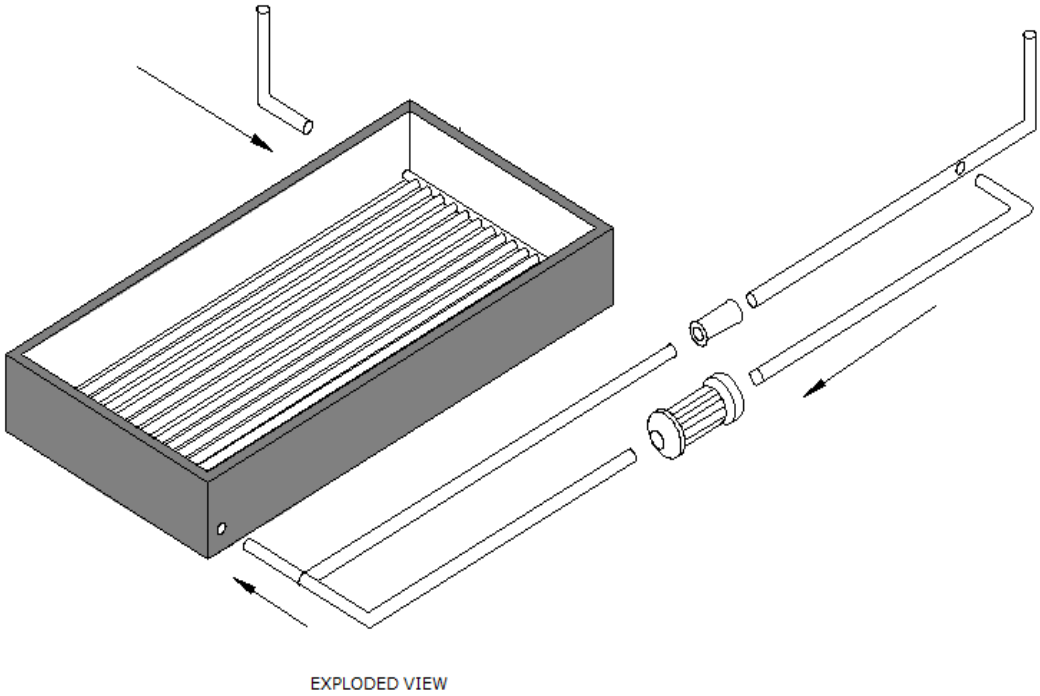

Figure 1f. Exploded Diagram for Solar Collector

5.0 Basic Operation of Solar Still

The still is filled to a predetermined level with water to be purified. Because the surface of the still is coated with a black material to maximise the absorption of solar heat, solar radiation is able to travel through the glass cover and reach the bottom, where it is mostly absorbed by the base. The moisture content of the air trapped between the water's surface and the glass cover increases as the

water starts to heat up. Water from the basin evaporates when it is heated and condenses on the inside of the glass lid. Only condensed water trickles through the slanted glass cover in the downward direction of the collection trough and is kept in the bottle during this process, as the pollutants present in the original water settle in the base itself. The solar still's basin needs to be cleaned daily to get rid of contaminants and settled salt. We can absorb more heat energy without wasting it if we only remove these.

6.0 Materials and Method of Fabrication

As shown in the schematic diagrams (Figure 1a to 1e), the distillation set-up consisted of four main parts:

i. A solar still without any moving parts. Solar still basin will be made up of a fiber reinforced plastic (FRP) to withstand the harsh conditions produced by water and sunlight. The advantages of FRP over other reinforcing materials such as glass fiber, carbon fiber etc are their specific strength properties, easy availability, light weight, high toughness, non-corrosive nature, low density, good thermal properties, renewability and biodegradability.
ii. A Flat-plate collector which is a metal box with a glass cover (called glazing) on top and a black-colored absorber plate on the bottom. The sides and bottom of the collector will be insulated to minimize heat loss.
iii. A DC water pump powered by solar energy from a solar panel and inverter system.
iv. The distillate water will collect in a plastic channel fixed at the lower end side of both the glass covers. The distillate collected is continuously drained through flexible pipe and stored in dedicated containers placed outside on both sides.

7.0 Measuring Instruments: Measurement of temperature:

The temperature of the condensing cover and water vapour were measured using copper-constantan thermocouples. Zeal thermometer (standard thermometer) was used to aid calibrate the thermocouples employed in the setup. A mercury thermometer that has been calibrated will be used to record the ambient air temperature.

Measurement of solar radiation: The solar intensity was measured with the help of a calibrated solarimeter, having least count of 20 W/m^2.

Setup: In an active solar still, the flat plate collector is often connected to the solar still in a way that allows hot water from the collection plate to reach the basin of the still when it is in forced circulation mode. The connectors for the collection plate's input and outlet were removed from the basin's bottom. The input pipe featured a valve to regulate the flow of water via the collecting plate. Water running through tubes receives energy from the sun that is absorbed by the collecting plate. In order to receive the most solar radiation possible, the double slope solar still was positioned east-west, and the collector plate was inclined at 11.5o (Kaduna's latitude) facing south.

8.0 Fabricated Equipment

Figures 2a to2d show the pictorial view of the fabricated equipment. Table 1 shows a summary of the materials used in the fabrication.

Table 1. Summary of the Materials Component of the Solar Still Considered

S/No	Component	Material(s)	Properties and Comments
1	Collector/Glazing (Trans- parent)	Plastic Glass	• Low water absorptance • High thermal conductivity • Transparent to short wave radiation (Transmittivity = 0.9) • Low iron content • Can withstand the effect of weather, wind, sunshine, rain, dust, etc
2	Basin (Absorber)	Galvanized Iron	• High radiation absorptivity • Stable to corrosion • High thermal conductivity
3	Solar Reflector	Galvanized Iron	• Minimum corrosion problem • High thermal conductivity • High reflectivity • Cheaper and readily available
4	Cover (Casing)	Plywood/iron	• Has uniform strength • Has no cleavage • Very durable even though it is more expensive than hard wood • Stronger, Light weight and cheaper • Good insulator
5	Insulator	Fiber Glass	• Very cheap • Poor conductivity and radiation of heat • Very effective for insulation
6	Sealant	(i) Araldite (ii) Putty	• Can withstand high temperature • Good resistance to organic liquids • Joint bounded with it are difficult to break • Slow curing epoxy • Poor adhesive strength • Soften under high temperature • Cheap and readily available
7	Drain Pipe	PVC	• Stable to corrosion • Not poisonous to water • Cheap and readily available
8	Support Structure	Iron stand	• High tensile strength • Cheap and easily constructed
9	Collection trough	Rubber troughs	• Stable to corrosion • Not poisonous to water

Figure 2a. Pictorial view of Solar Collector before cover is placed on it

Figure 2b. Pictorial view of Solar Collector after Cover is placed on it

Figure 2c. Pictorial view of Solar Still built to Specification

Figure 2d. Pictorial view of Solar Collector and Solar Still connected together

9.0 Instrumentation

Pictorial views of the instruments and equipment used for various measurements are presented below.

<table>
<tr><td> 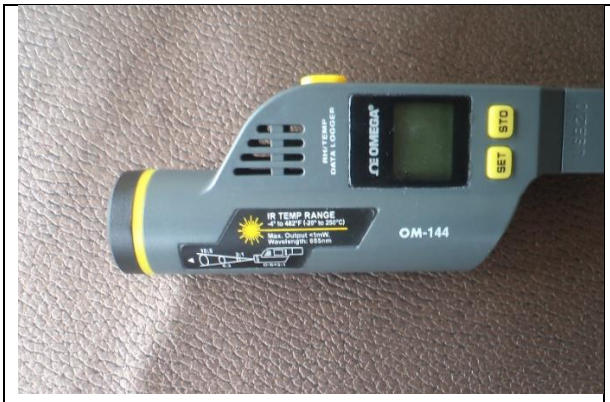
</td><td>  </td></tr>
<tr><td>Hygrometer/Ambient Temperature Analyser</td><td>Analog and Digital thermocouple readers</td></tr>
<tr><td> 
</td><td>  </td></tr>
<tr><td>Inverter</td><td>Thermocouple coils</td></tr>
</table>

	
Water flow Sensors	Solarimeter

9.0 Testing the Fabricated Setup

The following parameters have been be measured every half an hour for a period of 9 hours during each runs conducted. These details are very important parameters necessary for scale up:

i. Ambient Temperatures,
ii. Water temperature from the solar collector
iii. Solar Intensity
iv. Amount of distillate for various times of the day

The data generated during the testing of the fabricated rig is presented on Tables 1 to 3 and Figures 3 to 5.

Table1. Amount of pure distilled Water collected during Interval (litres)

Time	Day1	Day2	Day3	Day4	Day5	Day6	Day7	Average
9.00-9.30	0.12	0.09	0.11	0.15	0.12	0.08	0.11	
9.30-10.00	0.22	0.18	0.16	0.21	0.21	0.22	0.19	
10.00-10.30	0.29	0.27	0.26	0.23	0.28	0.28	0.26	
10.30-11.00	0.39	0.40	0.39	0.41	0.47	0.46	0.32	
11.00-11.30	0.40	0.45	0.48	0.49	0.55	0.47	0.37	
11.30-12.00	0.46	0.55	0.55	0.64	0.67	0.58	0.56	
12.00-12.30	0.79	0.82	0.80	0.87	0.86	0.91	0.75	
12.30-1.00	0.88	0.91	0.87	0.99	0.96	0.96	0.94	
1.00-1.30	0.98	1.02	1.07	1.14	1.17	1.11	0.94	
1.30-2.00	1.21	1.22	1.18	1.25	1.32	1.31	1.15	
2.00-2.30	1.09	1.19	1.19	1.29	1.25	1.25	1.12	
2.30-3.00	0.99	1.02	1.02	0.92	1.17	1.07	0.94	
3.00-3.30	0.71	0.81	0.81	0.81	0.98	0.90	0.79	
3.30-4.00	0.50	0.60	0.59	0.61	0.73	0.57	0.55	
4.00-4.30	0.34	0.31	0.30	0.32	0.43	0.33	0.27	
4.30-5.00	0.22	0.24	0.24	0.24	0.22	0.29	0.20	
Average Ambient Temperature (ºC)	33.5	30.2	32.3	30.6	29.5	30.2	31.3	**31.1**

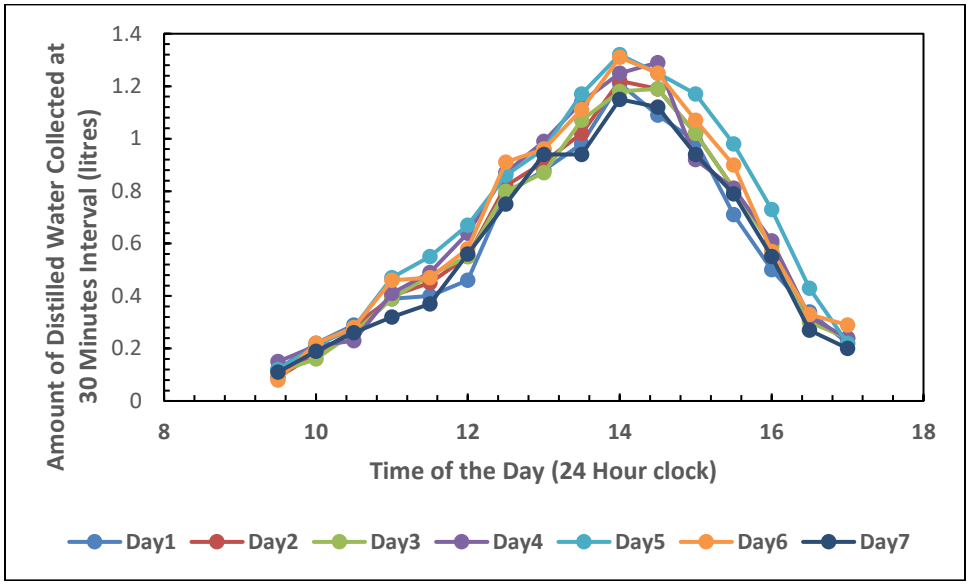

Figure 3. Amount of pure distilled Water collected during Interval (litres) for various times of the day for selected days in October, 2020

Table 2. Water temperature into still from solar collector (°C) for selected days in October, 2020

Time	Day 1	Day 2	Day 3	Day 4	Day 5	Day 6	Day 7
9.30	32.2	31.09	32.45	35.20	31.91	31.44	32.05
10.00	37.0	36.79	37.23	42.24	38.11	36.09	38.33
10.30	40.0	39.62	41.68	44.15	41.05	38.92	41.98
11.00	51.0	50.88	50.97	57.54	50.77	51.18	51.17
11.30	57.0	56.75	57.98	64.12	56.78	57.25	58.08
12.00	60.0	58.68	61.03	67.88	59.55	58.18	62.36
12.30	68.4	65.90	69.57	74.93	68.33	64.88	68.78
13.00	70.3	68.75	71.50	77.35	70.88	67.15	73.48
13.30	78.0	78.28	79.34	86.48	77.98	79.08	79.94
14.00	73.9	73.27	75.17	83.93	73.50	72.97	78.27
14.30	65.0	63.57	66.11	74.06	64.55	64.27	62.68
15.00	62.0	61.64	63.06	66.75	63.34	62.64	64.54
15.30	58.0	57.72	58.99	65.42	5755	57.02	58.99
16.00	47.0	45.57	47.80	53.56	47.67	44.47	47.80
16.30	40.5	40.2	41.19	45.90	40.99	41.22	40.19
17.00	38.0	37.36	38.65	41.24	37.94	36.16	37.05

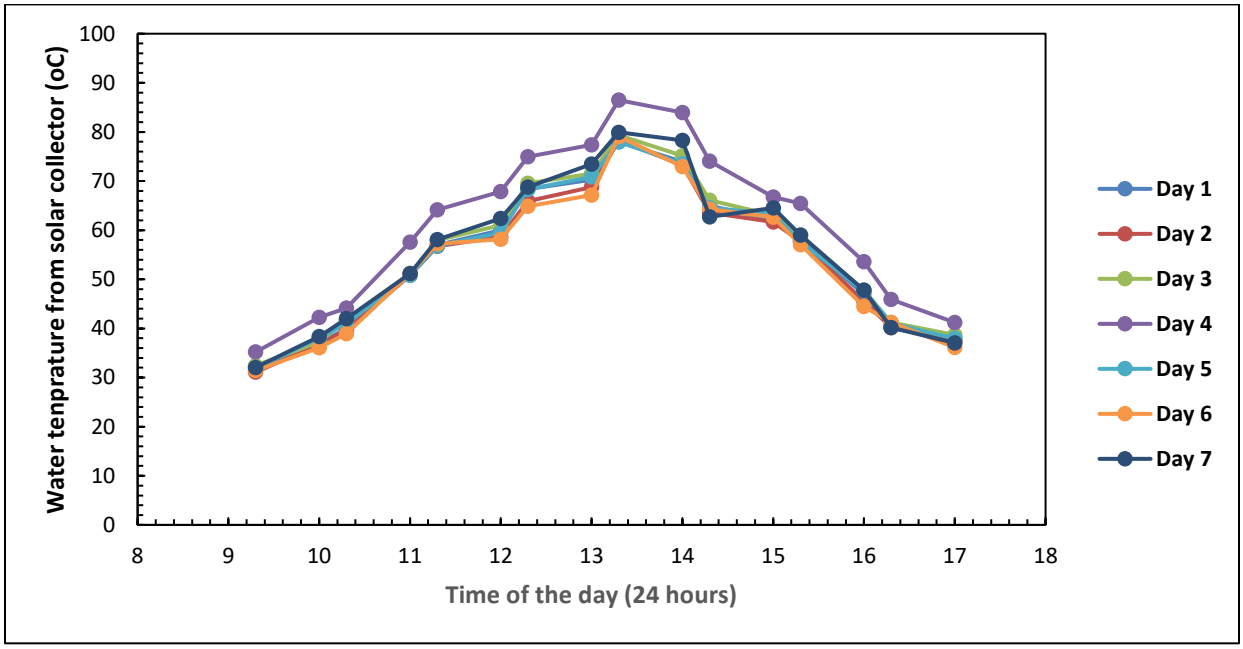

Figure 4. Water temperature into still from solar collector (^oC) for various times of the day for selected days in October, 2020

Table 3. Solar Hourly Global Radiation Values (W/m^2)- for selected days in October, 2020

Time	Day1	Day2	Day3	Day4	Day5	Day6	Day7
8.0	320.67	317.50	319.00	335.95	313.29	310.09	305.11
8.5	360.72	354.03	357.42	374.29	352.42	348.82	350.34
9.0	410.98	402.64	409.28	430.74	401.53	397.42	388.59
9.5	474.76	465.59	473.76	497.45	463.84	459.09	453.07
10	533.78	515.84	533.18	557.84	521.50	516.17	521.65
10.5	576.87	550.37	575.87	607.66	563.60	557.83	561.02
11	615.87	613.86	616.47	646.29	601.70	595.55	600.36
11.5	705.86	691.68	703.86	741.05	689.63	682.57	680.04
12	786.98	769.75	779.14	820.10	768.88	761.01	758.99
12.5	768.98	753.98	765.24	810.50	751.29	743.60	749.52
13	750.87	750.11	748.93	780.38	733.60	726.09	730.71
13.5	730.98	717.48	732.17	764.78	714.17	706.86	705.47
14	721.98	714.59	721.98	760.08	705.37	698.15	680.60
14.5	660.97	652.38	655.22	690.98	645.77	639.16	631.91
15	588.87	586.21	575.92	609.72	575.33	569.44	558.07
15.5	470.48	464.36	469.54	492.02	459.66	454.95	454.98
16	387.87	397.83	388.22	406.63	378.95	375.07	370.19
16.5	320.65	320.48	322.29	340.40	313.28	310.07	312.30
17	236.87	234.79	235.90	246.70	231.42	229.05	232.59

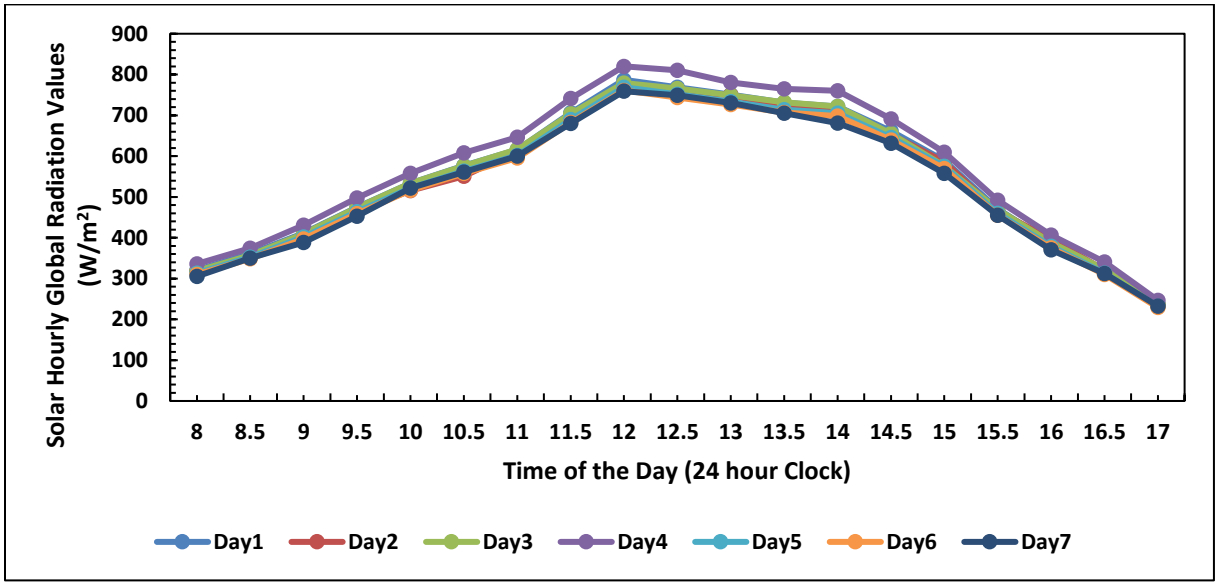

Figure 5. Solar Hourly Global Radiation Values (W/m^2) for various times of the day for selected days in October, 2020

10.0 Analysis of Data generated by the fabricated rig.

The distillate variation during a seven-day period is displayed in Table 1 and Figure 3. The average daily ambient temperature is also displayed in Table 1. The water temperature into the still from the solar collector is displayed in Tables 2 and 4 (oC), and the solar hourly global radiation values (W/m^2) for different times of the day are displayed in Tables 3 and 5. A solarimeter was used to measure the average solar intensity for each of the days that were taken into consideration, and type K thermocouples were used to create the temperatures.

Over the course of the seven days that were taken into consideration for the rig's testing, the average daily temperature was 31.1 °C. It was discovered from the daily measurement (Figure 5) that the hours of 8:00 am to 9:00 am are when the least amount of solar radiation is received, and this is also the time when the least quantity of distillate is obtained. Furthermore, it was noted that for the seven days under consideration, the largest distillate production was achieved between the hours of 1:00 pm and 2:00 pm, despite the fact that solar radiation was at its highest between 12:00 noon and 1:00 pm.

11.0 Conclusion

Lack of freshwater is a major problem in many Nigerian communities, particularly in remote and rural locations. The primary reasons for doing this review are this reality as well as the prevalence of untreated well water and water from streams and rivers in the majority of the nation. The outcomes produced by this construction demonstrate that single-effect solar stills are an affordable way to purify water in rural parts of the nation.

This study has demonstrated that utilising a solar still basin for water distillation is a cost-effective way to obtain portable drinking water in rural locations. Bacteria, salt, heavy metals, and other contaminants and impurities must all be totally eliminated throughout the distillation process.

Since solar stills don't require power, which is unavailable in the majority of Nigeria's rural areas, they have proven to be among the greatest water purifying technologies available.

The design's outcomes have consequences for creating a stable and effective single-slope solar still system. It is simple to adjust the inclination angle with this kind of construction. No matter where it is located, this has the ability and potential to create distilled water for residential, commercial, and industrial uses. The manufacturers advise mass producing this equipment so that it can be used in remote locations without access to portable drinking water.

Acknowledgement

The authors wish to acknowledge the funds provided for this research and publication by TETFund Centre of Excellence for Renewable Energy, Kaduna Polytechnic, Kaduna, Nigeria. The funds were provided by the Tertiary Education Trust Fund (TETFUND), Nigeria, under the TETFUND Special Intervention for Establishment of Centres of Excellence (TETF/ES/DS&D/KADPOLY/COE /2021/VOL11).

References

Abdulhaiy M. Radhwan (2004) Transient performance of a stepped solar still with built-in latent heat thermal energy storage**;** *Desalination* 171, pp 61–76

Ahsan, A. and T. Fukuhara (2009) Condensation mass transfer in unsaturated humid air inside tubular solar still. Ann. *J. Hyd. Eng*., 53: pp 97-102.

Ahsan, A. and T. Fukuhara (2010) Mass and heat transfer model of tubular solar still. *Solar Energy*, 84: 1147-1156.

Abu- Hijleh, B.A.K. and Rababa'h, H.M. (2003) Experimental Study of Solar Still with Sponge Cubes in Basin, *J. Energy Conversion and Management*, 44, pp 1411-1418.

Dinesh Kumar, Patel Himanshu and Zameer Ahmad (2013) Performance Analysis of Single Slope Solar Still; *International Journal of Emerging Technology and Advanced Engineering*, 3 (3)

Dunkle, R.V. (1961) Solar Water Distillation: The Roof Type Still and Multiple Effect Diffusion Still, International Developments in Heat Transfer, ASME (1961), *Proc. of Intl. Heat Trans. Conf., University of Colorado*, pp. 895-902.

El-Sebaii, A.A., A.A. Al-Ghamdi, F.S. Al-Hazmi, S. Faidah Adel (2009) Thermal performance of a single basin solar still with PCM as a storage medium; *Applied Energy*, 86, pp. 1187-1195

International Occupational Safety and Health Information Centre. Metals. *In Basics of Chemical Safety*, Chapter 7. Geneva: International Labour Organization.

Kabeel A E, S.A. El-Agouz (2011) Review of researches and developments on solar stills. *Desalination*, 276: pp 1–12.

Khalifa A. J.N, N, Al-Jubouri AS, Abed M.K. (1999) An experimental study on modified simple solar stills. *Energy Conversion and Management*; 40(18), pp 35–47.

Kwatra, H.S. (1996). Performance of a solar still: Predicted effect of enhanced evaporation area in yield and evaporation temperature, *Solar Energy* 56(3), pp 261-266.

Mink G., Aboabboude M.M. and Karmazsin E. (1998), *Solar Energy*, Volume 62, Issue 4, April 1998, pp 309-317

Nafey, A.S. M. Abdelkader, A. Abdelmotalip, A.A. Mabrouk (2001) Solar still productivity enhancement; *Energy Conversion and Management*, 42, pp 1401-1408

Patil B.L., Dr. J.A. Hole, Sagar Wankhede (2017) Parameters Affecting Productivity of Solar Still and Improvement Techniques: A Detailed Review; *International Journal of Engineering Technology, Management and Applied Sciences*, 5 (2)

Rubio E., Miguel A. Porta, José L. Fernández (August, 2000) Cavity geometry influence on mass flow rate for single and double slope solar stills *Applied Thermal Engineering*, Volume 20, Issue 12, 1 August 2000, Pages 1105-1111

Sethi, A.K. and V.K. Dwivedi (2013) Design, Fabrication, and Performance Evaluation of Double Slope Active Solar Still under Forced Circulation Mode; *Int. J. of Thermal & Environmental Engineering*; Volume 6, No. 1 pp 27-34

Somanchi, N. S., Sri Lalitha Swathi Sagi, Thotakura Ashish Kumar, .Sai Phanindra Dinesh Kakarlamudi and Ajay Parik, Modelling and Analysis of Single Slope Solar Still at Different Water Depth; *Aquatic Procedia*, Volume 4, 2015, Pages 1477-1482

Sow O, Siroux M. and Bernard Desmet (April 2005) Energetic and exergetic analysis of a triple-effect distiller driven by solar energy, *Desalination*, Volume 174, Issue 3, pp 277-286

Stephen, G., *et al.* (2012) *Low-Cost Solar Desalination Device*. Thesis Summary, Boston: North-eastern University

Tripathi, R., and Tiwari, G. N. (2005), Effect of Water Depth on Internal Heat and Mass Transfer for Active Solar Distillation; *Desalination*, 173, pp. 73–88

Nigerian Journal of Renewable Energy Research
Volume 1, Number 1, pp 82-101, 2023
 eISSN 1597-8907: pISSN 1597-8877

PRODUCTION OF BIO-OIL FROM BIOMASS USING FAST PYROLYSIS: A CRITICAL REVIEW

[1, 2,*]A.O. Kuye and [2]I. Edeh
[1]TETFund Centre of Excellence for Renewable Energy, Kaduna Polytechnic, Kaduna, Nigeria
[2*]Department of Chemical Engineering, University of Port Harcourt,
Port Harcourt, Nigeria

[*]Corresponding author: ayo.kuye@uniport.edu.ng
https://doi.org/10.5281/zenodo.11501426
https://www.njrer.org/download/vol_1_No_1_pap_6.pdf

ARTICLE INFORMATION

Article history:
Received 28 Jun, 2023
Revised 26 Sep, 2023
Accepted 03 Oct, 2023
Available online 30 Dec, 2023

Keywords:
Biofuel
bio-oil
biomass conversion
pyrolysis
fast pyrolysis

Abstract
Biofuels are liquid, gas and solid fuels produced from the conversion of biomass feedstock. The liquid product of this conversion through fast pyrolysis is a dark brown liquid known as bio-oil. The use of fast pyrolysis provides a higher yield of bio-oil compared to the other methods, such as gasification and combustion. The bio-oil produced can be readily stored, transported, and used as fuel and a source of chemicals. It is considered to be a relevant technology because; it provides energy security, environmental gains, economic stability and foreign exchange. Biomass is regarded as a renewable energy source with the highest potential to contribute to energy need of the modern society. The biomass resources in Nigeria include the following; wood, grasses, shrubs, animal wastes arising from forestry, agricultural, municipal and industrial activities as well as aquatic biomass. This review considers biomass feedstock and its conversion through fast pyrolysis to bio-oil. It further discusses various classifications of biofuel and bio-oil.

1.0 Introduction

The increasing industrialization and motorization of the world has led to a steep rise for the demand of petroleum-based fuels. Today fossil fuels take up 80% of the primary energy consumed in the world, of which 58% alone is consumed by the transport sector (Nigam and Singh, 2011). The sources of these fossil fuels are becoming depleted. Through its consumption, fossil fuels contribute significantly to greenhouse gas (GHG) emissions which can lead to many negative effects including climate change, receding of glaciers, rise in sea level, loss of biodiversity, etc. (Gullison *et al.,* 2007). The increasing energy consumption and GHG emissions have led to a move towards alternative, renewable, sustainable, efficient and cost-effective energy sources with lesser emissions. Four of the strategically important sustainable alternative energy sources are biofuels,

hydrogen, natural gas and syngas (synthesis gas). Within these four, biofuels are the most environment-friendly energy source.

The term biofuel refers to liquid, gas and solid fuels predominantly produced from biomass (Demirbas, 2006). Biomass can be defined as the biodegradable fraction of products, waste and residues from organic non-fossil material of biological origin that is readily available on recurring sustainable basis (Bridgewater, 1999). Biomass may be considered as the energy derived from plants, such as trees, grasses, agricultural crops/residues, organic fractions of municipal solid wastes, paper, cardboard, food waste, animal manure, green waste and other waste (Demirbas, 2009; Sambo, 2000). It is in abundance and stands as the third energy resource after oil and coal (Yaman, 2004; Radmanesh *et al.*, 2006). The significant advantage of using biomass is that it can be converted to liquid, solid and gaseous fuels (Yaman, 2004). It can also contribute to mitigating the effects of climate change as it will replace conventional fossil fuels (Radmanesh *et al.*, 2006; Tsai *et al.*,2005). Biomass availability in Nigeria is discussed in Section 2.

Various routes exist by which biomass can be converted into bioenergy and other industrial products. Such routes include: biological, chemical and thermal processes. Biological method involves the use of fermentation (bacterial and fungal) and anaerobic digestion, chemical processes involve the transesterification of oil to produce biodiesel, while thermal conversion processes include direct combustion, gasification and pyrolysis. These processes are described further in Section 3. Out of all these processes, pyrolysis produces energy fuels with high fuel-to-feed ratios, making it probably the most efficient process for biomass conversion and the method most capable of competing and eventually replacing non-renewable fossil fuel resources (Demirbas, 2006). Pyrolysis is discussed further in Sections 4 and 5.

The liquid product of the fast pyrolysis of biomass is called *bio-oil*. This *bio-oil* is a dark brownish viscous, free-flowing organic liquid that is made up of highly oxygenated compounds, which bear some resemblance to fossil crude oil (Czernik and Bridgwater, 2004). The synonyms for *bio-oil* include pyrolysis oils, pyrolysis liquids, bio crude oil (BCO), wood liquids, wood oil, liquid smoke, wood distillates, pyroligneous acid and liquid wood (Mohan *et al.*, 2006). *Bio-oil* is considered as relevant technologies for the following reasons: energy security, environmental concerns, foreign exchange savings, and socio-economic issues related to the rural areas. Typical *bio-oil* properties are presented in Section 6.

2.0 Biomass Availability In Nigeria

Majority of the world poor live in sub-saharan Africa. Nigeria is the most populous country in sub-saharan Africa with nearly one quarter of sub-sahara Africa's population and is one of the poorest countries in the world despite the huge resources from crude oil export (Etiosa *et al.*, 2007). The current population of Nigeria stands at 167 million with an annual growth rate of 2.3 per cent (Zubem, 2012). Nigeria is located in West Africa, between latitudes 4 and 14^{o}north of the equator and longitude 3 and 14^{o}east of Greenwich, along the Gulf of Guinea (Sambo, 2009; Obioh, 2009). It borders the Gulf of Guinea, between Benin (773 km) on the west and Cameroon (1, 690 km) on the east (www.nationsencyclopedia.com, accessed on December 14, 2012). It also borders the Republic of Niger (1,497 km), Chad (87km), and Atlantic Ocean (853km) at the north, north-east, and south, respectively. The land mass of the country extends from the Gulf of Guinea in the south to the Sahel (the shore of the Sahara Desert) in the north and this amounts to a total land area of

910, 768km^2 (www.nationsencyclopedia.com, accessed on December 14, 2012; Obioh, 2009). Approximately 33% or 300,550 km^{2}of the total land area is arable, while 3.1% or 28, 234 km^2 is under permanent crops and approximately 2, 820 km^2 or 0.31% is under irrigation (CIA, 2009). About 13 000 km^2 of the total compact area of 923, 768 km^{2}which Nigeria occupies is water and the terrain thus varies from coastal swamp and tropical forest in the south, to savannah and semi-desert in the north (Obioh, 2009). The availability of biomass resources follows the same pattern as the vegetation of the nation (Sambo, 2000). Thus, the rain forest in the south generates the highest quantity of woody biomass while the guinea savannah vegetation of the north central region generates more crop residues than the Sudan and Sahel savannah zones. Global climate models predict increased precipitation in some areas in Nigeria and this should result in increased biomass availability (Obioh, 2009). However, countering the increased biomass availability will be the increased flooding in the south and drought in the North. As would be expected, the net effect of climate change on biomass availability will depend on the relative magnitudes of these changes.

Biomass is the major energy source in Nigeria contributing nearly 78% of Nigeria primary energy supply (Edirin and Nosa, 2012). In Nigeria, the following biomass resources are available; fuelwood, agricultural waste and crop residue, sawdust and wood shaving, animal dung/poultry droppings, industrial effluents/municipal solid wastes (Sambo, 2009). Table 1 shows the estimated biomass resources in Nigeria.

Table 1. Biomass Resources and the estimated quantities in Nigeria in the year 2000

Resources	Quantity (million tonnes)	Energy value ('000 MJ)
Fuel wood	39.1	531
Agro-waste	11.244	147.7
Saw dust	1.8	31.433
Municipal Solid Waste	4.075	-

Source: Sambo (2008)

2.1 Fuelwood

Nigeria is naturally endowed with a vast area of land dominated with forest. In 1981, about 13,071,464 hectares of forest land was recorded (Sambo, 2008). The forest resources if harvested, can be an important source of bio fuel. In the recent times, about 80 million cubic metres, equivalent to 43.4 x 10^9 kg (or 43.4 million tonnes) of fuelwood with an average daily consumption ranging from 0.5-1.0 kg of dry fuelwood per person is being consumed in the country annually for cooking and domestic purpose (Ohunakin, 2010). These consumers of the fuelwood are over 60% population of the country and they consume about 95% of fuelwood (Energy Commission of Nigeria, 2003; Energy Commission of Nigeria and United Nations Development Programme, 2005).

The largest sources of fuelwood at present are from open forest, communal woodlots and private farmlands (Presidency, 2003). Apart from cooking and other domestic purposes such as lighting, fuelwood can also be used in cottage industrial activities, such as cassava and oil seeds processing. It could be used in the chemical process industries in the production of steam for generation of electricity, driving of pumps, etc. The demand for fuelwood has continued to increase, due to the

inefficient combustion method used. Over the period 1989-2000, about 32-40% of the total primary energy consumption in Nigeria emanated from fuelwood and charcoal (Presidency, 1992). This value increased to 37.4% in the year 2000, which corresponds to 39 million tons per annum, as can be seen from Table 1(Sambo, 2009). Also, it has been projected that the energy consumption would increase to 91 million tons by 2030 (Energy Commission of Nigeria, 1998).

2.2 Agricultural biomass

Nigeria is greatly endowed with fertile hectares of land that support the cultivation of agricultural biomass. Agricultural biomass is a relatively broad category of biomass that includes: the food-based portion of crops and non-food-based portion of crops, as seen in the energy crop presented above. The food-based portion of crops is the part of the plant that is either oil or simple sugars. Examples include: Rapeseed (used for canola oil), sun flower, soybeans, corn, sugarcane and sugar beets. Corn and sugar beets can be used for ethanol production through fermentation while the oilseed crops can be used to produce biodiesel. On the other hand, the non-food-based portion of crops is that part which is usually discarded as a residue. Crop residues are those residues that are associated with agriculture either as on-the-farm crop wastes, such as cornstalks or as processing wastes such as rice husk, corn shells, palm kernel shell, cassava peels, etc., (Sambo, 2000). Other examples of non-food-based portion of crops include: perennial grasses, animal waste and landfill grasses. Animal wastes such as cattle dung, poultry droppings and abattoir wastes are also available at places where cattle are reared, poultry farms and abattoir, etc. Agricultural biomass consists of complex carbohydrate and could serve as good sources of fuels. Cornstalks, rice husk, cassava peels, etc, can be fermented into ethanol while nutshell can be refined into biodiesel or combusted to produce heat. Also, animal wastes can be used in the production of biogas. Biogas digesters of various designs are capable of sustaining household, industrial and institutional energy needs (Presidency, 2003). The remaining part of this waste after digestion can be used as a fertilizer.

However, crop residue (agro-waste) is available in Nigeria in large quantities especially in the rural areas where crops are cultivated. From Table 1, the agro-waste (crop residues) in Nigeria was estimated in the year 2000 to be about 11.244 million tons of the entire biomass resources of that year and this amounted to 147,700 MJ of energy (Sambo, 2000). These wastes are currently burned directly as a starter or supplement materials to fuelwood. They have a great potential for bio fuel production. Recently, some of these biomasses have been used by different researchers to produce *bio-oil*. These include rice husks and saw dust (Zheng *et al.*, 2006) and cassava plantation, like cassava stalk and cassava rhizome (Pattiya *et al.*, 2006).

2.3 Saw dust

Saw dust is a typical example of lignocellulose biomass (biomass that is mostly plant cell walls which have high carbon content). It is readily available in Nigeria, as can be seen from Table 1. It is associated with the lumber industry and the main by-product of sawmill. The saw dust generated from sawmills are often discarded, burnt as wastes or used for cooking but may also constitute an environmental hazard if not properly used. However, as noted earlier, sawdust can also be converted to bio-oil. In the recent times, Zheng *et al.*, (2006) investigated the use of saw dust in the production of *bio-oil*. Also, Heo *et al.* (2009) investigated fast pyrolysis of waste furniture sawdust in a fluidized bed.

2.4 Municipal Solid Waste (MSW)

The portion of MSW that is wood includes items such as discarded furniture, pallets, packaging materials, processed lumber, and yard and tree trimmings (U.S. Department of Energy and U. S. Department of Agriculture, 2005). These wastes are generated in the high-density urban areas and they are usually burned to produce heat. Out of 56.2 million tons of biomass resources generated in the year 2000, approximately 4.1 million tons was municipal solid waste. As can be seen from Table 1, this quantity is more than twice of the quantity of saw dust generated that year. That is to say that large quantity of *bio-oil* can be generated from MSW compared to saw dust. A number of indigenous outfits are producing economically viable systems for converting municipal waste to energy (Sambo, 2009).

3.0 Biomass Conversion Processes

3.1 Biological Conversion

Biological conversion may be carried out either through fermentation or anaerobic digestion. Fermentation is enzyme-catalyzed, energy-yielding chemical reactions that occur during the breakdown of complex organic substrates in the presence of microorganism, such as yeast or bacteria to produce alcohol and carbon dioxide (Klass, 1998). In fermentation, the microorganism feeds on the sucrose or glucose produced after pretreatment processes of the biomass (sugar or starch) and converts them to alcohol and carbon dioxide.

$$C_6H_{12}O_6 \rightarrow 2C_2H_5OH + 2CO_2 \qquad (1)$$

The alcohol thus, produced is usually called bioethanol. Apart from sugar and starch, any lignocellulosic biomass can be used as feedstock. Here, conversion can be achieved by hydrolysis, i.e. by breaking the biomass into its component parts. Lignocellulosic conversion would greatly increase the supply of raw materials available for bioethanol production. The lignin residues could be used as fuel for the fermentation process (United Nations Industrial Development Organization, 2007).

The second method of biological conversion process is anaerobic digestion. It is the treatment of biomass with a mixed culture of bacterial to produce methane (biogas) as the primary product (Ralph and Thomas, 2008). The methane gas produced can be used directly for cooking, heating, or electricity generation using fuel cell technology. It can also be compressed like natural gas, for transport application. Anaerobic digestion usually takes place in a low oxygen environment. The four stages involved in anaerobic digestion are hydrolysis, acidogenesis, acetogenesis and methanogenesis.

3.2 Chemical Conversion

As mentioned earlier, chemical conversion involves the transesterification of oils into biodiesel and glycerol. Transesterification is the reaction of an alcohol with vegetable oil containing triglycerides to produce monoalkyl esters and glycerol (Meher *et al.*, 2006). The vegetable oils used include: soybean oil, rapeseed oil (canola oil), palm oil and coconut oil. Glycerol is the by-product of transesterification and it settles at the bottom of the reaction vessel after the reaction has been completed.

During the transesterification process, intermediate glycerols (mono and diacylglycerols) are formed. These intermediate products, and some other impurities such as unseparated glycerol, free fatty acids, residual alcohol, and catalyst can contaminate the final product (biodiesel). This can lead to severe operational problems, such as engine deposits, filter clogging, or fuel deterioration when using biodiesel.

3.3 Thermal Conversion

There are basically three methods of thermal conversion of biomass to biofuel. The first method is called combustion, which is the direct burning of biomass to produce useful energy, such as hot water, steam and electricity. Combustion is widely practiced, although the efficiency is very low compared to gasification and pyrolysis. When used in many applications, it could lead to fouling of equipments. Gasification is the second thermal conversion process and it is used to convert biomass to synthesis gas. This synthesis gas is a mixture of carbon monoxide and hydrogen. It can be combusted to generate heat which in turn could be used to produce steam, used in an engine or turbine for electricity generation. Biomass gasification technologies are similar to coal gasification and both produce similar product gases. It is noted that since biomass contains more volatile matter, its gasification occurs at lower temperatures and pressures when compared to coal (Ralph and Thomas, 2008).

The third thermal conversion process is called pyrolysis. Pyrolysis is always the first stage in combustion and gasification followed by total or partial oxidation. In gasification a fuel gas is mainly produced, while in pyrolysis, pyrolysis liquid, char and gas are the main products (Bridgwater, 2007; Mohan *et al.*, 2006; Bridgwater *et al.*, 2002; Bridgwater and Peacocke, 2000). The yield of the liquid product is very dependent on the temperature, heating rate and residence time of the raw material. Lower process temperature of about 400^{o}C and longer vapor residence time of about 20s favour the production of char while higher temperature of about 800^{o}C and longer vapour residence times favours gas formation (Bridgwater, 2007). The highest liquid yield is obtained with fast or flash pyrolysis, where the biomass is heated at a very fast rate (1000^{o}C/s) to a moderate temperature of about 500^{o}C with very short vapour residence time (<2s).

Typical products yield obtained from different pyrolysis mode is given in Table 2. A more detailed description of the thermal processes is given in the next section with much emphasis on fast pyrolysis.

Table 2: Typical product yields (dry wood basis) obtained by different modes of pyrolysis of wood

Process	Conditions	Liquid (%)	Char (%)	Gas (%)
Fast pyrolysis	Moderate temperature,short residencetime particularly vapour	75	12	13
Carbonisation	Low temperature,very long residencetime	30	35	35
Gasification	High temperature,long residence times	5	10	85

Bridgwater (2004)

4.0 Pyrolysis of Biomass

Pyrolysis is defined as a thermo-chemical process of the decomposition to smaller molecules by thermal energy (Demirbas,2007). The products of pyrolysis are gas, liquid and solid which can be used as improved fuels or intermediate energy carriers. Pyrolysis to a liquid offers the possibility of decoupling (time, place, and scale), easy handling of the liquids, and more consistent quality, compared to any solid biomass (Mohan et. al., 2006). There are three types of pyrolysis, depending on temperature, heating rate and residence time. These are flash, fast and slow pyrolysis. Flash pyrolysis is a rapid heating rate process occurring at 400-900^{o}C with small residence time. The product of flash pyrolysis is gas and it can be used for energy generation. The second type of pyrolysis is called fast pyrolysis. This is a thermal process in which the feedstock is rapidly heated in the absence of air, vaporizes and condenses to a dark brown mobile liquid which has a heating value of about half of the conventional fuel oil (Bridgwater and Peacocke, 2000; Zhang *et al.*, 2006). Thus, it is differentiated from flash pyrolysis as the heating rates are not extremely high and the temperature is lower than 600^{o}C (Ioannidou, 2009). By comparison with slow pyrolysis, the heating rates are lower but the residence times are longer. The operating temperature for slow pyrolysis is between 450^{o}Cand 700^{o}C. The product of slow pyrolysis is mainly solid char, which could be used for combustion or as activated carbon.

Fast pyrolysis is mostly used in the conversion of biomass into liquid products. The advantages include low production costs, high thermal efficiency, low fossil fuel input, and carbon dioxide neutrality (Mohan *et. al.*, 2006). The essential features of the fast pyrolysis process have been summarized by Bridgwater and Peacocke (2000) and include:

i. Very high heating and heat transfer rates that requires a finely ground biomass feed
ii. Carefully controlled temperature of about 500^{o}C
iii. Short vapour residence times of typically less than 2 seconds
iv. Rapid cooling of the pyrolysis vapours to give the bio-oil product

A typical fast pyrolysis process is shown in Figure 1.

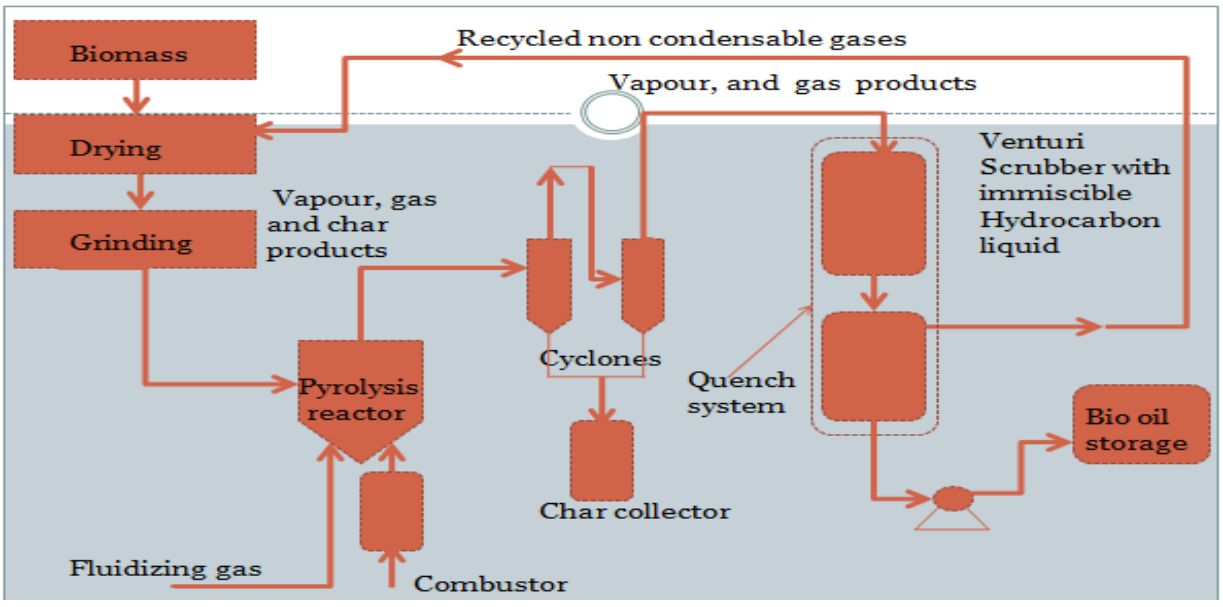

Figure 1: Process flowsheet of a fast pyrolysis process

It involves the following stages; grinding, drying, pyrolysis reactor, char separation and liquid recovery and storage. Grinding is required to reduce the biomass particle size to the range of 2 mm to 200 mm. The actual particle size is dependent on the type of pyrolysis reactor used (Bridgwater and Peacocke, 2000; Bridgwater *et al.*, 2002; Bridgwater, 2007). The dryer, operating between 120^{o}C and 130^{o}C is used to reduce the biomass moisture content to typically less than 10% water. After grinding and drying, the biomass is fed into the pyrolysis reactor.

The pyrolysis reaction takes place in the pyrolysis reactor at a temperature of about 500^{o}C and short residence time of about 2s. These conditions affect the yield of the *bio-oil* produced. According to Bridgwater (2004), yield of up to 75% wt on dry feed basis can be obtained. As would be expected different types of reactors have been developed by so many organizations; some of these are discussed in the next section. The products of pyrolysis reaction include; gases, vapours and char. These are sent immediately to the cyclone, where the char is separated and then sent to the char collector. The separation of char is necessary, since it contains some alkali and alkaline earth metals which act as a cracking catalyst for the *bio-oil* produced. These could lead to the production of side reactions, which in turns, increases the viscosity of *bio-oil*, resulting in its instability (Part *et al.,* 2008). It is important to note that some of these char particles always pass through the cyclones and are mixed with the liquid product. These can be removed by using hot vapour filtration.

After solid separation, vapours and gases are quenched rapidly to avoid continuous cracking of the organic molecules. The non condensable gases are recycled and used as source of heat to the dryer while the *bio-oil* produced is sent to the *bio-oil* storage tank for immediate applications. It could also, be upgraded, if need be. Some parts of the vapours, like aerosols are very difficult to condense, as a result of this, electrostatic precipitators are often used to capture these particulate material (Bridgwater and Peacocke, 2000; Bridgwater *et al.*, 2002; Bridgwater, 2007).

5.0 Fast Pyrolysis Reactors

An integrated fast pyrolysis process consists of the following; biomass reception, storage and handling, biomass drying and grinding, reactor, product collection, storage and, when relevant, upgrading. But amongst these components of the fast pyrolysis process, reactors are at the heart of the process and it probably represents only about 10-15% of the total capital cost of an integrated system (Bridgwater, 2011). Most research and development has focused on developing and testing different reactor configurations on a variety of feedstocks, although increasing attention is now being paid to control and improvement of liquid quality and improvement of liquid collection systems (Bridgwater, 2011). Some of these developed reactors include the following; fluidized bed, ablative (vortex and rotating blade), rotating cone and vacuum and they are discussed in details below. Also the advantages, disadvantages and yields of *bio-oil* produced using these reactors and many other reactors not discussed have been summarized and presented in Table 3.

5.1 Fluidized Bed Reactors

Fluid bed reactors give a high yield of *bio-oil* of between 70 wt. % and 75 wt. %. The required particle size of the biomass is usually less than 2-3mm and the rate of particle heating is the rate limiting step. The residence time of solids and vapours is controlled by the fluidizing gas flow rate and is higher for char than for vapours (http://www/pyne.co.uk).

Fluidized bed reactors include, deep bubbling, circulating and transported fluidized bed respectively. These reactors operate under atmospheric pressure and temperatures ranging from about 450°C to 800°C. Bubbling fluid bed, otherwise known as fluid bed, has been popular compared to the circulating fluid bed, because, it is a well understood technology that is simple in construction and operation, good temperature control, very efficient heat transfer to biomass particles due to high solid density and large heat storage capacity (http://www/pyne.co.uk).

On the other hand, circulating fluid beds (CFB) have many of the features of the bubbling fluid beds described above, except that they have shorter residence times for chars and vapors. These give rise to higher gas velocities, faster vapour and char escape and higher char content in the *bio-oil* than in the bubbling fluidized beds. CFB also, have a higher processing capacity or throughput, better gas-solid contact and improved ability to handle solids that are more difficult to fluidize. This technology is usually used at a very high throughput in the petroleum and petrochemical industries (http://www/pyne.co.uk). The technological strength and the market attractiveness favour the circulating fluidized bed for its commercial potential. The heat supply typically comes from a secondary char combustor (Smolders *et al.*, 2006).

Furthermore, some researchers have used the fluidized bed pyrolyser with different feedstocks to produce *bio-oil* under variable conditions. Examples of such researchers include, Hang *et al.* (2012) and Pattiya and Suttiback (2011). Hang *et al.* (2012) developed a cylindrical bubbling fluidized bed reactor having 2 kg/h pyrolysis capacity to produce biocrude oil using fast pyrolysis. The reaction conditions evaluated included biomass feeding rate, biomass particle size, nitrogen flowrate, heating temperature and cooling temperature were varied to determine their respective effects on the yield of the products. The results show that the biocrude yield increased from 54.6% to 57.8%, when the biomass particle size was increased, leading to a decrease in the biocrude yield from 56.9% to 51.3%. Hang *et al.* (2012) also found that increasing the nitrogen flowrate would lead to an initial increase in the biocrude oil yield from 53.9% to 54.8% and a later decrease to 50.6%. According to them, the maximum biocrude oil yield of 57.0% was obtained at 500^{o}C and that the bubbling condition vapour residence time and heat transfer played an important role on the thermal conversion of biomass and its final products.

Also, Pattiya and Suttiback (2011) worked on the production of *bio-oil* via fast pyrolysis of agricultural residues from cassava plantations (cassava rhizome and cassava stalk) in a fluidized bed reactor with a hot vapour filtration unit. They investigated the effects of reaction temperatures, biomass particle size and the use of simple hot vapour filtration on pyrolysis product yields and properties. The results show that at the maximum biofuel yields were obtained at pyrolysis temperatures between 469^{o}C and 475^{o}C for cassava rhizome and stalk, respectively. For these feedstocks, the particle size was in the range 250-425 µm resulting in biofuel yields of 61 – 69%. According to them, the use of hot vapour filtration unit led to the reduction in the yield of *bio-oil* obtained by 6-7wt%, but gave a better quality in terms of initial viscosity, solid content, ash content and stability.

5.2 Entrained Reactor

This type of reactor allows the use of biomass particle size of between 1 and 5mm, unlike the fluid bed reactor. The biomass is charged into a hot down-flow reactor, which is maintained at a temperature of 700-800^{0}C for a residence time of less than 1s. The draw backs of the reactor

include poor heat transfer, and lower liquid yield. An early process was developed at Georgia Tech Research Institute (USA) and a first unit transferred to Egemin (Belgium) for further development and scale up (Venderbosch and Prins, 2010).

5.3 Ablative pyrolysis reactors

This reactor uses a biomass particle size of up to 20mm, as against less 2mm for fluid bed and up to 5mm for entrained flow reactor. The biomass particle is moved to a very high velocity by a carrier gas (steam or nitrogen) and then introduced tangentially to the vortex (tubular reactor). As the particles slide down across the inner side of the reactor, at a very high velocity and reactor wall temperature of 625^0C, they are pressed on the wall and thus, melted. Vapours generated at the surface are quickly swept out of the reactor by the carrier gases to result in vapour residence times of 50-100 milliseconds. Although, a high liquid yield of 65% can be obtained using ablative reactor, which may compare favourably well with that obtained using fluid bed, the major problem it has include scalability and wearing of the reactor wall due to high particle velocity (Venderbosch and Prins, 2010). Some researchers have used the ablative fast pyrolysis reactor to produce *bio-oil* from different feedstocks. Thus, Dietrich *et al.,.,* (2007) reported practical results obtained from a 6 Mg/d dry biomass ablative fast pyrolysis pilot plant and diesel combined heat and power (CHP) plant built and operated by PYTEC ThermochemischeAnglagen GmbH. According to them the ablative pyrolyser system is a completely new and compact design, comprising a revolving feeding system for wood chips and a rotating hot disk as heat surface. The advantages that this design has are firstly, neither a heat carrier nor a transport gas is required and hence, loss of input energy is minimized. Secondary, the biomass-to-oil (BTO) process accepts standard wood chips or chopped straw. This means that no grinding or milling is required unlike the fluidized bed reactors and thus, operating cost is minimized. The *bio-oil* yield obtained using the ablative pyrolyser was 60 wt. %.

5.4 Vacuum Reactor

Vacuum reactor is not a true fast pyrolysis process as it has a high residence time and lower heat transfer rate compared to other reactors used in fast pyrolysis. The slow heating rate gives rise to a lower *bio-oil* yield (35-45%). It does not require carrier gas and large particle size of biomass can be processed. Operating at a vacuum requires special solids feeding and discharging devices to maintain a good seal at all times (Venderbosch and Prins, 2010). The advantages include the *bio-oil* produced is very clean with no or little char compared to that produced using fluid bed technologies and it can use larger feed particles (2-5 cm) than fluidized bed processes. The major drawback is the high moisture content present in the *bio-oil* which has the tendency of reducing the heating values during combustion and could also, cause phase separation during storage (Lu, *et al.,* 2009). Vacuum pyrolysis reactor has been successfully scaled up to 3000 kg/hr in 2000, but due to lack of market for *bio-oil*, it was abandoned in 2002 (Venderbosch and Prins, 2010).

5.5 Rotary Cone Pyrolysis Reactor

This reactor is similar to the circulating fluidized bed reactor in the sense that it allows the mixture of hot sand and biomass to enhance the thermal pyrolysis reaction. The difference is that the former uses centrifugal force resulting from a rotary cone in transport while the later uses carrier gas. The biomass feed and sand are introduced at the base of the cone while spinning causes centrifugal force to move the solids upward to the lip of the cone. As the solids spill over the lip of the cone, pyrolysis vapours are directed to a condenser. The char and sand are sent to a combustor where the sand gets re-heated before it is reintroduced at the base of the cone with the fresh biomass feed

Table 3. Advantages, disadvantages and *bio-oil* yield of different pyrolysis reactors (PYTEC, 2005; Boulard, 2002; Fernandez and Menendez, 2011; Zhao *et al.*, 2001; Ren, *et al.*, 2012)

Reactor type	Advantages	Disadvantages	Oil yield (%)
Fixed bed	1.Simple design 2. Reliable 3. Biomass size independent	1. Long solid residence time 2. Different to remove char	35 - 50
Bubbling fluidized bed	1.Simple design 2. Easy operation 3. Suitable for large scale	1. Small particle sizes are Needed	70-75
Circulating fluidized bed	1.Well-understood technology 2. Good control 3. Large particle sizes can be used	1.Suitable for small scale 2. Complex hydrodynamics 3. Char is finer	70-75
Rotating cone	1.No carrier gas required 2. Less wear	1. Complex process 2. Small particle 3. Small scale	65
Vacuum	1.Produces clean oil 2.Can process larger particles of 3-5 cm 3. No carrier gas required 4. Lower temperature required 5. Easier liquid condensation	1. slow process 2. solid residence time is too high 3. Required large scale equipment 4. Poor heat and mass transfer rate 5. Generates more water	35-50
Ablative	1.Inert gas is not required 2. Large particle sizes can be Processed	1.Reactor is costly 2. Low reaction rate	70
Auger	1.Compact 2. No carrier gas is required 3. Lower process temperature	1. Moving parts in hot zone 2. Heat transfer is suitable for small scale	30-50
PyRos	1.Compact and low cost 2. High heat transfer 3. Short gas residence time	1. Complex design 2. High impurities in the oil 3. High temperature is required	70-75
Plasma	1.High energy density 2. High heat transfer 3. High temperature 4. Very good control	1. High electrical power consumption 2.High operating costs 3. Small particle sizes is required	30-40

Microwave	1.Compact 2.High heating rate 3.Large size biomass can be processed 4. Uniform temperature distribution 5. High temperature	1.High electrical power consumption 2. High operating costs	60-70
Solar	1.Use renewable energy 2. High heating rate 3. High temperature	1. High costs 2. Weather dependent	40-60

Table 4. Organic chemicals in the Bio-oil

S/N	Chemical	Molecular formula
1.	9,9-bis[4-(4-nitrophenoxy)phenyl] fluorine	$C_{37}H_{24}N_20_6$
2.	1,2-benzenediol	$C_6H_60_2$
3.	2,6-dimethoxy-phenol	$C_8H_{10}0_3$
4.	Vanillin	$C_8H_80_3$
5.	1,2,4-trimethoxybenzene	$C_9H_{12}0_3$
6.	4^1-hydroxy-3^1-methoxy-acetophenone	$C_9H_{10}0_3$
7.	4,7-dimethyl-5-decyne-4,7-diol	$C_{12}H_{22}0_2$
8.	1,2,3-trimethoxy-5-methyl-benzene	$C_{10}H_{14}0_3$
9.	Butylated hydroxytoluene	$C_{15}H_{24}0$
10.	2,6-dimethoxy-4-[2-propenyl]-phenol	$C_{11}H_{14}0_3$
11.	4-hydroxy-3,5-dimethoxy-benzaldehyde	$C_9H_{10}0_4$
13.	4^1-hydroxy-3^1,5^1-dimethoxy-acetophenone	$C_{10}H_{12}0_4$
14.	1-[2,4,6-trihydroxyphenyl]-2-pentanone	$C_{11}H_{14}O_4$

Table 5. Typical properties of wood Pyrolysis *Bio-oil* and Heavy Fuel oil (Czernik and Bridgwater, 2004)

Property	*Bio-oil*	Heavy fuel oil
Moisture content (wt %)	15-30	0.1
pH	2.5	
Specific gravity	1.2	0.94
Elemental composition (wt%)		
C	54-58	85
H	5.5-7.0	11
O	35-40	1.0
N	0-0.2	0.3
ash	0-0.2	0.1
HHV (MJ/kg)	16-19	40
Viscosity, at 500^{o}C (cP)	40-100	180
Solids (wt %)	0.2-1.0	1
distillation residue (wt %)	up to 50	1

Table 6; Typical Properties of *Bio-oil*, compared to those of light and Heavy Fuel oil (http://dynamotive.com)

Bio Therm Property	Light *bio-oil*	Heavy fuel oil	Physical fuel oil
heat of combustion			
BTU/lb	7100	18200	17600
MJ/L	19.5	36.9	39.4
viscosity (centistokes)			
at 50^{o}C	7	4	50
at 80^{o}C	4	2	41
ash content (wt %)	< 0.02	< 0.01	0.03
sulfur content (wt %)	Trace	0.15-0.5	0.5-3
nitrogen content (wt %)	Trace	0	0.3
pour point (^{o}C)	-33	-15	-18
turbine emissions (g/MJ)			
NO_x	< 0.7	1.4	N/A
SO_x	0	0.28	N/A

(Ringer *et al.*, 2006). The design has a yield of 70% *bio-oil*. It does not require the use of carrier gas and this makes the *bio-oil* product recovery easier. Some of the disadvantages are: scale-up is very difficult and the entire system is complex, as it requires equipment, such as rotating cone, a bubbling bed for char combustion, and pneumatic transport of sand back to the reactor.

6. *Bio-oil* Properties

The complexity of the components of *bio-oil* leads to the difficulty in its analysis and characterization (Wildschut, 2009). Usually, gas chromatography-mass spectrometry (GC-MS) is the equipment used to analyze the composition of the *bio-oil* (Sipila *et al.*, 1998). Apart from oxygen, water and acids mentioned above, *bio-oil* contains so many other chemicals some of which are presented by Chen *et al.* (2006) and listed in Table 4.

The physiochemical properties of the *bio-oil* are different from conventional fossil fuels. These physiochemical properties include appearance, odour, heating value, moisture content, oxygen content, density, viscosity, distillation, aging and components (See Tables 5 and 6).

These require consideration before any application, storage, transport, upgrading or utilization is attempted.

a. Odour

Bio-oil has an acrid smoky smell which has the tendency of irritating the eyes on prolong exposure.

b. Density

The density of *bio-oil* is larger than that of light fuel oil. The reason is that the *bio-oil* contents a high per cent of water molecule and macromolecule, such as cellulose, hemicelluloses, oligomeric phenolic compounds (Oasmaa and Czernik, 1999). The density of *bio-oil* at 15^{0}C can be measured using pycnometer and ASTM D 4052 (Sipila *et al.*, 1998)

c. Aging of *bio-oil*

Bio-oil has the ability to undergo changes in chemical composition during storage or handling. This is because it contains some compounds which can react with themselves to form larger molecules, resulting in an increase in the viscosity and/or water content of the *bio-oil*. The aging rate depends exponentially on the temperature of the *bio-oil* during storage, *bio-oil* composition, pyrolysis condition, efficiency of solid removal and the liquid recovery system (Oasmaa and Czernik,1999).

d. pH

Bio-oil contains some amount of organic acids, such as acetic and formic acids. This however, lowers the acidity of the *bio-oil* to about 2.5 (Table 5). The presence of acids in the *bio-oil* makes it to be corrosive to some common construction materials, like carbon steel and aluminum. It can also affect some sealing materials (Czernik and Bridgwater, 2004; Oasmaa and Czernik, 1999; Soltes and Lin, 1984). Therefore, there is need for upgrading in order to meet the standard of fuels before application.

e. Heating value

Heating value is the standard measurement for the energy content of fuel. It is divided into lower heating value (LHV) and higher heating value (HHV), depending on the water produced through hydrogen in vapour or liquid phase. It can be determined by using oxygen-bomb colorimeter method (Demirbas, 2009). The heating value of *bio-oil* is usually lower than that of conventional fossil oil, due to the high percentage of water and oxygen contents see Table 5.

f. Oxygen content

The properties of wood derived crude *bio-oil* differ significantly from that of conventional fossil fuel derived fuel oil. As can be seen from Table 5, oxygen ranges from 35-40%. This high oxygen content in the bio-oil is the primary reason for the difference between hydrocarbon fuels and *bio-oil* (Demirbas, 2006). Due to the high oxygen content, the heating value of *bio-oil* is 40-45% of that for fossil fuels. Also, the *bio-oil* tends to be polar like water and as a result of that it is immiscible in hydrocarbon liquids. The high oxygen content of *bio-oil* gives it its high viscosity, low energy density, corrosiveness, and thermal instability (Elliott *et al.*, 2009). However, in order to improve the quality of *bio-oil*, it is imperative among other things to reduce its oxygen. This can be done through hydrodeoxygenation (HDO) and catalytic hydrotreatment reaction, which has the tendency of reducing the oxygen content to less than 10 wt% under severe conditions (Wildschut *et al.*, 2009). The elemental compositions of the *bio-oil* (C, H, O and N), can be determined by using CHN-S analyzer, according to ASTM D 5373-93. The oxygen content will be calculated by the difference (Wildschut, *et al.*, 2009).

g. Moisture content

The moisture in the *bio-oil* emanates from water content of the biomass prior to pyrolysis. From Table 5, it is about 15-30%. One of the advantages of high moisture content in the *bio-oil* is that it has the ability to reduce the viscosity of the *bio-oil* and hence, improve its flow characteristics (Czernik and Bridgwater, 2004; Oasmaa and Czernik, 1999; Lu *et al.*, 2009). Another advantage is that it facilitates the atomization of the *bio-oil*, when used in combustion (Lu, *et al.*, 2009). On the other hand, the disadvantage of the high moisture content in the *bio-oil* is that it lessens the heating values in combustion and may cause phase separation during storage (Lu, *et al.*, 2009). In order to reduce the moisture contents, it is required that the process of production be optimized

with respect to the intending application of the *bio-oil*. The moisture content in the *bio-oil* can be determined by Karl-Fischer titration, using ASTM D1744 (Sipila *et al.*, 1998).

h. Ash content

The presence of ash in *bio-oil* can cause erosion, corrosion and kicking problems in the engines and valves (Zhang *et al.*, 2007). The ash content, according Czernik and Bridgwater (2004) is usually is 0-0.2 for wood pyrolysis oil (Table 4). It can be determined according to ASTM D 482

7. Conclusion

Bio-oil can be produced from the fast pyrolysis of biomass. The *bio-oil* has the advantages of being a storable and transportable fuel and it is a source of chemicals. It has been successfully tested for use in boiler, diesel engine and gas turbine. Fluid bed reactor has been identified as the most preferred type of reactor due to its ease of operation and scale-up. Nigeria has a great potential for the various kinds of biomass, such as saw dust, agricultural residue, wood crop and municipal waste. Saw dust has been identified as a biomass with the highest yield of *bio-oil*.

Acknowledgement

The authors wish to acknowledge the funds provided for this research and publication by TETFund Centre of Excellence for Renewable Energy, Kaduna Polytechnic, Kaduna, Nigeria. The funds were provided by the Tertiary Education Trust Fund (TETFUND), Nigeria, under the TETFUND Special Intervention for Establishment of Centres of Excellence (TETF/ES/DS&D/KADPOLY/COE /2021/VOL11).

REFERENCES

Anja, O., Yrjo, S., Vesa, A., Eeva, K. and Kai, S. (2010), Fast Pyrolysis *Bio-oil*s from Wood and Agricultural Residue, *Energy fuel*, 24, 1380-1388.

Bozell, A. E. and Barth, T. (1999), *Org. Geochem.* pp. 1517-1526

Boulard, D. (2002), Ensyn, Personal Communication & Presentation, August 16

Bridgwater, T., (2007), Biomass pyrolysis, Aston University IEA Bioenergy

Bridgwater, A.V. (2004), Biomass Fast Pyrolysis, *Review paper UDC: 662.73/75 BIBLID: 0354 – 9836*, 8, p.21 – 49

Bridgwater, A. V. (2003), *Chem. Eng. J*. 91 (2-3), 87-102

Bridgwater, A. V.,Czernik, S. and Piskorz, J., (2002), The status of biomass fast pyrolysis, in fast pyrolysis of biomass, volume 2, CPL press, Newbur, p. 1 – 19

Bridgwater, A. V., and Peacocke, G.V.C. (2000), Fast pyrolysis processes for biomass, *Renewable and sustainable Energy Review* Vol. 4, Pergamon, p. 1 - 73

Bridgwater, A.V. (1999), Principles and practice of biomass fast pyrolysis processes for liquids, *J. Anal. Appl. Pyrolysis*, 51, 3-22

Bridgwater, A.V., Meier, D. and Radlein, D. (1999), An Overview of Fast Pyrolysis of biomass, *Organic Geochemistry*, 30, 1479 – 1493.

Brown, R.C. (2003), Biorenewable resources: Engineering new products from agriculture, Iowa State Press, Ames.Chen, M.Q., Wang, J., Wang, X.Y., Zhang, X. C.,

Zhang, S. P., Ren, Z.W. and Yan, Y.J. (2006), Fast pyrolysis of Biomass in a spout – fluidized Bed Reactor Analysis of Combustion and Combustion Characteristics of liquid product from Bio – mass", *The Chinese Journal of Process Engineering*, Vol.6, No.2.

Chiaramonti, D., Oasmaa, A., Solantausta, Y. (2007), "Power generation using fast pyrolysis liquids from biomass. *Renew.SUST.Energ.Rev*.11, 1056-1086

Chiaramonti, D., Bonini, M., Fratini, E., Tondi, G., Gartner, K., Bridgwater, A. V., Grimm, H. P., Soldaini, I., Webster, A.,Baglioni, P.(2002), *Biomass Bioenergy* , vol1, pp 101-111.

CIA (2009), "The 2008 World Factbook-Nigeria Central Intelligence Agency (CIA), United States of America; http://www.cia.gov/library/publications.

Czernik, S. and Bridgwater, A. (2004), Overview of Applications of Biomass Fast Pyrolysis Oil, *Energy & Fuels*, pp. 590-598

Demirbas A, (2011), "Competitive liquid biofuels from biomass", Applied Energy, 88, 17–28

Demirbas, A. (2009), *Biofuels: Securing the Planet's Future Energy Needs*, Springer-Verlag, London Ltd, UK.

Demirbas, A. (2007), Biodiesel: A Realistic Fuel Alternative for Diesel Engines, Springer-Verlag London Limited, ISBN 978-1-84628-994-1, London, UK.

Demirbas, A. (2006), Biofuels sources, bio fuel policy, bio fuel economy and global bio fuel projections, *Energy Conversion and Management*, Elsevier Ltd.

Dietrich, M., Stefan, S., Hannes, K. and Jens, M. (2007), Practical Results from Pytec's biomass-to-oil (BTO) process with ablative pyrolyser and diesel CHP plant, *Success & Vision for Bioenergy*, ISBN 978-1-872691-28-2.

Dynamotive Energy Systems.http://www.dynamotive.com/industrial-fuels/biooil/ [accessed 06/23/2023].

Edirin, B. A. and Nosa, A. O. (2012), A comprehensive Review of Biomass Resources and Biofuel production potential in Nigeria, *Research Journal in Engineering and Applied Sciences*, Vol. 1, 3, pg. 149-155.

Energy Commission of Nigeria (1998), World Solar Programme, 1996-2005, Projects of the Government of Nigeria: Project Document, ECN Abuja.

Energy Commission of Nigeria (2003), National Energy Policy of the Federal Republic of Nigeria.

Energy Commission of Nigeria and United Nations Development Programme (2005), Federal Republic of Nigeria Renewable Energy Master Plan, Published by the ECN and UNDP.

Elliott, D. C., Hart, T. R., Neuenschwander, G.G., Rotness, L. J. and Zacher, A. H. (2009), "Catalytic Hydroprocessiong of Biomass Fast Pyrolysis *Bio-oil* to Produce Hydrocarbon Products", Environmental Progress and Sustainable Energy, Vol. 28, No. 3, pp. 441-449,

Etiosa, U., Matthew, A. and Agbarese, E. (2007), Promoting Renewable Energy Efficiency in Nigeria, CREDC

Fengel, D., Wood, W. G. (1984), Chemistry, Ultrastructure, Reactions, *Walter de Gruyter*: Berlin, New York, pp 167-175

Fernandez, Y., Menendez, J. A. (2011), Influence of feed characteristics on the microwave-assisted pyrolysis used to produce syngas from biomass wastes, *Journal of Analytical and Applied Pyrolysis*, 91 (2), pp. 316-322

Gullison R. E, Frumhoff P. C, Canadell J. G, Field C. B, Nepstad D. C, Hayhoe K, *et al.* (2007), Tropical forests and climate policy, *Science*, 316, pp 985 – 986.

Hang, S., C., Yeon, S. C. and Hoon, C. P. (2012), Fast pyrolysis characteristics of lignocellulosic biomass with varying reaction conditions, *Renewable Energy*, 42, pg. 131-135

Heo, H. S., Park, H. J., Park, Y. K., Ryu, C., Suh, D. J., Suh, Y. W., Yim, J.H. and Kim, S.S. (2009), "*Bio-oil* production from fast pyrolysis of waste furniture sawdust in a fluidized bed", Bioresource Technology, Elsevier Ltd.

http://www.biomassenergycentre.org.uk, accessed on 19/07/2023. http://www/pyne.co.uk

Ioannidou, O., Zabaniotou, A., Antonakou, E.V., Papazisi, K. M., Lappas, A. A. and Athanassiou, C. (2009), Investigating the potential for energy, fuel, materials and chemicals production from corn residues (cobs and stalks) by non-catalytic pyrolysis in the reactor configuration, *Renewable and Sustainable Energy Reviews*, pp 750-762

Katzen R., Schell D.J. (2006), Lignocellulosic Feedstock Biorefinery: History and Plant Development for Biomass Hydrolysis, *Biorefineries-Industrial Processes and Products*, Vol. 1, ISBN 3-527-31027-4, Wiley-VCH Verlag GmbH & Co. KGaA, Weinheim, Germany, pp. 129-136.

Klass, D. L. (1998), Biomass for Renewable Energy, Fuels and Chemicals, Academic Press, San Diego, CA.

Lu, O., Yang, X.L., Zhu, X.F. (2009), Overview of fuel properties of biomass fast pyrolysis oils, *Energy. Conservation and. Management*, 50, pp 1376-1383

McCarthy, J. and Islam, A. (2000), Lignin chemistry, technology, and utilization: a brief history. In Lignin: Historical, Biological and Materials Perspectives, Glasser, W. G., Northey, R. A.,

Schultz, T. P., Eds.: ACS Symposium Series 742, *American Chemical Society*, Washington, DC, pp 2-100

Meher L.C., Vidya S.D., Naik S.N. (2006), Technical aspects of biodiesel production by transesterification-a review, *Renewable and Sustainable Energy Review*, Vol. 10, Pg. 248-26

Meier, D. (2004), New ablative pyrolyzer in operation in Germany, *PyNe Newsletter* 17.

Menendez, J. A., Dominguez, A., Inguanzo, M., Pis, J. J. (2004), Microwave pyrolysis of sewage sludge: analysis of the gas fraction, *Journal of Applied Pyrolysis*, Vol. 71, pp. 657-667

Mohan, D., Pittman, C.U. and Steele, P. H. (2006), Pyrolysis of wood/Biomass for Bio – oil: A Critical Review, *Energy & Fuels*, 20, pp 848 – 889.

Moris, E., Williams, P.T., Horne, P.A. (2000), *Biomass Bioenergy*, pp. 223-236.

Nigam P. S. and A. Singh, (2011), Production of liquid biofuels from renewable resources, *Progress in Energy and Combustion Science*, 37, pp 52-68.

North Central Sun Grant Centre (2007), Composition of the Herbaceous Biomass Feedstocks, SDSU.

Oasmaa,A., Kuoppala, E., Gust, S. and Solantausta, Y. (2003), Fast Pyrolysis of Forestry Residue.1. Effect of Extractives on Phase Separation of Pyrolysis Liquids, *Energy & Fuels*

Oasmaa, A. and Czernik, S. (1999), Fuel Oil Quality of Biomass Pyrolysis Oils-State of the Art of the End Users, *Energy and Fuels*, pp 914-921

Obioh, I. B. (2009), Energy Systems: Vulnerability-Adaptation-Resilience (VAR), Regional Focus: Sub Saharan Africa, HELIO International, Nigeria.

Ohunakin, S. O. (2010), Energy Utilisation and Renewable Energy Sources in Nigeria, *Journal of Engineering and Applied Sciences*, Vol. 5, Issue, pp. 171-177

Olakor, F. (2012), Nigeria's population stands at 167 million – NPC, *Nigeria Punch Newspaper*, 21st December, 2012.

Park, H. J., Park, Y. and Kim, J. S. (2008), Influence of reaction condition and the char separation system on the production of *bio-oil* from radiata pine saw dust by fast pyrolysis, *Fuel Processing Technology*, Elsevier B.V, 797 – 802.

Paster, M., Pellegrino, J.L. and Carole, T. M. (2003), Industrial Bioproducts: Today and Tomorrow, *Department of Energy Report prepared by Energetics*, Inc., Columbia, MD.

Pattiya, A., Titiloye, J.O. and Bridgwater, A.V. (2006), Fast Pyrolysis of Agricultural Residues from Cassava Plantation for *Bio-oil* production, *The 2nd Joint International Conference on Sustainable Energy and Environment*, Bangkok, Thailand.

Pattiya, A. and Suttiback, S. (2011), Production of *bio-oil* via fast pyrolysis of agricultural residues from cassava plantations in a fluidized-bed reactor with a hot vapour filtration unit, *Journal of Analytical and Applied pyrolysis*, 95, pp 227-235

Pine L., Piskorz J, Radlein, D., Scott D. S. (2009), In *Proceedings of International Symposium on Advances in Thermochemical Biomass Conversion*, Bridgwater, A. V Ed., Blackie Academic, London, pp 1432

Pittman, C. U., Mohan, D., Eseyin, A., Li, Q., Ingram, L., Hassan, E. M., Mitcheu, B., Guo, H. and Steel, P. H. (2012), Characterization of *Bio-oil*s produced from fast pyrolysis of corn stalks in an Auger Reactor, *Energy & fuels, American Chemical Society*, 26, 3816-3825.

Putun, A. E. and Apaydin, E. (2004), Rice straw as a *bio-oil* source via pyrolysis and steam pyrolysis", Energy 29, 2171 – 2180.Putun, A.E., Apaydin, E., Pu¨tu¨n, E. (2001), *Bio-oil* production from pyrolysis and steam pyrolysis of soybean-cake:product yields and composition", *Energy*, pp 703-713.

PyNe (2006), Pyrolysis Network of IEA Bioenergy. (http://www/pyne.co.uk).

PYTEC (2005), Bio-fuel based on agricultural and forest residues-the alternative renewable energy of our future, Press Release.

Ralph, W.P. and Thomas, A.H.(2008), Integrating Biomass Feedstocks into Chemical Production Complexes using New and Existing Processes, Minerals processing Research Institute, Louisiana State University, Baton Rouge

Radmanesh, R., Courbariaux, Y., Chauki, J., Guy, C. (2006), A unified lumped approach in kinetics modelling of biomass pyrolysis, *Fuel*, 1211-20

Ren, S., Lei, H., Wang, L., Bu, Q., Chen, S., Wu, J., Ruan, R. (2012), Biofuel production and kinetics analysis for microwave pyrolysis of Douglas fir sawdust pellet, *Journal of Analytical and Applied Pyrolysis*, 94 (0), pp 163-169

Ringer, M., Putsche, V. and Scohill, J. (2006), Large-scale Pyrolysis oil Production: A Technology Assessment and Economic Analysis, *Technical Report*, NREL/TP-510-37779, US.

Rowell, R. M. (1984), The Chemistry of solid wood, *American Chemical Society*, Washington, DC.

Sambo, A.S. (2000), Strategic Developments in Renewable Energy in Nigeria, *International Association for Energy Economics*

Sambo, A.S. (2008), Renewable Energy Policy and Regulation in Nigeria, paper presented at the International Renewable Energy Conference, Rockview Hotel, Abuja.

Sambo, A. S. (2009), Strategic Developments in Renewable Energy in Nigeria, *International Association for Energy Economics*.

Shadia, R. T., Mohamed, H. S., Abdelgbani, M. G. A., Hala, A. Y., Nihal, M. E. D., Joseph, Y. F. and Ismail, K. A. (2011), "*Bio-oil* from rice straw by pyrolysis: Experimental and Techno-Economic Investigations", *Journal of American Science*, 9 pages.

Soltes, E.J. and Lin, J.C.K. (1984), " Hydroprocessing of Biomass Tars for Liquid Engine Fuels", in: *Progress in Biomass Conversion*

Sipila, K., Knoppala, E., Fagernas, L. and Oasmaa, A. (1998), Characterization of Biomass-based Flash Pyrolysis oils, *Biomass & Bioenergy*, Vol. 14, pp.103-113

Smolders, K., Van de Velden, M. and Baeyens, J. (2006), Operating parameters for the bubbling fluidized bed (BFB) and circulating fluidized bed (CFB) processing of biomass. In: Proceedings of the use of renewable, *Achema,* Frankfurt, paper 1030.

Su-Hwa, J., Bo-Sung, K. and Joo.Sik, K. (2008), "Production of bio-oil from rice straw and bamboo sawdust under various reaction conditions in a fast pyrolysis plant equipped with a fluidized bed and a char separation system", Elsevier *J. Anal. Appl. Pyrolysis*, pp 240-247.

Teter S.A., Xu F., Nedwin G.E., Cherry J.R. (2006), "Enzymes for Biorefineries", Biorefineries Industrial Processes and Products, Vol. 1, Wiley-VCH Verlag GmbH & Co. KGaA, Weinheim, Germany, Pg. 357-382.

The Presidency (1992), Report on the National Fuelwood Substitution Programmme. The Presidency (2003), Federal Republic of Nigeria, National Energy Policy.

Tsai, W.T., Lee, M.K., Chang, Y.M. (2007), "Fast pyrolysis of rice husk: product yields and compositions", Bioresources Technology 98, pp 22-28

U.S. Department of Energy (DOE) and U. S. Department of Agriculture (USDA) (2005), Biomass as feedstock for a bioenergy and bioproducts industry: The technical feasibility of a billion-ton annual supply, DOE/GO-102995-2135, Washington, DC.

United Nations Environment Programme (2009), Towards Sustainable Production and use of Resources: Assessing Biofuels.

United Nations Industrial Development Organization (2007), Industrial Biotechnology and Biomass Utilization, Prospects and Challenges for the Developing World, Vienna.

Vassiler, S., Baxter, D., Andersen, L., Vassileva, C. (2010), An Overview of the Chemical Composition of Biomass, *IEA Bioenergy Task 32 Workshop*, Lyon, France.

Venderbosch, R. H., Prins, W. (2010), Fast Pyrolysis Technology Development, Society of Chemical Industry and John Wiley & Sons, Ltd (www. Interscience.wiley.com); DOI: 10. 1002/bbb.205; *Biofuels*, Bio prod. Bioref. 4: pp178-208

Wildshut, J. (2009) Pyrolysis oil upgrading to Transportation Fuels by Catalystic Hydrotreatment, Thesis, University of Groningen

www.orcbs.msu.edu/newhazard/wastemanualdocs/05classification.html

www.nationsencyclopedia.com/economies/Africa/Nigeria.html, accessed on December 14, 2012).

Yaman,S. (2004), Pyrolysis of biomass to produce fuels and chemical feedstocks, *Energy Conservation and Management*, pp 651-71

Zhang,Q.,Chang,J.,Wang and Xu,Y. (2006), Upgrading Bio-oil Over Different Solid Catalysts, *Energy& Fuels*, Vol.20, No.6, pp.2717-2720

Zhang, S. P., Yan Yongjie, Li T, *et al.* (2007): Upgrading of liquid fuel from the pyrolysis of biomass", pp 545–550.

Zhao, X., Hunang, H., Wu, C., Li, H., Chen, Y. (2001), Biomass pyrolysis in an Argon/Hydrogen plasma reactor, *Chemical Engineering Technology*, 24 (5), pp. 197-199

Nigerian Journal of Renewable Energy Research
Volume 1, Number 1, pp 101-108, 2023
 EISSN 1597-8907: PISSN 1597-8877

Instructions for Authors

The Nigerian Journal of Renewable Energy Research (NJRER) is an open-access publication that facilitates prompt dissemination of papers across the full spectrum of renewable energy. Manuscripts that align with the rigorous scientific standards and are of notable significance are welcomed. On average, papers are published approximately 6 months post their approval.

PRE-SUBMISSION CHECKLIST

Before submitting, please use this list to ensure your paper meets all the necessary criteria. For comprehensive details, refer to the relevant sections in this Author's Guide. Ensure you have:

- Nominated one author as the main point of contact, including:
- Email address
- Complete postal details
- Uploaded all essential files:
  - The paper itself, with keywords included.
  - Arrange your paper with a single column layout per page.
  - All figures (with corresponding captions).
  - Tables (with titles, descriptions, footnotes).
  - Check that references to figures and tables within the text correspond with provided files.
  - Clearly highlight if any illustrations need to be colour printed.
  - Graphical abstracts or highlights (if relevant).
  - Any supplementary files.
- Additional Checks:
  - Run a spell-check and grammar-check.
  - Ensure all references in your list are also mentioned in your text and the other way around.
  - Acquire permissions for copyrighted content, even from online sources.
  - Include a statement about competing interests (even if none exist).
  - Familiarise yourself with the journal's policies mentioned in this guide.
  - Provide referee recommendations and their contact details, as per the journal's prerequisites.

Digital submission of papers is preferable. Make sure the content, tables, and illustrations are in a single Microsoft Word document (Arial font is preferred).

Send your papers as an email attachment to the Editorial Office at: editor@njrer.org. Within a week, the primary author will receive a manuscript number.

The introductory letter should detail the main author's full contact information. This should accompany the file (named after the first author's surname) sent as an email attachment to the Editor. Authors can also propose two to four potential reviewers for their manuscript, although NJRER might nominate others.

Submissions to *The Nigerian Journal of Renewable Energy Research* are accepted solely as email attachments.

TYPES OF MANUSCRIPTS

The *Nigerian Journal of Renewable Energy Research (JRER)* considers:

1. **Original Articles**: Describing novel, thoroughly verified findings. These should be as succinct as necessary for clarity.
2. **Short Communications**: Suitable for concise research results, new theories, novel methods or equipment. They don't need to follow the layout of full-length papers and range from 6 to 12 manuscript pages.
3. **Reviews**: Synopses covering contemporary topics are appreciated. Reviews should not exceed 12 to 18 manuscript pages and undergo a peer-review process.

Procedure: Submit original articles via editor@njrer,org. For review articles, send an outline and your CV to the Editor in Chief for consideration.

Paper Length: Typically, original articles range between 4,000 to 6,000 words (excluding captions and references), while review articles can be up to 10,000 words. Please mention the word count during submission.

Review Process: Every manuscript undergoes a review by the editor, Editorial Board members, or expert external reviewers. Our aim is to revert with feedback within 3 weeks. The editorial team will reassess manuscripts that are approved but need revisions. JRER's objective is to publish manuscripts within 8 weeks of submission.

MANUSCRIPT STRUCTURE FOR REGULAR ARTICLES

Manuscripts should be typed with double-spacing and pages numbered beginning from the title page.

- **Title**: A concise description of the paper's content.
- **Title Page**: Should contain full names and affiliations of all authors, and the contact details of the corresponding author.
- **Abstract**: A self-explanatory summary between 100 to 200 words, highlighting the scope, significant data, and major conclusions.
- **Keywords**: Provide 3 to 10 keywords for indexing purposes.
- **Abbreviations**: List uncommon abbreviations. General abbreviations like ATP or DNA don't need to be expanded.
- **Introduction**: A clear outline of the problem, related literature, and the proposed approach.
- **Materials and Methods**: Detailed enough for reproducibility, with references to established methods.
- **Results**: Presented clearly and in past tense.
- **Discussion**: Interpretation of the findings in light of existing knowledge.
- **Acknowledgments**: Keep it brief.

Tables and figures should be concise, understandable without referencing the main text, and be on separate pages. Graphics should be high-resolution and created using appropriate software before embedding in the Word document.

REFERENCES

Adhere to the 7th Edition - APA Style (American Psychological Association) for referencing. Ensure the proper format, which includes author name(s), publication year, article title, journal title (italicised), volume (italicised), issue number, page range, and DOI or URL. The first line of each reference should align left, with subsequent lines indented.

Example:

Ruxton, C. (2016). Tea: Hydration and other health benefits. *Primary Health Care*, *26*(8), 34-42. https://doi.org/10.7748/phc.2016.e1162

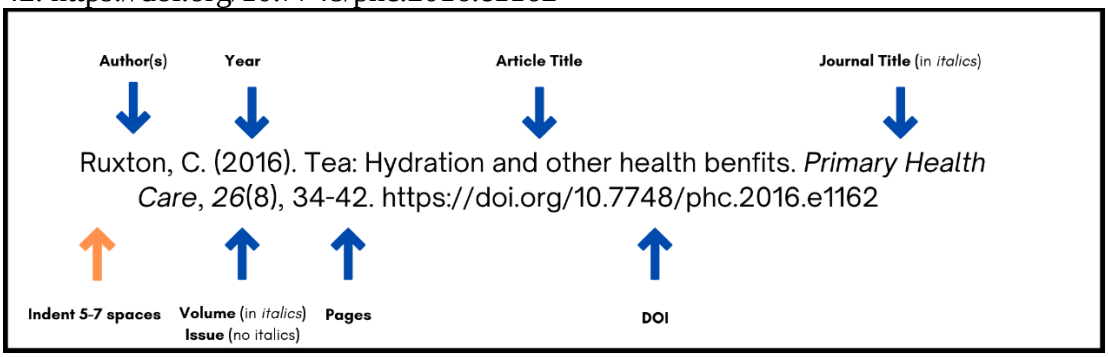

Material Type	In-Text Example	Reference List Example
Journal Article: Single author	"Black tea is the second most consumed beverage in the world after water" (Ruxton, 2016, p. 34). **OR** Ruxton (2016) suggests "Unsweetened tea can be part of a recommended diet" (p. 40). **Include page numbers for direct quotes.**	Ruxton, C. (2016). Tea: Hydration and other health benefits. *Primary Health Care*, *26*(8), 34-42. https://doi.org/10.7748/phc.2016.e1162 **Where a DOI is available it must be included at the end of the reference, in the format https://doi.org/10.xxxx**
Journal Article: 2 authors	... connection and optimism (Aspy & Proeve, 2017), but others contend ... **OR** Aspy and Proeve (2017) have found ...	Aspy, D. J., & Proeve, M. (2017). Mindfulness and loving-kindness meditation: Effects on connectedness to humanity and to the natural world. *Psychological Reports*, *120*(1), 102-117. https://doi.org/10.1177/0033294116685867

	Cite both authors each time the reference occurs.	
Journal Article: 3 to 20 authors	(Wilmott *et al.*, 2018) OR Wilmott *et al.* (2018) noted that… **Cite only the surname of the first author followed by *et al.* and the year.**	Wilmott, C., Fraser, E., & Lammes, S. (2018). 'I am he. I am he. Siri rules: work and play with the Apple Watch', *European Journal of Cultural Studies, 21*(1), 78-95836-839. **Provide the names of all authors in the reference list.**
Journal Article: 21 or more authors	Research indicated that "lost sense of smell is a factor" (Khan *et al.*, 2017, p. 344). **OR** Khan *et al.* (2019) used criteria which included "reduced or lost sense of smell" (p. 344). **Cite only the surname of the first author followed by *et al.* and the year. Include page numbers for direct quotes.**	Khan, A., Huynh, T. M. T., Vandeplas, G., Joish, V. N., Mannent, L. P., Tomassen P., van Zele, T., Cardell, L.O., Arebro, J., Olze, H., Forster-Ruhrmann, U., Kowalski, M. L., Olszewska-Ziaber, A., Fokkens, W., van Drunen, C., Mullol, J., Alobid, I., Hellings, P.W., Hox, V., …Bachert, C. (2019). The GALEN rhinosinusitis cohort: Chronic rhinosinusitis with nasal polyps affects health-related quality of life. *Rhinology, 57*(5), 343-351. https://doi.org/10.4193/Rhin19.158 **Provide the names of the first 19 authors, insert an ellipsis […] (but no ampersand [&]), then add the final author's name.**
Journal Article from most Library databases: No DOI	Nairne and Wilkinson (2018) assert that "our relationship with ourselves is essential to how we each show up professionally" (p. 106). **OR** "Our relationship with ourselves is	Nairne, D. C., & Wilkinson, H. (2018). What's love got to do with it? *Vermont Connection*, *39*(1), 106-112. **An article retrieved from most Library databases that does not have a DOI can be presented as though it were a print article.**

	essential to how we each show up professionally" (Nairne & Wilkinson, 2018, p. 106).	
Journal Article from the Cochrane Database of Systematic Reviews	The review included 78 trials employing a variety of intervention approaches (Hodder *et al.*, 2019). **OR** Hodder *et al.* (2019) identified 78 relevant trials that employed a variety of intervention approaches.	Hodder, R. K., O'Brien, K. M., Stacey, F. G., Tzelepis, F., Wyse, R. J., Bartlem, K. M., Sutherland, R., James, E. L., Barnes, C., & Wolfenden, L. (2019). Interventions for increasing fruit and vegetable consumption in children aged five years and under. *Cochrane Database of Systematic Reviews*. https://doi.org/10.1002/14651858.CD008552.pub6 **Articles in the Cochrane Database of Systematic Reviews can only be retrieved from this database, therefore the name of the database (in italics) is included as the source of the article.**
Online Journal Article: No DOI (With an Article Number)	Marion *et al.* (2018) explore whether evil characters in film share ... **OR** ... including stereotypical depictions of evil characters in film (Marion *et al.*, 2018).	Marion, T., Reese, V., & Wagner, R. F. (2018). Dermatologic features in good film characters who turn evil: The transformation. *Dermatology Online Journal*, *24*(9), Article 4. https://escholarship.org/uc/item/1666h4z5 **For an online journal article with no DOI (other than those retrieved from a Library database), provide the direct URL for the article.** **For journal issues with article numbers (rather than consecutive pagination) replace with page numbers with the word 'Article' followed by the article number or eLocator.**
Print Journal Article: No DOI assigned	… Aussie Rules is the people's game (Duncan, 2016)… **OR** Duncan (2016) states that a sense of belonging…	Duncan, S. (2016). Voices from the grandstands: The attitudes of Australian football fans towards the concept of creating, developing and binding communities. *Sporting Traditions*, *33*(2), 19-40. **Note: Where a print journal article has a DOI you must include it, even though you did not access the electronic version.**
Online Journal Article: No page numbers	... in all outcomes (Christensen *et al.*, 2019). **OR**	stensen, G., Dafoe, A., Miguel, E., Moore, D. A., & Rose, A. K. (2019). A study of the impact of data sharing on article citations using journal policies as a natural experiment. *PLoS ONE*, *14*(2), Article e0225883. https://doi.org/10.1371/journal.pone.0225883

	Christensen *et al.* (2019) examine ... **For direct quotes of online material without pagination, name the sections and paragraph number:** The authors' "objective was to identify control journals that did not require data posting" (Christensen *et al.*, 2019, Broad Analysis section, para. 4).	
Secondary Sources: When you are referring to the ideas or words of an author who has been cited in another work. Also called 'secondary citation'. ***Only recommended where the original work cannot be obtained.***	Constituting a "global movement toward a more naturalistic approach for childbirth" (Goldbas, 2012, as cited in Sullivan & McGuiness, 2015, p. 20). **OR** Goldbas's overview (2012, as cited in Sullivan & McGuiness, 2015) indicates… **Provide names of both authors. Where the year is known for the original work, include it as well as the year of the publication you read.**	Sullivan, D. H., & McGuiness, C. (2015). Natural labor pain management. *International Journal of Childbirth Education*, *30*(2), 20-25. https://scholarworks.waldenu.edu/sn_pubs/51/ **Provide the full reference for the journal article that you actually read.**

Proofs and Copies:
Digital proofs will be forwarded to the main author as a PDF attachment via email. These page proofs are deemed the conclusive rendition of the manuscript. Save for typographical or small administrative oversights, no alterations will be made to the manuscript during this phase. Given that NJRER will be freely accessible online to engage a broad readership, authors will enjoy complimentary electronic access to their article's full content (in PDF format). Authors can effortlessly download the PDF, enabling them to produce countless prints of their papers.

Copyright:
Submitting a manuscript insinuates: that the detailed work has not been previously published (barring being in abstract form or part of a published talk or dissertation); it's not being reviewed for publication elsewhere; and, should the manuscript gain acceptance for publication, authors concur to the immediate transfer of copyright to the publishing entity.

Fees and Costs:
Authors are obliged to cover an assessment fee of either $100 or N30,000.00 and if the paper is accepted for publication, the Publication fee is $100 or N30,000.00. Please note that publishing an article in the **Nigerian Journal of Renewable Energy Research** is not dependent on the author's capacity to settle these fees. Similarly, a commitment to handle the fee doesn't assure the manuscript's acceptance for publication. Under certain conditions, authors might petition the editorial team to consider a reduction or exemption of some handling charges in advance. The payment process is presented on the Journal website.